UNIVERSITY OF OKLAHOMA

GRADUATE COLLEGE

EXTENDED SURFACTANTS: CHARACTERIZATION AND MICROEMULSION PROPERTIES

A DISSERTATION

SUBMITTED TO THE GRADUATE FACULTY

in partial fulfillment of the requirements for the

Degree of

DOCTOR OF PHILOSOPHY

By

ANURADEE WITTHAYAPANYANON
Norman, Oklahoma
2008

Downloaded from SHAREOK. Persistent Handle URL: https://hdl.handle.net/11244/318447

EXTENDED SURFACTANTS: CHARACTERIZATION AND MICROEMULSION PROPERTIES

A DISSERTATION APPROVED FOR THE
SCHOOL OF CHEMICAL, BIOLOGICAL, AND MATERIALS ENGINEERING

BY

_____
Dr. Jeffrey H. Harwell, Chair

_____
Dr. David A. Sabatini

_____
Dr. John F. Scamehorn

_____
Dr. Tohren C.G. Kibbey

_____
Dr. Edgar J. Acosta

© Copyright by ANURADEE WITTHAYAPANYANON 2008
All Rights Reserved.

DEDICATION

This dissertation is dedicated to my parents, Papa Bancha and Mama Pui, my aunties, Yee Yai, Yee Moi, Yee Jin, and Yee Lek, my brothers, P' Axe and N' Arm and my fiancé, Trung Hoang

ACKNOWLEDGEMENTS

Though the following dissertation is an individual work, many people have contributed to its production. I owe my gratitude to all those people who have made this dissertation possible and because of whom my graduate experience has been one that I will cherish forever.

My deepest gratitude is to my advisors, Dr. David A. Sabatini and Dr. Jeffrey H. Harwell. I have been unbelievably fortunate to be one of their students. Dr. David A. Sabatini not only gives me the freedom to think and explore on my own, but also supports with immeasurable time and guidance when my steps faltered. His unwavering faith and confidence in my abilities and in me is what has shaped me to be the person I am today. In addition, I am thankful to him for giving an opportunity to present my work at the national conferences and industrial companies. I am also very grateful to Dr. Jeffrey H. Harwell for his continual support and encouragement. His advice and guidance are paramount in providing a well rounded experience.

I am also deeply indebted to Dr. John F. Scamehorn for his support, encouragement and practical advice. I am thankful to him for being former master co-advisor, providing the opportunity of the lifetime in studying a PhD, carefully reading and commenting on my writing, and helping me understand and enrich my ideas. My warm appreciation goes to Dr. Tohren C.G. Kibbey for his participation as a committee member, his valuable time to read and comment this dissertation, and kind permission to use his laboratory devices such as the UV spectrophotometer and

the liquid chromatography. A very special thank to Dr. Edgar J. Acosta for generous advice, valuable guidance and friendship during my years in the United States.

Most importantly, none of this would have been possible without the love, patience, and encouragement of my family and my fiancé. My family, to whom this dissertation is dedicated to, no one has ever given more loving and unconditional support than I have been given by them. Thank to my fiancé A' Trung for his friendship, love, patience, humor, and willingness to accept each other for better and for worse.

My graduate studies would have never been an enjoyable and memorable experience without my student-colleagues and friends at the University of Oklahoma. Thank to Trung Hoang, Trung Pham, Pheung, Thu, Linh, Tri, P' Noi, P' Chan, P' Khwan, P' Oam, P' Him, P' Tu, P' Cheng, Anand, Laura, Chirs, and Sezin. Their support and care helped me overcome setbacks and stay focused on my graduate study. I greatly value their friendship. I also would like to express a special thank to my wonderful undergraduate students, Emily, Todd, Kathy, and Jimmy, for both friendship and lab-assistant throughout my time being a graduate student.

This is also a great opportunity to express my appreciation to the staff members of both Civil Engineering and Environmental Science department and the Chemical, Biological, and Materials Engineering department for their kind assistance and encouragement during my years of study.

Finally, I appreciate the financial support from the Institute for Applied Surfactant Research (IASR) at the University of Oklahoma, the U.S. Environmental

Protection Agency (USEPA) that funded parts of the research discussed in this dissertation.

TABLE OF CONTENTS

	Page
ACKNOWLEDGEMENTS	iv
TABLE OF CONTENTS	vii
LIST OF TABLES	ix
LIST OF FIGURES	xi
ABSTRACT	xiii
CHAPTER 1. Introduction	1
References	5
CHAPTER 2. Formulation of Ultralow Interfacial Tension Systems Using Extended Surfactants	8
Abstract	8
Introduction	9
Experimental Procedures	15
Results and Discussion	17
References	33
CHAPTER 3. Hydrophilic-Lipophilic Deviation (HLD) Method for Characterizing Conventional and Extended Surfactants	38
Abstract	38
Introduction	39
Experimental Procedures	46
Results and Discussion	50
Conclusions	67
References	69
CHAPTER 4. Interfacial Properties of Extended- Surfactants-Based-Microemulsions	72
Abstract	72
Introduction	73
Experimental Procedures	78
Results and Discussion	84
References	102

CHAPTER 5. Conclusions 108

APPENDIX A. Dynamic Interfacial Tension and the Critical Micelle Concentration (CMC) of Extended Surfactants (Chapter 2) 113

APPENDIX B. *K*- and σ-Values of Conventional and Extended Surfactants (Chapter 3) 115

APPENDIX C. Dynamic Interfacial Properties and Turbidity Measurement of Extended-Surfactant-Based-Microemulsions (Chapter 4) 119

APPENDIX D. Microemulsion-Enhanced Cleaning Performance 124

LIST OF TABLES

Table 2.1. Properties of the extended surfactants 14

Table 2.2. Summary of the optimum salinity (S*) and the optimum dynamic IFT (IFT*) with various kinds of oils for C_{14-15}-$(PO)_8$-SO_4Na surfactant 25

Table 2.3. Summary of the optimum salinity (S*) and the optimum dynamic IFT (IFT*) with various kinds of oils for C_{12}-$(PO)_{14}$-$(EO)_2$-SO_4Na surfactant 26

Table 2.4. Selected composition parameters of vegetable oils and Calculated EACN 28

Table 2.5. Critical micelle concentration (CMC) and area per molecule (A_{min}) of conventional and extended surfactants 30

Table 3.1. Summary of the optimum salinity (S*) and the minimum interfacial equilibrium tension (IFT*) of the 0.07 M sodium dihexyl sulfosuccinate (AMA) with a wide range of oils 51

Table 3.2. Summary of the s value of conventional and extended surfactants 57

Table 3.3. HLB number vs σ value of various surfactants 63

Table 4.1. Properties of conventional and extended surfactants 80

Table 4.2. Comparison of microemulsions properties at the optimum condition between the $C_{12,13}H_{25,27}$-$(PO)_8$-SO_4Na, 100 B and the SDS/sec-butanol mixture for a wide range of alkane oils at constant 0.07 M surfactant concentration and 27 ^oC 86

Table 4.3. Characteristic length (ξ*), interfacial rigidity (Er) at the optimum condition, and equilibrium time of conventional and extended surfactant systems for hexadecane 91

Table 4.4. Characteristic length (ξ*), interfacial rigidity (Er), and coalescence rate constant (K_c) of the $C_{12,13}$-$(PO)_4$-SO_4Na-alone and mixture systems at the optimum middle phase hexadecane microemulsions and 27 ^oC. The $C_{12,13}$-$(PO)_4$-SO_4Na concentration was fixed at 0.07 M, unless stated otherwise. The ratio of SMDNS/lipophilic linker was kept constant at 0.03 M and added on the top of the 0.07 M $C_{12,13}$-$(PO)_4$-SO_4Na concentration. The ratio of $C_{12,13}$-$(PO)_4$-SO_4Na/AOT used was the 50/50 at constant 0.07 M total surfactant concentrations 99

LIST OF FIGURES

Figure 2.1. Structure of extended surfactants: (a) alkyl-PO-sulfate C_{14-15}-$(PO)_8$-SO_4Na and (b) alkyl-PO-EO-sulfate C_{12}-$(PO)_{14}$-$(EO)_2$-SO_4Na 14

Figure 2.2. Dynamic IFT as a function of electrolyte concentration (salinity scan) for the systems triolein-C_{14-15}-$(PO)_8$-SO_4Na-brine (squares), triolein- C_{12}-$(PO)_{14}$-$(EO)_2$-SO_4Na-brine (triangles), triolein-C_{12-13}-$(PO)_8$-SO_4Na-brine (diamonds), and triolein-AOT-brine (cross), surfactant concentration 10 mM, all reading taken after 10 minute contact 18

Figure 2.3. Dynamic IFT versus surfactant concentration at optimum concentration electrolyte for the systems triolein-C_{14-15}-$(PO)_8$-SO_4Na-0.2 M brine (squares) and triolein- C_{12}-$(PO)_{14}$-$(EO)_2$-SO_4Na-0.015 M brine (triangles), all reading taken after 10 minute contact 21

Figure 2.4. Surface tension of extended surfactants with and without salt: (a) C_{14-15}-$(PO)_8$-SO_4Na, (b) C_{12-13}-$(PO)_8$-SO_4Na, and (c) C_{12}-$(PO)_{14}$-$(EO)_2$-SO_4Na 31

Figure 3.1. Structure of extended surfactants, (a) R-$(PO)_x$-SO_4Na and (b) R-$(PO)_y$-$(EO)_2$-SO_4Na, adapter from Ref. [12] 48

Figure 3.2. Determine the K_{AMA}, σ_{AMA}, and EACN of limonene using a HLD equation of an anionic surfactant (0.07 M AMA surfactant) at the optimum salinity (see Table 3.1.), 25 ^oC and no additives 52

Figure 3.3. A plot of ln $S^*_{AMA+SDS}$ vs SDS composition (X_{SDS}) in the mixed AMA-SDS system with limonene at constant 0.07 M total surfactant concentration and controlled temperature 25 ^oC 57

Figure 3.4. A plot of ln S^*_{1+2} vs SDS composition (X_2) in various surfactant mixtures with limonene at constant 0.07 M total surfactant concentration and controlled temperature 25 ^oC 58

Figure 3.5. The σ value of mixed AMA-surfactant system with limonene oil at the optimum condition, 0.07 M total surfactant concentration, and 25 ^{o}C: (a) AMA/$C_{12,13}$-$(PO)_3$-SO_4Na vs. AMA/C_{12}-$(PO)_{14}$-$(EO)_2$-SO_4Na systems and (b) AMA/$C_{12,13}$-$(PO)_8$-SO_4Na vs AMA/C_{10}-$(PO)_{18}$-$(EO)_2$-SO systems 64

Figure 3.6. Comparison the optimum salinity (S*) obtained from the prediction using σ parameter and the experimental phase study of (a) AMA/AOT/Octane system (represented by the triangle bullet), and (b) AMA/AOT/Decane system (represented by the circle bullet). total surfactant concentration of 0.07 M at 25 ^{o}C 67

Figure 4.1. The structure of middle phase microemulsions at the optimum condition shown in accordance to (a) a zero net-curvature of coexisting oil and water droplets and (b) microscopic lattice model illustrating the characteristic length (ξ) of the surfactant dynamic membrane adapted from ref [4] and [19], respectively 76

Figure 4.2. Proposed structure of PO-extended surfactants, (R-$(PO)_x$-SO_4Na) adapted from ref [7] 79

Figure 4.3. Fish diagram of the $C_{12,13}$-$(PO)_8$-SO_4Na, 50 B/brine/hexadecane Microemulsion at constant 27 ^{o}C 95

Figure 4.4. The turbidity (a) and inverse turbidity (b) curves during Coalescence at 27 ^{o}C of the samples containing the 0.07 M $C_{12,13}$-$(PO)_8$-SO_4Na-alone, the 0.07 M $C_{12,13}$-$(PO)_8$-SO_4Na/0.03 M SMDNS/ 0.03 M dodecanol, the 0.07 M $C_{12,13}$-$(PO)_8$-SO_4Na/0.03 M SMDNS/0.03 M oleyl alcohol, and the 0.035 M $C_{12,13}$-$(PO)_8$-SO_4Na/0.035 M AOT mixtures turbidity samples resulted from shaking the optimum middle phase hexadecane microemulsions 100

ABSTRACT

Extended surfactants are surfactants with intermediate polarity groups, such as polypropylene oxide (PO) and polyethylene oxide (EO), inserted between the hydrophilic head and the hydrocarbon tail. With this unique molecular structure, extended surfactants provide an enhanced interaction with both oil and water phases. This results in microemulsion formation with desirable low interfacial tension (IFT) and high solubilization properties, especially for highly hydrophobic oils and vegetable oils. Such formulations have numerous potential applications in enhanced subsurface remediation, drug delivery, and detergency. However, due to the limited amount of information available on these recently developed surfactants, there is no easy and adequate technique to guide the formulation selection process and microemulsion characteristics for extended surfactant systems. In addition to the challenge in characterization, extended surfactant-based microemulsions also struggle with their slow kinetics. Therefore this present work seeks to characterize extended surfactant hydrophilicity/lipophilicity, and at the same time, evaluate both equilibrium and kinetic properties of extended surfactant-based microemulsions. The thermodynamically derived model known as hydrophilic-lipophilic deviation (HLD) approach used in combination with microemulsion phase behavior was proposed as a simple, yet convenient tool for characterizing extended surfactant behavior and predicting the optimal conditions for microemulsion systems. To our knowledge, this is the first report of the extended surfactant hydrophilicity/lipophilicity index and interfacial morphology of the extended

surfactant membranes (i.e. characteristic length and interfacial rigidity). The findings of this study not only emphasize the important role of inserting PO and EO groups on the hydrophilic-lipophilic nature of extended surfactants, but also demonstrate the impact these intermediate functional groups have on both equilibrium and dynamic microemulsion properties.

CHAPTER 1

Introduction

In general, microemulsions are a thermodynamic stable dispersion of oil and water stabilized by surfactants, and frequently, with a combination of additives or co-surfactants. Microemulsions, and in particular the middle phase microemulsion, have received significant attention from both scholars and practitioners due to their unique properties, in particular their ability to significantly reduce interfacial tension (IFT) and enhance the solubilization of hydrophilic and lipophilic ingredients. Therefore, microemulsions have been a key component of successful technologies in various applications such as an enhanced oil recovery, subsurface remediation, and cleaning technology [1-7].

Formulating microemulsions with desirable low IFT and high solubilization properties has been a challenging task as it is both an art and a science [8]. Indeed, the formation of microemulsions involves a deep understanding of the physiochemical environment at the surfactant-oil-water interface. Based on decades of intensive research, we now know that forming a microemulsion requires a balanced and substantial interaction between surfactant-oil and surfactant-water phases. This concept was first introduced by Winsor [9] in 1948 and has remained a conceptual foundation for a microemulsion formation until these days.

According to Winsor's model [8, 10, 11], the maximum in co-solubilization of oil and water and the minimum in IFT coexist at the optimum condition, where

the surfactant-oil and the surfactant-water interactions are equal (R-ratio = 1). In addition, the solubilization enhancement and IFT reduction are improved by increasing both of these individual interactions, while maintaining them as equal. Using Winsor's terms, an effective way of enhancing these interactions is to increase the size of surfactant hydrophilic head group and hydrocarbon tail. However, this approach is limited by the loss in solubility associated with long hydrocarbon tails. Extended surfactants have been proposed as an alternative surfactant structure to achieve the Winsor's approach without sacrifying water solubility [8, 11-15].

Unlike conventional surfactants, extended surfactants are surfactants in which intermediate polarity groups, such as a short-chain polypropylene oxide (POs) or polypropylene-polyethylene oxide (POs-EOs), are inserted between the surfactant hydrophilic head and hydrocarbon tail. Due to this unique structure, extended surfactants offer not only an extended length, but also a smooth transition between hydrophilic and hydrophobic regions at the oil-water interface [8, 11, 12]. In addition, despite the relatively large molecular weight of these surfactants, they are water-soluble and can be formulated in relatively high electrolyte concentration without surfactant precipitation. To date, extended surfactants have been a foremost candidate for forming microemulsions with high solubilization and low IFT properties, especially for highly hydrophobic oils, triglycerides and vegetable oils.

However, since extended surfactants are a relatively new class of surfactants, our understanding of their fundamental properties is still quite limited. The goal of this dissertation is to provide a better understanding of extended surfactant in the

microemulsion formation. The framework of the dissertation is divided into two main areas; the extended surfactants' ability to form microemulsions and their properties and an empirical model to characterize the hydrophilic-lipophilic nature of extended surfactants. While Chapter 2 and 4 focus on the first area, Chapter 3 provides new information of extended surfactants using an alternative approach.

Chapter 2 introduces the use of the dynamic IFT measurement of dilute extended surfactant formulations as a simple technique to investigate how the unique structure of extended surfactant achieves ultra low IFT property with a wide range of oils (i.e. petroleum hydrocarbon, triglyceride, and vegetable oils etc.). The study reveals the crucial role of additional PO and EO groups in facilitating an enhanced interaction with triglyceride molecules, thus resulting in the efficient IFT reduction. These results are then integrated with the hydrophilic-lipophilic deviation (HLD) concept[11, 16] to evaluate the hydrophobicity of different triglyceride and vegetable oils as well as scale the hydrophilic-lipophilic nature of extended surfactants. This work demonstrates the shortcoming of the existing HLB method in capture the hydrophilic-lipophilic characteristic of extended surfactant.

Chapter 3 is a follow-up on the inadequacy of existing techniques for determining the hydrophilic-lipophilic nature of extended surfactants addressed in Chapter 2. The ultimate goal of this work is to be able to use empirical models to guide for conditions to form microemulsions and their microemulsion properties under various circumstances. However, one major problem is the lack of an accurate determination of the surfactant characteristic, especially for extended surfactants.

Therefore, in this work, we utilize the simple hydrophilic-lipophilic deviation (HLD) technique in combination with mixed surfactant phase study to determine the surfactant characteristic (σ) and the σ/K parameter of conventional and extended surfactants. These parameters were evaluated as surfactant behavior indicators, as an alternative to the HLB number. In the final analysis, the combination of the σ parameter established and the HLD equation will be demonstrated its practical use for guiding the optimum formulation (in this case, optimum salinity) for a microemulsion system.

Chapter 4 builds on the observation that the optimum middle phase microemulsions produced by extended surfactants require a prolonged time to reach equilibrium (ranging from weeks to months). This slow kinetic behavior could be a major barrier in applying the extended-surfactant-based formulations for practical uses, regardless of desirable low IFT and high solubilization properties. Therefore, the study in this chapter was designed to illustrate both equilibrium and dynamic aspects of extended-surfactant-based microemulsions. Previous remarks found in Chapter 2 and 3 indicate that the time for extended-surfactant-based microemulsions to approach equilibrium is dependent on the coalescence rate of corresponding macroemulsion droplets. This finding leads to the speculation that this slow coalescence phenomenon is a result of the extended surfactants' unique structure – the presence of PO groups. The interfacial film properties (such as characteristic length (ξ) and interfacial rigidity (E_r)) in extended surfactant systems will be characterized using the net-average curvature model [17, 18] to provide an insight

into the role of PO groups inserted in extended surfactant molecules. Lastly, the work culminates by demonstrating an approach to overcome the slow coalescence rate of extended-surfactant-based systems, while still maintaining favorable low IFT and high solubilization.

Finally, Chapter 5 summarizes major conclusions of this dissertation. The goal of this dissertation is that these remarks and the corresponding understanding will bring us a step closer to fully exploiting the exciting potential of extended-surfactant-based microemulsions.

References

1. Shah, D.O., Schechter, R. S., ed. *Improved Oil Recovery by Surfactant and Polymer Flooding*. 1977, Academic Press: New York.
2. Johansen, R.T., Berg, R. L., ed. *Chemistry of Oil Recovery*. ACS Symposium Series. Vol. 91. 1978, American Chemical Society: Washington DC.
3. Harwell, J.H., *Transport and Remediation of Subsurface Contaminants*, R.C. Knox, Editor. 1992, American Chemical Society: Washington DC. p. 124.
4. Knox, R.C., Shiau, B. J., Sabatini, D. A., Harwell, J. H., *Innovative Subsurface Remediation: field Testing of Physical, Chemical, and Characterization Technologies*, M.L. Brusseau, Editor. 1999, American Chemical Society: Washington DC. p. 49.
5. Tongcumpou, C., Acosta, E. J., Quencer, L. B., Joseph, A. F., Scamehorn, J. F., Sabatini, D. A., Chavadej, S., Yanumet, N., *Microemulsion Formation and*

Detergency with Oily Soils: II Detergency Formulation and Performance. J. Surfact. Deterg., 2003. **6**: p. 205 - 214.

6. Childs, J., Acosta E. J., Scamehorn, J. F., Sabatini, D. A., *Surfactant-Enhanced Treatment of Oil-Based Drill Cuttings.* J. Energy Res. Technol., 2005. **127**: p. 153 - 162.
7. Yanatatsaneejit, U., Rangsunvigit, P., Scamehorn, J. F., Chavadej, S., *Diesel Removal by Froth Flotation Under Low Interfacial Tension Conditions I: Foam Characteristics, Coalescence Time, and Equilibration time.* Sep. Sci. Technol., 2005. **40**: p. 1537.
8. Salager, J.L., Anton, R. E., Sabatini, D. A., Harwell, J. H., Acosta, E. J., Tolosa, L. I., *Enhancing Solubilization in Microemulsions-State of the Art and Current Trends.* J. Surfact. Deterg., 2005. **8**: p. 3 - 21.
9. Winsor, P.A., Trans. Faraday Soc., 1948. **44**: p. 376.
10. Bourrel, M., Schechter, R., *Microemulsions and Related Systems*. 1988, New York: Marcel Dekker.
11. Salager, J.L., *Microemulsions*, in *Handbook of Detergents: Part A: Properties*, G. Broze, Editor. 1999, Marcel Dekker: New York. p. 253.
12. Minana-Perez, M., Graciaa, A., Lachaise, J., Salager, J. L., *Solubilization of Polar Oils with Extended Surfactants.* Colloid Surfaces A., 1995. **100**: p. 217 - 224.

13. Scorzza, C., Gode, P., Martin, P., Minana-Perez, M., Salager, J. L., Villa, P., *Synthesis and Surfactant Properties of a New "Extended" Glucidoamphiphile Made from d-Glucose.* J. Surfact. Deterg., 2002. **5**: p. 331.
14. Scorzza, C., Gode, P., Martin, P., Minana-Perez, M., Salager, J. L., Usubillaga, A., Villa, P., *Another New family of "Extended" Glucidoamphiphiles. Synthesis and Surfactant Properties for Different Sugar Head Groups and Spacer Arm Lengths.* J. Surfact. Deterg., 2002. **5**: p. 337.
15. Sabatini, D.A., Acosta, E., Harwell, J. H., *Linker Molecules in Surfactant Mixtures.* J. Colloid Interface Sci., 2003. **8**: p. 316 - 326.
16. Salager, J.L., Morgan, J., Schechter, R. S., Wade, W. H., Vasquez, E., *Optimum Formulation of Surfactant-Oil-Water Systems for Minimum Tension and Phase Behavior.* Soc. Petrol. Eng. J., 1979. **19**: p. 107 - 115.
17. Acosta, E., Szekeres, E., Sabatini, D. A., Harwell, J. H., *Net-Average Curvature Model for Solubilization and Supersolubilization in Surfactant Microemulsions.* Langmuir, 2003. **19**: p. 186 - 195.
18. Acosta, E.J., Le, M. A., Harwell, J. H., Sabatini, D. A., *Coalescence and Solubilization Kinetics in Linker-Modified Microemulsions and Related Systems.* Langmuir, 2003. **19**: p. 566 - 574.

CHAPTER 2

Formulation of Ultralow Interfacial Tension Systems Using Extended Surfactants[£]

Abstract

Inspired by the concept of lipophilic and hydrophilic linkers, extended surfactants have been proposed as highly desirable candidates for the formulation of microemulsions with high solubilization capacity and ultra low interfacial tension, especially for triglyceride oils. The defining characteristic of an extended surfactant is the presence of intermediate polarity group(s) between the hydrophilic head and the hydrophobic tail. Currently only limited information exists on extended surfactants; such knowledge is especially relevant for cleaning and separation applications where the cost of the surfactant and environmental regulations prohibit the use of concentrated surfactant solutions. In this work, we look at surfactant formulations for a wide range of oils using dilute solutions of the extended surfactant classes sodium alkyl polypropyleneoxide sulfate (R-(PO)x-SO_4Na), and sodium alkyl polypropyleneoxide-polyethyleneoxide sulfate (R-(PO)y-(EO)z-SO_4Na). The interfacial tension of these systems was measured as a function of electrolyte and surfactant concentration for polar and non-polar oils. The results show that these

[£] This chapter or portions thereof has been published previously in Journal of Surfactants and Detergents under title of "Formulation of Ultralow Interfacial Tension Systems Using Extended Surfactants", Journal of Surfactants and Detergents, 2006, 9 (4), p. 331 – 339. This current version has been

extended surfactant systems have low critical micelle concentrations (CMC) and critical microemulsion concentrations (CμC) compared to other surfactants. We also found that the unique structure of these extended surfactants allow them to achieve ultra low interfacial tensions (IFT) with a wide range of oils, including highly hydrophobic oils (e.g. hexadecane), triolein and vegetable oils, while using only ppm levels of these extended surfactants. It was also found that the introduction of additional PO and EO groups in the extended surfactant yielded lower interfacial tensions and lower optimum salinity, both of which are desirable in most formulations. Based on the optimum formulation conditions, it was found that the triolein sample used in these experiments behaves as a very polar oil while all other vegetable oils are very hydrophobic. This unexpected triolein behavior is suspected to be due to uncharacterized impurities in the triolein sample, as will be further evaluated in future research.

Key words: extended surfactant, microemulsion, dilute surfactant solution, low interfacial tension, triglyceride and vegetable oils

Introduction

According to Winsor's premise (1), the oil and water solubilization capacity of microemulsion systems increases when the surfactant-oil and the surfactant-water interactions increase. Also, the optimum co-solubilization of oil and water is found when these two interactions are equal. An effective way of increasing these

interactions is to enhance both the hydrophilicity of the head group and the hydrophobicity of the tail group of the surfactant while maintaining balanced affinity for the oil and water. . However, surfactant solubility limits the magnitude to which this approach can be utilized; i.e., as the hydrophobic tail gets longer, the surfactant eventually loses its water solubility (2). Graciaa *et al*. (3,4) first introduced the use of a lipophilic linker to effectively extend the length of the surfactant tail further into the oil phase without sacrificing water solubility of the surfactant; a long chain alcohol is one example of such a linker molecule. Subsequently, the concept of the hydrophilic linkers was proposed as a way of compensating for the increased hydrophobicity of lipophilic linkers and to further improve the solubilization capacity of these systems (5,6,7). Hydrophilic linkers adsorb at the oil/water interface, thereby promoting surfactant-water interaction and loosening the surfactant packing at the interface (6). The combination of hydrophilic and lipophilic linkers has been shown to act as a pseudo surfactant, thereby reducing the amount of surfactant necessary for oil solubilization in middle phase microemulsions (8,9). However, not all linker molecules incorporate into the oil/water interface, rather some of these molecules partition either into the oil or water phases (3,8,9). To mitigate this undesirable separation, extended surfactants have been introduced (10,11,12,13,14).

Extended surfactants are surfactants in which groups of intermediate polarity, such as polypropyleneoxides or copolymers of propyleneoxides and ethyleneoxide, are inserted between the hydrocarbon tail and hydrophilic head group. Due to the

resulting unique molecular structure, the surfactant is stretched out further into both the oil and water phases, providing a smoother transition between the hydrophilic and hydrophobic regions of the interface, which provides a more suitable environment for solubilizing hydrophilic and lipophilic molecules. Additionally, the Gibbs adsorption equation leads us to expect that a thickening of the interfacial region between the two phases should result in an increase in adsorption at the interface and a reduction of interfacial tension.

Despite the relatively large molecular weight of these surfactants, they are water-soluble and can be formulated in relatively high electrolyte concentration while avoiding surfactant precipitation. Recently, several papers (11,14,15,16) have demonstrated the benefits of using these extended surfactants to enhance oil solubilization of microemulsion with highly hydrophobic oils, as well as triglyceride and vegetable oils.

Microemulsion formulation with triglycerides and conventional surfactants (surfactants other than extended surfactants) has proven to be a challenging task, likely due to the polar and at the same time hydrophobic nature of different regions in the triglyceride molecule. This is consistent with the extremely low solubilization parameters reported for these systems (17).

According to the Chun-Huh relationship, the oil/water solubilization capacity increases as the interfacial tension (IFT) of the microemulsion systems decreases, as shown in the following equation (18):

$$SP = \frac{C}{IFT^2} \qquad [1]$$

where SP is known as the solubilization parameter (mL of oil/ g of surfactant) of the microemulsion system, C is the Chun-Huh constant characteristic of the surfactant, and IFT is the interfacial tension between excess oil and water phases (mN/m). Since large solubilization parameters have been reported for extended surfactant systems (11), the Chun Huh relationship predicts that these systems should produce ultra low interfacial tensions.

To date the majority of extended-surfactant microemulsion systems have been Type IV single-phase microemulsions (14,15), due in large part to the occurrence of stable macroemulsions in regions where Type III microemulsion systems were expected. These Type IV systems, which require elevated surfactant concentrations, are not particularly useful for most applications (detergency and soil, ground water, and wastewater remediation, etc.) where economics require that the surfactant be used at ppm-levels in the formulation (15,16,19). In cleaning applications such as detergency and oil extraction, an additional requirement is to achieve low interfacial tension within a reasonable contact time (minutes to tens of minutes).

Recently, it has been shown that an extended surfactant $C_{14\text{-}15}$-$(PO)_4$-SO_4Na that could not form Type III middle phase microemulsions was still capable of producing ultra low interfacial tension using only ppm-levels of the surfactant (15). These conditions were identified using electrolyte and surfactant concentration

scans, and the dynamic and equilibrium interfacial tensions of these systems were measured. In the absence of middle phase microemulsions, which required higher surfactant concentrations, the optimum salinity was defined as the electrolyte concentration that produced the lowest interfacial tension (15), and the critical microemulsion concentration (CμC) was defined as the minimum surfactant concentration at which the ultra low interfacial tension are attained (9,20).

In this work we study the formulation of dilute extended surfactant formulations with a wide range of oils, including petroleum hydrocarbons and vegetable oils. In the majority of studies, two extended surfactants were compared: C_{14-15}-$(PO)_8$-SO_4Na and C_{12}-$(PO)_{14}$-$(EO)_2$-SO_4Na. Although the molecular structure and molecular weight of these surfactants are quite different (see Figure 2.1), the HLB (hydrophilic lipophilic balance) values are only slightly different (see Table 2.1). The main difference between the two surfactants in Figure 2.1 is the additional PO and EO groups in C_{12}-$(PO)_{14}$-$(EO)_2$-SO_4Na. To evaluate the effect of alkyl chain length, a limited number of experiments included a third surfactant C_{12-13}-$(PO)_8$-SO_4Na (see Table 2.1). A hydrophobic anionic surfactant, sodium dioctyl sulfosuccinate, was also formulated with Canola oil to compare the performance of conventional anionic surfactants with the performance (IFT reduction) of these extended surfactants.

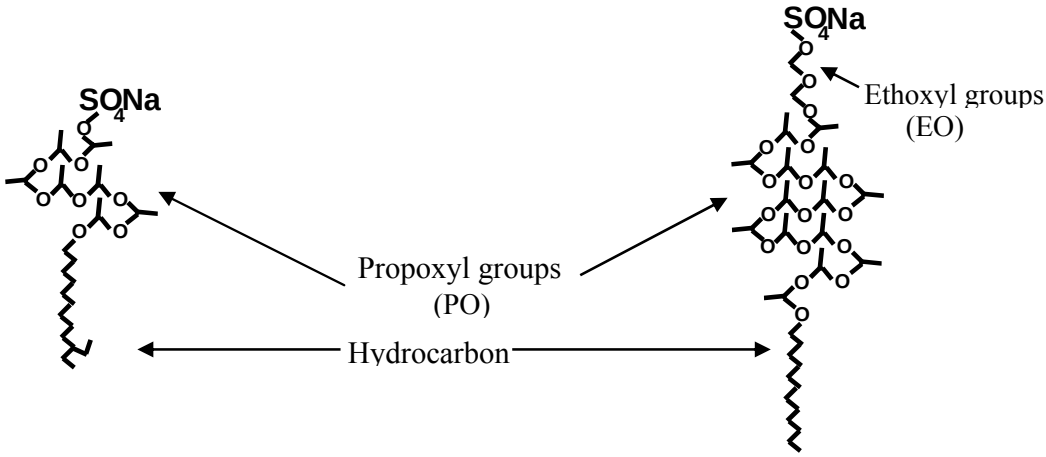

Figure 2.1. Structure of extended surfactants, (a) Alkyl –PO sulfate $C_{14\text{-}15}$-$(PO)_8$-SO_4Na, (b) Alkyl-PO-EO sulfate C_{12}-$(PO)_{14}$- $(EO)_2$-SO_4Na.

Table 2.1. Properties of the extended surfactants

Extended surfactant	**Hydrocarbon chain**	**#PO**	**#EO**	**% Active**	**HLB[a]**	**MW g/mol**
Alkyl-xPO-SO_4Na						
1. $C_{12,13}H_{25,27}$-$(PO)_8$-SO_4Na	12-13	8	-	29.1	31.6	712.8
2. $C_{14,15}H_{29,31}$-$(PO)_8$-SO_4Na	14-15	8	-	29.6	30.6	715.5
Alkyl-xPO-2EO-SO_4Na						
1. $C_{12}H_{25}$-$(PO)_{14}$-$(EO)_2$-SO4Na	12	14	2	24.1	31.8	1104

Notes

[a] Calculated based on the Davies' group contribution factors: J T Davies. Proceedings 2nd Intern. Congress Surface Activity, vol. I, 426, Butterworth, London (1957).

The oils considered in this study are decane, hexadecane, triolein, canola oil, peanut oil, soya oil, corn oil, sunflower oil, and palm oil. The optimum electrolyte concentration (S*), and the interfacial tension at optimum formulation were studied for these systems. These results are analyzed using the surfactant affinity difference concept proposed by Salager et al (21,22). Based on this approach, the relative hydrophocity of the different oils is discussed, as well as the hydrophobicitiy of the extended surfactants. The values of interfacial tension at optimum formulation and critical microemulsion concentration will be used to determine the efficacy and efficiency of these systems. Also, the relation between the properties of the surfactant formulations (optimum salinities, interfacial tension and critical microemulsion concentration) and the properties of each surfactant (HLB, CMC, surface area per molecule) are discussed. We thus demonstrate how the unique structure of extended surfactants allows us to achieve ultra low IFT at low surfactant concentrations with highly hydrophobic alkane oils and high molecular weight triglyceride and vegetable oils.

Experimental procedures

Materials. The extended surfactants evaluated in this work contain polyethylene and/or polypropylene oxide groups in between the hydrocarbon tail and sulfate head group. Two main classes of extended surfactant were used in this work. The first class of extended surfactant is a sodium alkyl polypropylene oxide sulfate (R-(PO)x-SO_4Na) with the alkyl (R) group consisting of a branched hydrocarbon

chain with 12 to 13 carbons (C_{12-13}) or 14 to 15 carbons (C_{14-15}) and with eight propylene oxide units. The R-(PO)x-SO_4Na surfactants were 29.4 wt% active with 0.1 wt% Na_2SO_4, 2.5 wt% of free oil and 68 wt% water. These surfactants were donated by Sasol North American Inc (Lake Charles, LA).

The second class of extended surfactants evaluated is sodium linear-alkyl polypropoxylated polyethoxylated sulfate (R-(PO)y-(EO)z-SO_4Na) synthesized and donated by Huntsman Petrochemical Corp (Houston, TX) with 12 carbons in its hydrophobic tail (C_{12}), 14 propylene oxides and 2 ehtylene oxide groups. This surfactant consists of 24.1 wt% active, 1-2 wt% Na_2SO_4 and 74-75 wt% water. The surfactant structures and properties are summarized in Table 2.1 and Figure 2.1. The extended surfactants were used as received from the manufacturers. Sodium dioctyl sulfosuccinate (Aerosol-OT, anhydrous 99+) was purchased from Fisher Scientific and used as received.

The following oils were purchased from Sigma-Aldrich (Saint Louis) at the concentration shown and used without further purification: glyceryl trioleate (triolein-65%, practical grade), canola oil (commercial canola cooking oil), peanut oil (sigma), soya oil (fluka), corn oil (sigma), sunflower oil (sigma), palm oil (commercial palm cooking oil), decane (99%+, anhydrous), hexadecane (99%+, anhydrous), and sodium chloride (99%+).

Methods. Dynamic interfacial tension (IFT) is the measurement of the time-dependent interfacial tension using a spinning drop tensiometer (University of Texas, model 500). According to standard procedures (9,15,19) surfactant and sodium

chloride concentrations were prepared in the aqueous solution and used as the dense phase. The IFT measurements were commenced immediately after injecting 1-3 μL of the oil into a spinning drop tube containing the surfactant formulation. The interfacial tension values were obtained as a function of time. Unless stated otherwise, interfacial tension values are reported throughout this work for a ten minute reading. We have demonstrated that the dynamic IFT values reached equilibrium within 10 minutes. As an typical example, at the optimum salinity (0.13 M), the dynamic IFT values of C_{12}-$(PO)_{14}$-$(EO)_2$-SO_4Na at 10 minutes and 2 hours are 0.0017 mN/m and 0.0019 mN/m, respectively. Additionally, 10 minutes dynamic IFT is a sufficient representation time of cleaning applications (e.g. time scale of a washing cycle (19)).

Surface tension measurements on the surfactant solutions were performed with a Kruss K-10T tensiometer by Wilhelmy vertical plate technique at 30 ^oC. Surfactant solutions were equilibrated for 2 hrs before data collection.

Results and Discussion

*Salinity scans of dilute solutions***.** Figure 2.2 illustrates the use of electrolyte scans with dilute surfactant solutions (10 mM). In particular, Figure 2.2 presents the values of dynamic interfacial tension as a function of the electrolyte concentration for the systems triolein/C_{14-15}-$(PO)_8$-SO_4Na /brine, triolein/C_{12}-$(PO)_{14}$-$(EO)_2$-SO_4Na/brine, triolein/$C_{12,13}$-$(PO)_8$-SO_4Na/brine, and triolein/AOT/brine. The electrolyte concentration of 0.13M is the optimum salinity (S*) for the C_{14-15}-$(PO)_8$-

SO_4Na system and 0.21M is the optimum salinity (S*) for the $C_{12\text{-}13}$-$(PO)_8$-SO_4Na system. In both cases the interfacial tension reaches a minimum value close to 0.01 mN/m. Similarly for the C_{12}-$(PO)_{14}$-$(EO)_2$-SO_4Na system, a minimum interfacial tension value close to 0.001 mN/m is observed at 0.09 M sodium chloride. For the conventional surfactant AOT the interfacial tension remains above 1 mN/m for all values of electrolyte concentration.

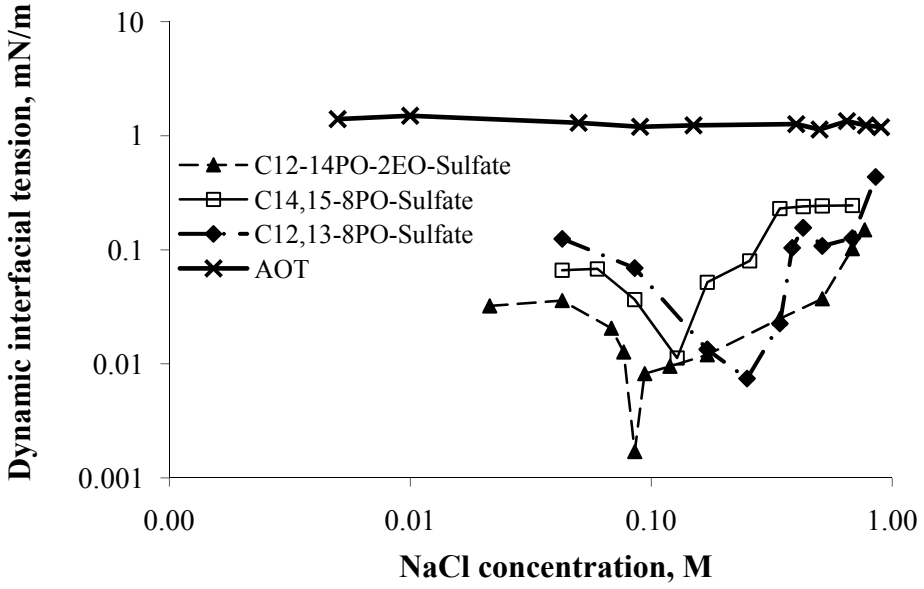

Figure 2.2. Dynamic interfacial tension as a function of electrolyte concentration (salinity scan) for the systems triolein – $C_{14\text{-}15}$-$(PO)_8$-SO_4Na – brine (squares), triolein – C_{12}-$(PO)_{14}$-$(EO)_2$-SO_4Na – brine (triangles), triolein – $C_{12\text{-}13}$-$(PO)_8$-SO_4Na (diamonds), and triolein – AOT - brine (cross), surfactant concentration 10 mM. All readings taken after 10 minutes contact.

To interpret these results, it is helpful to consider the different interactions in microemulsion systems. The Winsor R-ratio helps explain the interrelation between the different interactions (1,2):

$$R = \frac{A_{SO_{NET}}}{A_{SW_{NET}}} = \frac{A_{SO} - A_{OO} - A_{LL}}{A_{SW} - A_{WW} - A_{HH}} \qquad [2]$$

where $A_{SO\text{-}NET}$ is the net interaction between the surfactant and oil; $A_{SW\text{-}NET}$ is the net interaction between the surfactant and water; A_{SO} is the interaction between the surfactant and oil; A_{SW} is the interaction between the surfactant and water; A_{OO} is the interaction energy among oil molecules; A_{LL} is the interaction among the tails of the surfactant molecules; A_{WW} is the interaction energy among the water molecules; and A_{HH} is the interaction among the surfactant heads.

As mentioned in the introduction section, the optimum formulation is obtained when the net interactions $A_{SW\text{-}NET}$ and $A_{SO\text{-}NET}$ are equal (this results in R=1). Also, the solubilization increases and the interfacial tension decreases when each of these interactions is larger but equal. The addition of electrolyte in each of these formulations is used to suppress the double layer around the anionic group of the surfactant, thus reducing $A_{SW,}$ and $A_{SW\text{-}NET}$. A larger optimum electrolyte concentration suggests that the surfactant-oil interaction (A_{SO}) is small since more electrolyte is required to reduce A_{SW} to the A_{SO} value.

In the particular case of Figure 2.2, C_{12}-$(PO)_{14}$-$(EO)_2$-SO_4Na showed the lowest optimum salinity (and the thus largest A_{SO}). Since A_{SO} is largest (and thus the balanced A_{SW} is also largest) the co-solubilization of oil and water is expected to be

largest, and according to equation 1 the interfacial tension is expected to be the lowest. In fact, the interfacial tension at optimum formulation for this surfactant is close to one order of magnitude lower than the optimum values observed for the PO extended surfactants (0.0017 mN/m vs 0.0113 mN/m, respectively). The results suggest that additional PO and EO groups (14PO, 2EO vs 8PO) increase the interaction with triglyceride molecules, likely because these groups match the polarity of the glycerol ester groups of the triglyceride (triolein in this case). This hypothesis would also explain why conventional surfactants (such as AOT in Figure 2.2) are not capable of producing microemulsions or solutions with ultra low interfacial tensions for triglyceride oils.

When comparing the optimum electrolyte concentration for $C_{14\text{-}15}$-$(PO)_8$-SO_4Na and $C_{12\text{-}13}$-$(PO)_8$-SO_4Na (0.13 M vs 0.21 M, respectively), it is clear that when the tail length of the surfactant is smaller, the optimum salinity increases, suggesting that the interaction A_{SO} is smaller. The optimum interfacial tension for both systems is comparable which suggests that the changes of the net interactions are minor, and that factors such as A_{LL}, and A_{HH} should be considered.

One important point of consideration is that, according to Table 2.1, the surfactant C_{12}-$(PO)_{14}$-$(EO)_2$-SO_4Na has a slightly higher HLB value than $C_{14,15}$-$(PO)_8$-SO_4Na which would imply that this is a more hydrophilic surfactant. Yet, as discussed above, the lower optimum salinity for this surfactant (Figure 2.2) indicates that this surfactant is more hydrophobic (larger A_{SO}) than its alkyl-PO-sulfate counterpart. This shows that the HLB parameter alone does not completely capture

the nature of the interactions between extended surfactant and triglycerides, probably due to the slightly polar environment induced by the presence of the PO groups in the surfactant.

Surfactant concentration scans. In this set of experiments, the electrolyte concentration was fixed at the optimum salinity, and the dynamic IFT was measured against triolein as a function of surfactant concentration for 0.2 M NaCl concentration. Figure 2.3 shows the dynamic interfacial tension for the systems triolein/ $C_{14\text{-}15}$-$(PO)_8$-SO_4Na /brine, and triolein/ C_{12}-$(PO)_{14}$-$(EO)_2$-SO_4Na/ brine.

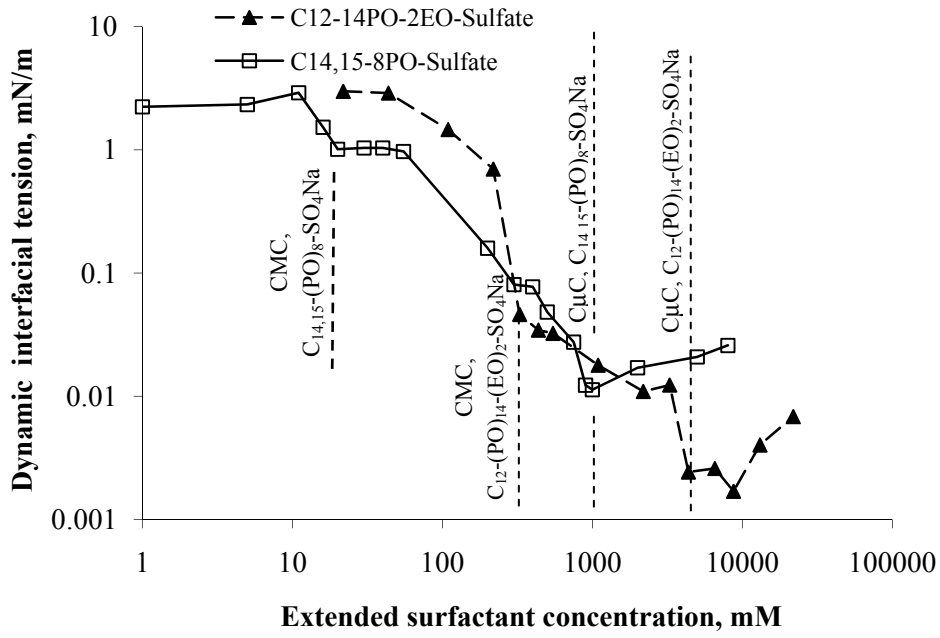

Figure 2.3. Dynamic surface tension versus surfactant concentration at optimum electrolyte concentration for the systems triolein/ $C_{14\text{-}15}$-$(PO)_8$-SO_4Na/ 0.2 M NaCl brine (squares) and triolein/ C_{12}-$(PO)_{14}$-$(EO)_2$-SO_4Na/ 0.015M brine (triangles). All readings after 10 minutes contact.

The trend of decreasing interfacial tension with the increase in surfactant concentration follows the trend previously observed in systems where equilibrium IFT values were measured (9,15). This decrease in interfacial tension follows two steps. The first step corresponds to the absorption of the surfactant at the oil/water interface, which occurs at concentrations less than the CMC. The second step corresponds to the change in curvature of the micelles which ends at the point where the first droplet of microemulsion forms (the CμC) (9). While an intermediate plateau typically separates the two steps, this is not completely obvious in the curves of Figure 2.3, potentially due to the dynamic nature of the experiment.

It should be noted that, at least to our knowledge, this is the first time that ultralow interfacial tension with triglycerides has been reported using surfactant concentrations in the range of 0.1 to 1.0 mM without the addition of co-oils and/or alcohol. This finding is of great significance for applications such as detergency and other cleaning processes where oil removal performance correlates with lower interfacial tensions (19).

The CμC value for $C_{14\text{-}15}$-$(PO)_8$-SO_4Na is close to 5 times smaller than the CμC of C_{12}-$(PO)_{14}$-$(EO)_2$-SO_4Na (1000 μM vs 4365 μM, respectively). While this suggests that $C_{14\text{-}15}$-$(PO)_8$-SO_4Na is a more efficient surfactant, a closer look at the data shows that the interfacial tension for C_{12}-$(PO)_{14}$-$(EO)_2$-SO_4Na is lower. As will be discussed later, the CμC obtained for these microemulsion systems correlates with the CMC of the pure surfactants.

One final observation related to Figure 2.3 is that there is a slight increase in the interfacial tension above the CμC. This is observed for both surfactants, and it seems to be correlated with the fact that gel phases were obtained instead of the middle phase microemulsions, which is consistent with previous observations (14). The physical explanation for this phenomenon is still unknown.

Formulation of ultralow interfacial tension systems with a range of oils. In the next set of experiments, salinity scans were conducted using the surfactants described above along with hydrophobic oils (decane, hexadecane) and a range of vegetable oils. Table 2.2 summarizes the optimum salinity and minimum interfacial tension obtained with these oils and the surfactant $C_{14\text{-}15}$-$(PO)_8$-SO_4Na. Table 2.3 summarizes the same set of data obtained with the surfactant C_{12}-$(PO)_{14}$-$(EO)_2$-SO_4Na. The optimum salinity presented in these tables gives an indication of how hydrophobic an oil phase is. This hydrophobicity can be expressed in terms of the equivalent alkane carbon number (EACN) as defined by Salager et al (21):

$$\ln(S^*) = K(EACN) + f(A) - \sigma + aT\Delta T \qquad [3]$$

where S* is the optimum salinity of microemulsion system, EACN is equivalent alkane carbon number of oil, f(A) is a function of alcohol type and concentration, σ is the surfactant characteristic, and T is the temperature effect. From Equation 3, the optimum salinity is a function of the equivalent alkane carbon number (EACN) of the oil. For hydrocarbons such as decane and hexadecane the EACN value corresponds to the alkyl chain length, 10 and 16 respectively.

Considering that for each surfactant the term $f(A) - \sigma + aT\Delta T$ is a constant we will call " b", equation 3 thus takes a linear form with respect to the logarithm of optimum salinity:

$$\ln(S^*) = K(EACN) + b \qquad [4]$$

This simplified formulation equation can be calibrated with two known values of optimum salinity and EACN. Using the optimum salinity values for decane and hexadecane (EACN values of 10 and 16 respectively) the resulting equations are as follows:

For $C_{14\text{-}15}$-$(PO)_8$-SO_4Na

$$\ln(S^*) = 0.053 \times EACN - 0.52 \qquad [5]$$

For C_{12}-$(PO)_{14}$-$(EO)_2$-SO_4Na

$$\ln(S^*) = 0.069 \times EACN - 3.1 \qquad [6]$$

One important observation from these equations is that the "*K*" values (0.053 and 0.069) are relatively small compared with the typical value of 0.17 for conventional anionic surfactants (1,2). In other words this means that, in microemulsion or ultralow IFT systems, extended surfactants are not as electrolyte sensitive as conventional anionic surfactants, probably due to the nonionic nature of the PO and EO groups that are next to the ionic head group. The EO and PO chains potentially arrange in the extended surfactants in such a way to allow the surfactant membrane to minimize the repulsion between the sulfate groups, which reduces their dependence on electrolyte in forming a low energy surfactant membrane.

Interestingly, the relatively invariable dynamic IFT value of the conventional surfactant AOT in Figure 2.2 seems to contradict the above explanation. In fact, the limited response of AOT to salinity reflects that AOT is ineffective and does not form microemulsions or ultralow IFT with these oils studied here.

Table 2.2. Summary of the optimum salinity (S*) and the optimum dynamic interfacial tension (IFT*) with various kinds of oils. The interfacial tension was measured after 10 minutes of contact using a spinning drop tensiometer at 0.2 wt% $C_{14\text{-}15}$-$(PO)_8$-SO_4Na.

Oil	**S* (M)**	**IFT* (mN/m)**	**EACN**
AOT			
Canola oil	1.60	1.2400	
$C_{14,15}H_{29,31}$-$(PO)_8$-SO_4Na			
Decane	1.00	0.0168	10
Hexadecane	1.40	0.0046	16
Triolein	0.2	0.011	-18[a]
Peanut oil	1.8	0.061	20[a]
Canola oil	2.0	0.020	22[a]

[a] Calculated using Equation 5

Table 2.3. Summary of the optimum salinity (S*), the optimum dynamic interfacial tension (IFT*) with various kinds of oils, The interfacial tension was measured after 10 minutes of contact using the spinning drop tensiometer at 0.2 wt% C_{12}-$(PO)_{14}$-$(EO)_2$-SO_4Na.

Oil	**S* (M)**	**IFT* (mN/m)**	**EACN**
Decane	0.088	0.021	10
Hexadecane	0.13	0.003	16
Triolein	0.015	0.0017	-16[a]
Soya oil	0.15	0.0048	18[a]
Corn oil	0.13	0.0015	16[a]
Canola oil	0.16	0.0013	18[a]
Sunflower oil	0.12	0.0052	14[a]
Peanut oil	0.15	0.0015	18[a]
Palm oil	0.12	0.0057	14[a]

[a] Calculated using Equation 6

Using equations 5 and 6, and the optimum salinity obtained through the electrolyte scans, the EACN values for each of the vegetable oils were calculated, as summarized in Tables 2.2 and 2.3. The most remarkable fact that comes out of these EACN values is that triolein has a highly negative EACN value whereas the vegetable oils have positive values. Although the EACN values for triolein, canola, and peanut oil were not exactly the same between the two surfactant systems, they were close enough to validate the relative magnitude of these values.

To explore the variation in EACN for triolein and the vegetable oils, three molecular structure parameters were considered: the average number of carbons in the saturated chains (ASC), the fraction of the unsaturated chains (UC), and the average number of double bonds of the unsaturated chains (DB). These values were calculated from typical composition data (23), and are summarized in Table 2.4.

To correlate these composition parameters to the calculated EACN values for these triglyceride molecules, the following linear regression was investigated (23):

$$EACN_{triglyceride} = c1*(ASC)+c2*(UC)+c3*DB+c4 \quad [7]$$

A sensitivity analysis revealed that the average number of double bonds (DB) had little impact on the EACN (an increment of 1 additional double bond changed the EACN value by less than 1%). The following simplified correlation was found (23):

$$EACN_{triglyceride} = 2.05*(ASC)+0.071*(UC)-24 \quad [8]$$

The R^2 correlation factor between the values calculated with Equation 8 and the values calculated using Equations 5 and 6 is 0.97. More importantly, Equation 8 reveals that there is a constant negative factor for triglycerides (c4 = -24) which could correspond to the polarity of the glycerol group. The positive value of "c1" indicates that the saturated hydrocarbon chains are the largest contributing factor to the hydrophobicity of triglycerides. On the other hand unsaturated chains do contribute to the hydrophocity of the triglyceride but not as much as their saturated counterparts.

Table 2.4. Selected composition parameters of vegetable oils and calculated EACN (23)

Oil	**Avg. length of saturated chain (ASC)**	**% Unsaturated chains (UC)**	**Avg. number of double bonds(DB)**	**EACN calculated** [a]
Triolein	N.A.	100	1	-17
Soya oil	16.5	85	1.7	16
Corn oil	16.3	87	1. 7	16
Canola oil	16.6	94	1.4	17
Sunflower oil	16.8	88	1.8	17
Peanut oil	19.5	82	1.4	22
Palm oil	16.1	50	1.2	13

[a] Calculated using Equation 8.

One last observation regarding the formulation of ultralow interfacial tension systems with vegetable oils is that the IFTs achieved with C_{12}-$(PO)_{14}$-$(EO)_2$-SO_4Na were close to one order of magnitude smaller than those obtained with $C_{14\text{-}15}$-$(PO)_8$-SO_4Na (see Figure 2.3 and Tables 2.2 and 2.3). Nonetheless the interfacial tension with decane and hexadecane were almost the same for both surfactants. This suggests that the interaction between extended surfactants and alkanes are driven by the alkyl groups while the interaction with triglycerides are driven by the PO and EO groups.

The EACN values for triolein in Tables 2.2, 2.3 and 2.4 should be qualified. As described in the Materials section, the triolein used in these measurements was a 65%, practical grade. The most likely explanation for the anomalous EACN values obtained for triolein in these experiments is that the sample contained significant levels of fatty acids and monoglycerides, which made it behave as though it were a much more polar oil. While beyond the scope of this research, this phenomenon will be further explored in future work.

Correlation between extended surfactant properties and performance. Because of the limited availability of extended surfactants, we are not able to systematically compare the effect of varying the number of EOs and POs for a constant alkyl chain length and PO groups of extended surfactants. However, Minana-Perez *et al* (11) reported that the presence of EO groups in extended surfactant structures was reported to give outstanding solubilization parameters (10-30 mL/g surfactant) and three-phase behavior with triglycerides such as soya oils. They also mentioned that extended surfactants consisting of both EO and PO groups in surfactant structure have a dual anionic and nonionic character, which was reflected in the lower K-value obtained for these surfactants (Equations 5 and 6). Because of the exciting potential of extended surfactants to lower the IFT of triglyceride, vegetable oils, highly hydrophobic oils such as hexadecane, it is valuable to characterize the interfacial properties of these extended surfactants, such as the critical micelle concentration (CMC) and the surface area per molecule of the surfactant (A_{min}). A_{min} and CMC values were measured from surface tension data

without added salt and with 0.2M NaCl, and at 30°C, as presented in Table 2.5. CMC values were determined as the intersection of two liner portions of surface tension (γ) versus log concentration (log C) diagram. The area per molecule (A_{min}, $Å^2$/molecule) is also determined from this same plot (24). Figure 2.4 shows the γ vs. log C for the three extended surfactants, $C_{14\text{-}15}$-$(PO)_8$-SO_4Na, $C_{12\text{-}13}$-$(PO)_8$-SO_4Na and C_{12}-$(PO)_{14}$-$(EO)_2$-SO_4Na.

Table 2.5. Critical micelle concentration (CMC) and area per molecule (A_{min}) of conventional and extended surfactants.

Surfactant	**No salt**		**0.2 M NaCl**	
	CMC (μM)	**A_{min} ($Å^2$)**	**CMC (μM)**	**A_{min} ($Å^2$)**
$C_{12}H_{25}SO_4Na$ (Varadaraj,1992)	7900	52.5	-	-
Branch $C_{12}H_{25}SO_4Na$ (Varadaraj,1992)	14200	95	-	-
$C_{14}H_{29}SO_4Na$ (Lange, 1968)	2100[a]	56[b]	-	-
$C_{12\text{-}13}H_{25\text{-}37}$-8PO-$SO_4Na$	130	153	14	68
$C_{14\text{-}15}H_{29\text{-}31}$-8PO-$SO_4Na$	33	133	5	116
$C_{12}H_{25}$-14PO-2EO-SO_4Na	80	200	8	147

[a] Lange,1968

[b] Huber,1991, Rosen,1996

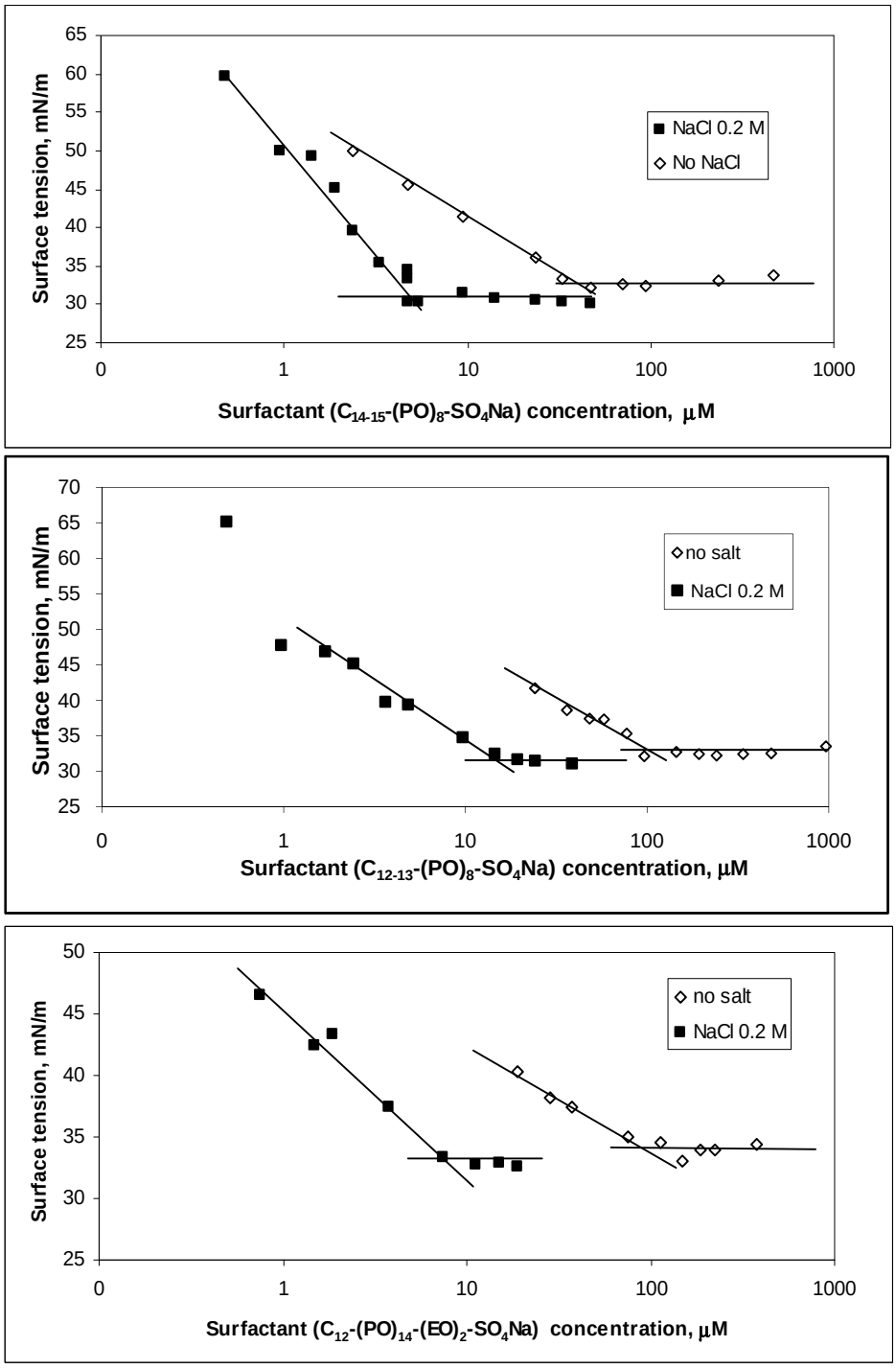

Figure 2.4. Surface tension of extended surfactants with and without salt, (a) C_{14-15}-$(PO)_8$-SO_4Na, (b) C_{12-13}-$(PO)_8$-SO_4Na and (c) C_{12}-$(PO)_{14}$-$(EO)_2$-SO_4Na.

According to Table 2.5, it is seen that all of the extended surfactants have CMC values much lower than conventional C_{12} and C_{14} surfactants (24,25). Furthermore, we observe a decrease in CMC of the extended surfactants as the alkyl chain length increses (130 μM for $C_{12\text{-}13}$-$(PO)_8$-SO_4Na and 33 μM for $C_{14\text{-}15}$-$(PO)_8$-SO_4Na); this four-fold decrease is similar in ratio to the decrease in conventional C_{12} to C_{14} surfactants in Table 5 (7900 to 2100 μM, respectively). We thus observe that the introduction of EO and/or PO groups has a significant effect on the CMC. Moreover, the lower CMC of $C_{14\text{-}15}$-$(PO)_8$-SO_4Na is consistent with the lower CμC observed for this surfactant. This is consistent with previous observations that the two phase transitions (monomer-micelle, and micelle-microemulsion) are correlated (9).

The data of Table 2.5 indicate that the extended surfactants have a large A_{min} as compared to conventional surfactants. Moreover, the presence of two EO groups in C_{12}-$(PO)_{14}$-$(EO)_2$-SO_4Na further increases A_{min} . Dahanayake *et. al.* (26) reported that the introduction of the second EO group does increase the A_{min}. This increase in surface area may create additional interfacial area were the polar glycerol groups can penetrate the palisade layer. In addition this larger surface area may help explain the shielding effect (lower K-values) provided by the PO and EO groups. Thus, adding POs and EOs can increase the area per molecule, but still achieves ultra low CMC values and ultra low interfacial tension values, suggesting that the increased hydrophobic interaction resulting from the extended tail helps offset the lower packing density.

Acknowledgements

The authors would like to thank George Smith, Huntsman Petrochemical Corp (Houston, TX) and Geoff Russell, Sasol North American Inc (Lake Charles, LA) for providing us the extended surfactant samples. Funding for this work has been provided through the United States Environmental Protection Agency Science to Achieve Results (STAR) program, through grant number Rd-83090301-0. Although the research described in this article has been funded by the United States Environmental Protection Agency, it has not been subjected to the Agency's required peer and policy review and therefore does not necessarily reflect the views of the Agency and no official endorsement should be inferred. Partial support was provided by industrial sponsors of the Institute for Applied Surfactant Research at University of Oklahoma.

References

1. Bourrel, M. and Schecter R. *Microemulsions and related systems*. Marcell Dekker Inc. New York, 1988
2. Salager, J. L.; Antón, R. E.; Sabatini, D.A.; Harwell, J., H.; Acosta, E. J.; Tolosa, L. I. Enhancing solubilization in microemulsions—state of the art and current trends. *J. Surfactant Detergents.* (2005), 8, 3-21.
3. Graciaa, A.; Lachaise, J.; Cucuphat, C.; Bourrel, M.; Salager, J. L. Improving solubilization in microemulsions with additives. 1. The lipophilic linker role. *Langmuir* (1993), 9(3), 669-72.

4. Graciaa, A.; Lachaise, J.; Cucuphat, C.; Bourrel, M.; Salager, J. L. Improving solubilization in microemulsions with additives. 2. Long chain alcohols as lipophilic linkers. *Langmuir* (1993), 9(12), 3371-4.
5. Uchiyama, H.; Acosta, E.; Tran, S.; Sabatini, D. A.; Harwell, J. H. Supersolubilization in chlorinated hydrocarbon microemulsions: solubilization enhancement by lipophilic and hydrophilic linkers. *Ind. Eng. Chem. Res.* (2000), 39(8), 2704-2708.
6. Acosta, E.; Uchiyama, H.; Sabatini, David A.; Harwell, J. H. The role of hydrophilic linkers. *J. Surfactant Detergents* (2002), 5(2), 151-157.
7. Sabatini, D.A, Acosta, E.J., Harwell, J.H. Linker molecules in surfactant mixtures. *J. Colloid Interface Sci.* (2003), 8, 316-326.
8. Acosta, E.; Tran, S; Uchiyama, H; Sabatini, D. A.; Harwell, J. H. Formulating chlorinated hydrocarbon microemulsions using linker molecules. *Environ. Sci. Technol*. (2002), 36(21), 4618-4624.
9. Acosta, E. J.; Harwell, J. H.; Sabatini, D. A. Self-assembly in linker-modified microemulsions. *J. Colloid Interface Sci.* (2004), 274(2), 652-664.
10. Miñana-Pérez, M.; Graciaa, A.; Lachaise, J.; Salager, J. L. Solubilization of polar oils in microemulsion systems. *Prog. Colloid Polym. Sci.* (1995), 98, 177-179.
11. Miñana-Pérez, M.; Antón, R. E.; Graciaa, A.; Lachaise, J.; Salager, J. L. Solubilization of polar oils with extended surfactants. *Colloid Surfaces A*. (1995), 100, 217-224.

12. Scorzza, C.; Godé, P.; Martin, P.; Miñana-Pérez, M.; Salager, J. L.; Villa, P. Synthesis and surfactant properties of a new "extended" glucidoamphiphile made from d-glucose. *J. Surfactant Detergents*. (2002), 5: 331.
13. Scorzza, C.; Godé ,P.; Goethals, G.; Martin, P.; Miñana-Pérez, M.; Salager, J. L.; Usubillaga, A.; Villa, P. Another new familly of "extended" glucidoamphiphiles. synthesis and surfactant properties for different sugar head groups and spacer arm lengths. *J. Surfactant Detergents*. (2002), 5, 337.
14. Huang, L.; Lips, A.; Co, C. Microemulsification of triglyceride sebum and the role of interfacial structure on bicontinuous phase behavior. *Langmuir*. 2004; 20(9), 3559 – 3563.
15. Childs J., Acosta E., Scamehorn J. F and Sabatini D. A, Surfactant-enhanced treatment of oil-based drill cuttings. *J. Energy Res. Technol.* 2005; 127, 153-162.
16. Yanatatsaneejit, U., Rangsunvigit, P., Scamehorn, J.F., Chavadej, S. Diesel removal by froth flotation under low interfacial tension conditions I: foam characteristics, coalescence time, and equilibration time. Submitted to Sep. Sci. Tech.
17. Christov, N. C.; Denkov, N. D.; Kralchevsky, P. A.; Broze, G.; Mehreteab A. Kinetics of triglyceride solubilization by micellar solutions of nonionic surfactant and triblock copolymer1. empty and swollen micelles. *Langmuir.* (2002), 18, 7880-7886.
18. Huh, C. Interfacial tensions and solubilizing ability of a microemulsion phase that coexists with oil and brine. *J. Colloid Interface Sci.* (1979), 71(2), 408-26.

19. Tongcumpou, C.; Acosta, E. J.; Quencer, L. B.; Joseph, A. F.; Scamehorn, J. F.; Sabatini, D. A.; Chavadej, S.; Yanumet, N. Microemulsion formation and detergency with oily soils: ii. detergency formulation and performance. *J. Surfactant Detergents* (2003), 6(3), 205-214.
20. Aveyard, R.; Binks, B. P.; Fletcher, P. D. I. Interfacial tensions and aggregate structure in pentaethylene glycol monododecyl ether/oil/water microemulsion systems. *Langmuir* 1989**,** 5, 1210.
21. Salager, J. L.; Morgan, J.; Schechter, R. S.; Wade, W. H.; Vasquez E. Optimum formulation of surfactant-oil-water systems for minimum tension and phase behavior. *Soc. Petrol. Eng. J.* (1979), 19, 107-115.
22. Salager, J. L.; Márquez, N.; Graciaa, A.; Lachaise, J. Partitioning of ethoxylated octylphenol surfactants in microemulsion-oil-water systems: influence of temperature and relation between partitioning coefficient and physicochemical formulation. *Langmuir*. (2000), 16, 5534-5539
23. Campbell, E. *et al* Editors, *Food fats and oils*. the Institute of Shortening and Edible Oils. Washington DC, 1999, P. 27.
24. Rosen, Milton J. *Surfactants and Interfacial Phenomena*. 2nd Ed. John Wiley & Sons, New York, 1989
25. Lange, H.and Schwuger, M.J. Micelle formation and Kraft-points in a homologous series of sodium-N-Alkyl sulfates including ODD-numbered members. *Kolloid Z.Z. Polym.*, 1968, 223, 145.

26. Dahanayake, M., Cohen, A. W., Rosen, M.J., Relationship of Structure to Properties of Surfactants 13 Surface and Thermodynamic Properties of Some Oxyethylenated Sulfates and Sulfonates, J. Phys. Chem., 1986, 90, 2413-2418.

CHAPTER 3

Hydrophilic-Lipophilic Deviation (HLD) Method For Characterizing Conventional And Extended Surfactants[£]

Abstract

An accurate determination of the hydrophilic-lipophilic nature of surfactants plays an essential role in guiding the formulation of microemulsion with the goal of achieving low interfacial tension (IFT) and high solubilization. While several empirical models have been proposed as simple tools for predicting surfactant characteristics and microemulsion conditions, only a few of these models are fundamentally-based yet convenient to use. In this work, the hydrophilic-lipophilic deviation (HLD) approach was used with mixed surfactant systems to determine the surfactant characteristic (σ) and $\frac{\sigma}{K}$ parameters of conventional and extended surfactants. To our knowledge, this is the first time that the HLD index has been used to represent the hydrophilic-lipophilic behavior of extended surfactants. It was observed that inserting PO and/or EO groups in extended surfactants play a key role in altering σ values and $\frac{\sigma}{K}$ values. Finally, the σ parameters found in this work were

[£] This chapter or portions thereof has been published previously in Journal of Colloid and Interface Science under title of "Hydrophilic-Lipophilic Deviation (HLD) Method for Characterizing Conventional and Extended Surfactants", Journal of Colloid and Interface Science, 2008, 325, p. 259 – 266. This current version has been formatted for this dissertation.

combined with the HLD equation and used to demonstrate its practical utility for guiding the optimum formulation (in this case, optimum salinity) for a microemulsion system.

Key words: microemulsions, hydrophilic-lipophilic balance, extended surfactants, hydrophilic-lipophilic deviation (HLD)

Introduction

Microemulsion formation has proven to be an effective approach in enhancing oil solubilization and reducing the oil-water interfacial tension (IFT) in many industrial applications. Examples include enhanced-subsurface remediation [1, 2] drug delivery [3-5] and detergency [6-9]. Forming an efficient microemulsion system requires an equal balance between surfactant-oil and surfactant-water interactions, which has proven to be a very challenging task for certain types of oils (e.g. hydrophobic oils and vegetable oils) [10-12]. In addition, different applications require specific degrees of solubilization and IFT reduction. It is no surprise, then, that formulating microemulsions for spcecific industrial use has been referred to by researchers as both an art and science [13]. This is because microemulsion design requires not only a great understanding of molecular interactions, but also a deep understanding of thermodynamic principles [14].

To date, information on microemulsions and related systems is mostly based on experimental phase behavior studies. While this process is a critical step in

determining the type and interfacial properties of microemulsion formulations, it is tedious and time-consuming work. As a consequence, several researchers have proposed empirical correlations as quick and convenient tools for predicting microemulsion conditions and properties. Excellent examples of these correlations are the Winsor R-ratio [14. 15], the hydrophilic-lipophilic balance (HLB) [16-18], the phase inversion temperature (PIT) [19], the hydrophilic-lipophilic deviation (HLD) [20, 21], and the net-average curvature model [22]. It is important to clarify that although both HLB and PIT approaches were originally developed for achieving stable macroemulsions, the direct relationship between the macroemulsion stability at optimum HLB or PIT and the optimum middle phase microemulsion has been clearly demonstrated in the literature [13, 14, 23]. With this relevant connection, the HLB and PIT techniques have been used to guide formulation of optimum microemulsion systems.

Although most empirical correlations show an encouraging agreement with the experimental data, the practical utility of these empirical approaches is still limited. This is due to the fact that fundamentally-established correlations like the Winsor R-ratio and the net-average curvature model are complex equations which require quantification of multiple parameters, while the simple and easy-to-use expressions exhibit several significant limitations. For example, the frequently used HLB method has demonstrated poor accuracy for predicting hydrophilic-lipophilic balance (HLB value) of some surfactant classes [18, 24]. Moreover, the HLB number does not account the impact of formulation variables on surfactant behavior

(i.e. surfactant structure and concentration, temperature, salinity, and the presence of alcohols or co-surfactants etc.). Furthermore, the HLB number neither indicates the relative efficiency nor effectiveness of emulsion systems [25]. However, due to its convenience, the HLB technique is still widely used for estimating the hydrophilic-lipophilic characteristic of surfactants and oils as well as guiding surfactant selection for emulsion [16-18] and microemulsion systems [13, 14, 23].

Salager *et. al.* [20, 24] proposed an empirical correlation known as the hydrophilic-lipophilic deviation (HLD) as a dimensionless form of the thermodynamically-derived surfactant affinity difference (SAD) equation to describe microemulsion systems. Similar to the Winsor R-ratio, the HLD value measures the departure from the optimum formulation, but the parameters are easier to quantify. Negative, zero, or positive HLD values suggest the formation of Winsor Type I, Type III or Type II microemulsions, respectively. Separate HLD equations were developed for anionic surfactants and nonionic surfactants. Since all surfactants used in the present work are anionic surfactants, the HLD equation for anionic surfactants will be reviewed in more detail here. Thus the overall goal of this work is to show the utility of the HLD approach and σ parameter for characterizing extended surfactants.

HLD concept

The general HLD equation for an anionic surfactant is described as follows [20, 24]:

$$\mathrm{HLD} = \ln \mathrm{S} - K(\mathrm{EACN}) - f(\mathrm{A}) + \sigma - a_T(\Delta \mathrm{T}) \qquad (1)$$

where S is the salinity in wt% NaCl (based on the aqueous phase), K is an empirical constant depending on the type of surfactant head group, EACN is the equivalent alkane carbon number, which is analogous to the ACN (alkane carbon number) and indicates the hydrophobicity of the oil phase, $f(A)$ is a function of the alcohol type and concentration, σ is a surfactant characteristic parameter, a_T is the empirical temperature constant related to the type of microemulsion system, and ΔT is the temperature difference measured from the reference temperature ($T_{ref} = 25\ ^oC$).

When using anionic surfactants, the optimum condition can be obtained by varying the NaCl concentration. Therefore, the optimum condition is also known as the optimum salinity or S*. At the optimum condition, the surfactant system interacts equally with the oil and water phases and thus has the greatest affinity to accumulate at the oil-water interface, resulting in formation of middle phase microemulsion with the minimum IFT and maximum oil solubilization. At this optimum salinity (S = S*), the HLD value equals zero since there is no deviation between the hydrophilic and lipophilic interaction energies. If the microemulsion is formed without the addition of alcohols ($f(A) = 0$) and at the reference temperature ($T = T_{ref} = 25\ ^oC$), the general HLD equation listed in Equation (1) can be simplified as shown below:

For a single anionic surfactant system:

$$\ln S^* = K(\text{EACN}) - \sigma \tag{2}$$

For mixtures of anionic surfactants:

$$\ln S^*_{mix} = K_{mix}(\text{EACN}) - \sigma_{mix} \tag{3}$$

We can estimate parameters in Equation 3 using the following linear mixing rules [21], where *i* refers to the individual components in the mixture and the x_i represents the mole fraction of surfactant i in the surfactant combination.

$$\ln S^*_{mix} = \sum x_i \ln S_i^* \tag{4}$$

$$\sigma_{mix} = \sum x_i \sigma_i \tag{5}$$

$$K_{mix} = \sum x_i K_i \tag{6}$$

The HLD equation for a mixture of two anionic surfactant systems at the optimum salinity with no addition of alcohol ($T = T_{ref} = 25\ ^oC$) nd $x_2 = 1\text{-}x_1$gives us:

$$\ln S^*_{mix} = \{[K_1(EACN)] - \sigma_1\} + \{(K_2 - K_1)(EACN) + (\sigma_1 - \sigma_2)\}x_2 \tag{7}$$

Then if the EACN of the oil used to scan the mixture of anionic surfactants is the same as the one used to determine the optimum salinity of surfactant 1 (S^*_1), Equation 7 can further be simplified as follows:

$$\ln S^*_{mix} = \ln S^*_1 + \{(K_2 - K_1)(EACN) + (\sigma_1 - \sigma_2)\}x_2 \tag{8}$$

Upon inspection we observe that Equation 8 is a linear equation when plotting the $\ln S^*_{mix}$ as a function of x_2. The slope and intercept of Equation 8 are as follows:

$$\text{Intercept} = \ln S^*_1 = \{[K_1(EACN)] - \sigma_1\} \tag{9}$$

$$\text{Slope} = \{(K_2 - K_1)(EACN) + (\sigma_1 - \sigma_2)\} \tag{10}$$

It is worth noting that, all the parameters of the HLD equation are easily and practically quantifiable. Since a majority of the HLD constants, alcohol and temperature functions (e.g. K, $f(A)$, and a_T) have already been established by Salager and his co-workers [23, 24, 26], the HLD expression is relatively easy to use and is more effective than the HLB method [23] for microemulsion formulation.

An interesting parameter in the HLD equation is the surfactant characteristic parameter (σ). Based on the literature [20], this σ parameter and its corollary of $\frac{\sigma}{K}$ value was determined from the extrapolation of an alcohol-free microemulsion system with a wide range of oils at the unit salinity (S = 1). The extrapolated $\frac{\sigma}{K}$ value indicates the preferred oil ACN (the optimum oil) that produces the minimum IFT with the evaluated surfactant system. This ACN value was later referred as the Extrapolated Preferred Alkane Carbon Number at Unity Salinity (EPACNUS) or N_{min} [20, 21, 24]. For comparison propose, this $\frac{\sigma}{K}$ ratio was proposed to be a better indicator than the σ itself in providing a relatively hydrophilic-lipophilic characteristic of surfactant molecule since it also takes into account the hydrophilic nature of surfactant (K constant) [24]. In spite its stated potential [24] in capturing the amphiphilic nature of surfactants, somewhat similar to the HLB number, the use of σ and $\frac{\sigma}{K}$ indicators as alternative surfactant characteristic parameters has yet to be fully explored due to limited database of the σ parameter.

During recent years numerous studies have evaluated a new class of surfactants called extended surfactants. By definition, extended surfactants contain intermediate polarity molecules, such as polyethylene and/or polypropylene oxide groups (EOs and POs, respectively), which are inserted between the hydrocarbon tail and hydrophilic head. Because of their unique structure, extended surfactants will extend the length of the surfactant tail further into the oil phase without losing water solubility, thereby providing a smoother transition between oil and water phases [13]. Extended surfactants have not only demonstrated their ability to provide ultra low IFT systems for cleaning applications [12, 28, 29], but also significantly improve the solubilization of bulky oil molecules, especially triglycerides and vegetable oils, in microemulsion systems [10, 13]. The enhanced triglyceride solubilization and IFT reduction of extended surfactants shows promise for use in a wide range of applications (i.e. aqueous-based solvent extraction, drug delivery vehicles, bioremediation, etc.) and has been a strong driving force for studying both fundamental properties and applications of extended surfactant-based microemulsions.

However, because extended surfactants are relatively new, information on their fundamental properties, such as hydrophilicity/lipophilicity, is currently unavailable. In our previous study [12], we mentioned the shortcomings of the HLB number to capture hydrophilic-lipophilic characteristic of extended surfactants due to the polar environment induced by the presence of the inserted PO and EO groups. The optimum salinity for a given oil system was another indicator used for judging

the hydrophilic-lipophilic nature of different extended surfactant structures. But since the optimum salinity is a function of the oil, it is difficult to utilize it as a fine-tuning parameter when different extended surfactants are present in the various oil environments.

Therefore, in this work, we propose to evaluate the σ and $\frac{\sigma}{K}$ parameters from the HLD equation as alternative indicators for comparing the hydrophilic-lipophilic nature of conventional and extended surfactants. Surfactants with similar tails but with and without the addition of PO and/or EO groups (extended and conventional surfactant, respectively) are systematically studied to provide insight into the role of PO and EO groups on the hydrophilic-lipophilic nature of surfactants. Then the utility of the σ and/or $\frac{\sigma}{K}$ value as a surfactant characteristic is examined and compared to the HLB number. Finally, we conclude our study with an experimental demonstration of the practical benefit of the σ parameter when combined with the HLD equation for guiding the optimum formulation of microemulsion systems.

Materials and methods

3.1 Materials.

Surfactants evaluated in this work can be categorized into three groups; conventional surfactants, conventional surfactants with a small number of polyethoxylated groups (EOs), and extended surfactants. In the first group, the three

conventional anionic surfactants studied were dihexyl sulfosuccinate, sodium salt (tradename Aerosol-MA or AMA, 80% in water), bis(2-ethylhexyl) sulfosuccinate, sodium salt (Aerosol-OT or AOT, 99%+ anhydrous), and sodium dodecyl sulfate (SDS). Both AMA and AOT surfactants were purchased from Fisher Scientific and used as received, while SDS was obtained from Sigma-Aldrich with 97% active and was subsequently purified to remove some impurities by recrystallization with water and ethanol before being used [30].

The second surfactant category is a conventional surfactant containing a small number of EO groups, i.e., an alkyl ether sulfate ($R\text{-}(EO)_n\text{-}SO_4Na$). Despite containing the addition of EO groups, the alkyl ether sulfate is not classified as an extended surfactant because a small number of EO groups does not significantly affect the total length of the surfactant molecule but rather serves to improve the salinity and hardness tolerance as well as reduce the Krafft temperature. The alkyl ether sulfate surfactant used in this work is a C12 to C15 alkyl with the addition of 2 EO groups connected to a sodium sulfate hydrophilic head ($C_{12\text{-}15}\text{-}(EO)_2\text{-}SO_4Na$). This surfactant is also known under the trade name of Steol 230 and was purchased from Stepan Company as 25.5 % active.

The last group of surfactants evaluated in this study, extended surfactants, contain EO and PO groups inserted between the surfactant head and hydrocarbon tail, thereby extending the total length of surfactant molecule further into both oil and water phases. Two types of extended surfactants were tested in this work:

extended surfactants containing PO groups alone (R-$(PO)_x$-SO_4Na) and extended surfactants containing both EO and PO groups (R-$(PO)_y$-$(EO)_2$-SO_4Na).

The extended surfactant studied containing only PO groups was a sodium alkyl polypropylene oxide sulfate (R-$(PO)_x$-SO_4Na) with a branched 12 to 13 carbons ($C_{12,13}$) and with various numbers of propylene oxide groups (POs). These R-$(PO)_x$-SO_4Na surfactants were provided by Sasol North American Inc. (Lake Charles, LA). The other type of extended surfactant studied is a sodium linear-alkyl polypropoxylated polyethoxylated sulfate (R-$(PO)_Z$-$(EO)_2$-SO_4Na). The R-$(PO)_y$-$(EO)_2$-SO_4Na is composed of a 12 carbon chain with different degrees of propylene oxide and two ethylene oxide groups. These extended surfactants were synthesized and donated by Huntsman Petrochemical Corp (Houston, TX). All extended surfactants were used without further purification. The two types of extended surfactant structures are illustrated in Figure 3.1.

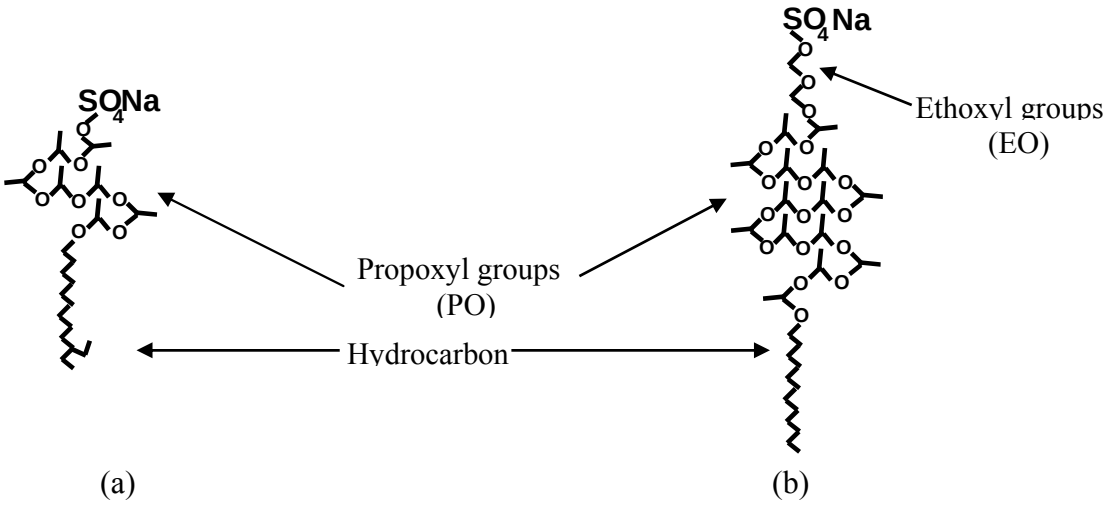

Figure 3.1. Structure of extended surfactants, (a) R-$(PO)_x$-SO_4Na, (b) R-$(PO)_y$-$(EO)_2$-SO_4Na, adapted from reference [12].

Six oils were studied in this research. The oils were purchased from Sigma-Aldrich (Saint Louis, MO) at the concentration shown and used without further purification: benzene (99.8%, anhydrous), pentane (97%+), heptane (99%, anhydrous), octane (99%+, anhydrous), decane (99%+, anhydropus), and (R)-(+) limonene (97%, 98%, ee(GLC)). Sodium chloride (99%+) was also purchased from Sigma-Aldrich.

3.2 Microemulsion phase study

Microemulsion phase studies were performed in flat-bottom test tubes with Teflon-lined screw caps. While holding surfactant concentrations, temperature, and pressure constant, equal volumes of oil and water (5mL) were added into the vial with different concentrations of NaCl (salinity scan). All test tubes were subsequently placed in a temperature-controlled water-bath at 25 ^{o}C, shaken once a day for 3 days and left to equilibrate for at least ten days. After the systems reached equilibrium, the relative phase heights and interfacial tension (IFT) values were quantified in each system to determine the optimum condition (in this case, the salinity producing the lowest IFT and highest volume of middle phase is known as the optimum salinity (S*) for the system.

3.3 Equilibrium interfacial tension (IFT) measurment

Equilibrium interfacial tension (IFT) was measured using samples of pre-equilibrated microemulsion phases in a spinning drop tensiometer (University of Texas, model 500). The excess water phase of the microemulsion, used as the dense

phase, was added into the spinning drop tube, and then 1-3 μL of the excess oil phase was subsequently added into the same tube.

Results and Discussion

Determining the K constant and σ parameter using a single anionic surfactant. According to the HLD concept, *K* and σ are key parameters for determining the hydrophilic-lipophilic nature of surfactants. While the *K* parameter depends on the hydrophilicity of a surfactant head group, the σ value correlates with the hydrophobicity of the surfactant tail. In this section, we illustrate a simple technique to establish these parameters (*K* and σ) from the HLD equation using a single anionic surfactant system. Later in the section, the limitation of using a single anionic surfactant system for extended surfactants will be demonstrated and the HLD concept will be extended to a mixed surfactant system. Thus, the goals of this section are (1) to establish *K* and σ values for AMA, (2) to demonstrate that such single surfactant systems do not work for extended surfactants and these oils, setting the search for multi-surfactant systems discussed in the next section.

To obtain accurate *K* and σ values of a single surfactant system, the surfactant should first form a microemulsion with a broad range of oils. A twin-tail sodium dihexyl sulfosucsinate surfactant (AMA) was selected in this work based on its ability to form middle phase microemulsions with a wide range of oils without the addition of additives and at ambient temperature. A typical microemulsion phase transition (Winsor Type I to III to II microemulsions) was observed by increasing

NaCl concentrations. The optimum salinity (S*) of each AMA-oil system was determined by measuring the phase volume and the minimum interfacial tension (IFT*). The S* and IFT* values of several AMA-oil systems are listed in Table 3.1. In keeping with Equation 2, ln S* was plotted as a function of the oil hydrophobicity as represented by the alkane carbon number (ACN) (see Figure 3.2).

Table 3.1. Summary of the optimum salinity (S*) and the minimum equilibrium interfacial tension (IFT*) of the 0.07 M sodium dihexyl sulfosuccinate (AMA) with a wide range of oils.

Oil	S* (wt%)	IFT* (mN/m)	EACN
Benzene	2.5	0.292	0
Pentane	6.8	0.0450	5
Heptane	8.0	0.0593	7
Octane	9.0	0.0803	8
Decane	15.5	0.273	10
Limonene	6.8	0.0538	5.7[a]

[a] calculated using Equation 8 at optimum salinity (S*)

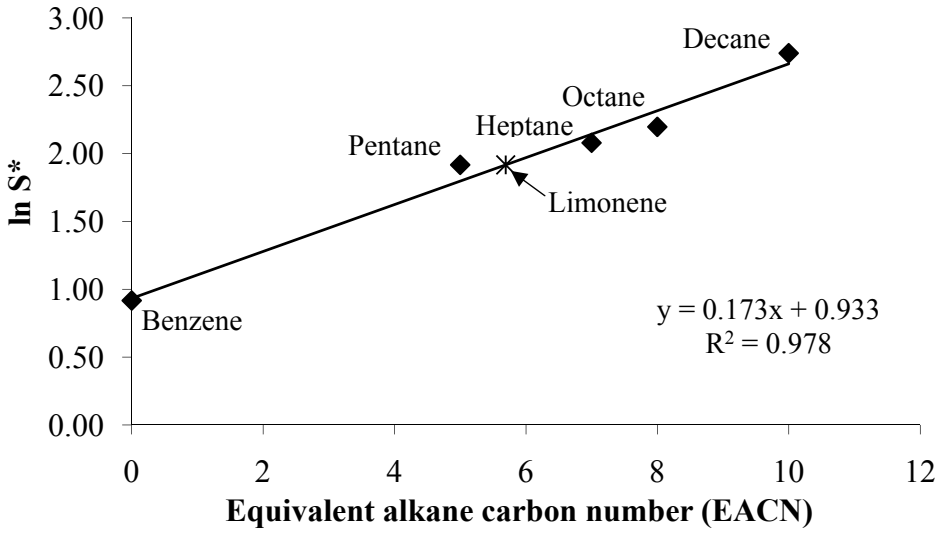

Figure 3.2. Determine the K_{AMA} , σ_{AMA}, and EACN of limonene using a HLD equation of an anionic surfactant (0.07 M AMA surfactant) at the optimum salinity (see Table 3.1), 25 ^{o}C and no additives.

In Figure 3.2 and Table 3.1, we observe an increase in the optimum salinity with increasing oil hydrophobicity. To interpret this result, we refer to the well-known Winsor R-ratio [13, 14]. The Winsor R-ratio correlates interactions between oil, surfactant, and water molecules using the following equation:

$$R = \frac{A_{SO_{NET}}}{A_{SW_{NET}}} = \frac{A_{SO} - A_{OO} - A_{LL}}{A_{SW} - A_{WW} - A_{HH}} \tag{11}$$

where $A_{SO\text{-}NET}$ is the net interaction between the surfactant and oil; $A_{SW\text{-}NET}$ is the net interaction between the surfactant and water; A_{SO} is the interaction between the surfactant and oil; A_{SW} is the interaction between the surfactant and water; A_{OO} is the interaction energy among oil molecules; A_{LL} is the interaction among the tails of the

surfactant molecules; A_{WW} is the interaction energy among the water molecules; and A_{HH} is the interaction among the surfactant heads.

The optimum salinity is obtained when the system has an equal balance between the $A_{SO\text{-}NET}$ and $A_{SW\text{-}NET}$ (resulting in R = 1). The addition of electrolyte helps to reduce the repulsive force between anionic head groups, thereby lowering the A_{SW} and $A_{SW\text{-}NET}$. A larger optimum salinity for high EACN oils indicates a larger oil-oil interaction (A_{OO}). Large oil molecules interact more strongly with each other, forcing out the surfactant tail, as a result, a smaller net interaction between surfactant-oil molecule ($A_{SO\text{-}NET}$). Therefore, more electrolyte is required to reduce the $A_{SW\text{-}NET}$ value in keeping with the lower $A_{SO\text{-}NET}$ value.

By applying a linear regression model to the experimental data plotted in Figure 3.2, the slope and intercept of this plot are as follows:

$$\ln S^{*} = 0.173 * (ACN) + 0.933 \tag{12}$$

In comparison to the original HLD equation (Equation 2), the slope and intercept of equation 12 are by definition the *K* and σ values of the AMA surfactant; 0.17 ± 0.02 and -0.93 ± 0.10, respectively. The *K* constant and σ value determined for AMA here are consistent with the values reported in the literatures for this anionic surfactant [21, 23, 27]. For example, Acosta *et. al.* [27] reported a *K* value of 0.16 for alkyl sulfosuccinate surfactants. Once the *K* and σ values of AMA surfactant have been established, Equation 12 can now be utilized for evaluating the hydrophobicity of non-alkane oils. Analogous to the ACN number, the equivalent alkane carbon number or EACN represents the hydrophobicity of non-alkane oils.

For instance, Table 3.1 shows the EACN of limonene determined in this manner. The result shows that the EACN of limonene is 5.7, which suggests that limonene should behave similar to hexane, (alkane oil having an ACN value of 6). This can be observed from Figure 3.2 where the ln S* value of limonene is shown with its corresponding EACN value of 5.7.

This example illustrates a simple and ideal scenario of determining the *K* constant and σ value of a single anionic surfactant system. However, the process is not so simple for some conventional anionic surfactants and particularly extended surfactants. In the case of conventional anionic surfactants, a majority of them are unable to form microemulsion without additives and at ambient temperature since they are susceptible to the precipitation or phase separation before middle phase microemulsion occurs. Extended surfactants often produce gel, liquid crystal or stable macroemulsion phases in the region where they would form microemulsions. The formation of these phases are undesirable and normally require prolonged times to equilibrate [12]. This makes it difficult to evaluate the *K* and σ value of extended surfactants using the single surfactant approach presented above. Another concern regarding the use of the anionic surfactant HLD equation for extended surfactants is that extended surfactants exhibit dual anionic-nonionic characteristic [10].

Hence, we propose a strategy of using the surfactant mixture system (the combination of a conventional anionic surfactant (AMA) and the extended surfactant) as an alternative approach to assessing the *K* and σ value of both conventional and extended surfactants. The mixed surfactant system not only allows

us realization of the middle phase microemulsions without undesirable phases in a reasonable time frame (the goal of the next section), but also provides an adequate utilization of the HLD equation of anionic surfactants. In addition, it must be noted that impurities such as free oil content (unsulfated propoxylated alcohol) present in extended surfactants could affect the σ value established in this work. To increase confidence in the σ-value, a high purity grade of extended surfactants is needed, which is not currently available.

Determining the K constant and σ parameter using a mixed anionic surfactant Salager *et.al.* [21] present results validating the linear mixing rule for establishing the optimum salinity and HLD parameters through the use of many mixed anionic surfactant systems. As a consequence, the original HLD equation can reasonably be expanded to a mixture of anionic surfactants system using a linear mixing rule. The idea of this section is to formulate microemulsion with limonene oil using a mixture of two anionic surfactants at different mixture ratios. The optimum salinity obtained from the microemulsion phase study yields the slope of the modified HLD equation (first shown earlier; repeated below for convenience):

$$\text{Slope} = \{(K_2 - K_1)(EACN) + (\sigma_1 - \sigma_2)\} \tag{10}$$

where *K* is a constant of the HLD equation reflecting the hydrophilic head, and σ is the hydrophobic characteristic of the surfactant tail. The subscript 1 and 2 indicate surfactant component 1 and 2 in a mixture, respectively. Limonene was studied oil in this work instead of hexane (by definition having ACN of 6) due to the low volatility of limonene. Additionally, the EACN of limonene determined in this work

(5.7) is consistent with the values reported by other researchers (ranging from EACN of 5.6 to 5.9) [27].

By substituting the EACN of the studied oil, Equation 10 has four remaining parameters (K_1, K_2, σ_1, and σ_2). If one of the surfactant in the mixture has knwon K constant and σ values, and if the K constant of the second surfactant is known (K_2), the σ value of the second surfactant (σ_2)can be calculated using the given slope and Equation 10. A positive slope gives a negative σ parameter and vice versa. The more negative σ values suggest the more hydrophilic surfactant and the tendency of forming normal micelles in an equilibrium with an excess oil phase (O/W microemulsions), while the more positive σ values imply the more hydrophobic surfactant and the formation of reverse micelles in equilibrium with an excess water phase (W/O microemulsions). Future research should further evaluate the relationship between σ and micelle type/size.

To illustrate this approach, we evaluated a mixture of AMA and sodium dodecyl sulfate (SDS) with limonene. Figure 3.3 shows the plot between ln S* and SDS mole fraction (x_{SDS}), yielding the slope of Equation 10 for a mixed AMA-SDS system (1.132). K_{AMA} and σ_{AMA} values were determined previously in this work to be 0.17 and -0.93, respectively. The K_{SDS} constant for an alkyl sulfate surfactant has been reported as 0.1 by Salager and his group [21, 23] and summarized in Table 3.2. The K constants of all surfactants listed in Table 3.2 were either determined in this work or reported from the literatures [20, 21, 23, 24]. The EACN of limonene is 5.7, as reported above. Thus, by using Equation 10, the σ_{SDS} is the only remaining

unknown and the σ and corresponding $\frac{\sigma}{K}$ values are calculated to be -2.46 ± 0.35 and -24.6 respectively.

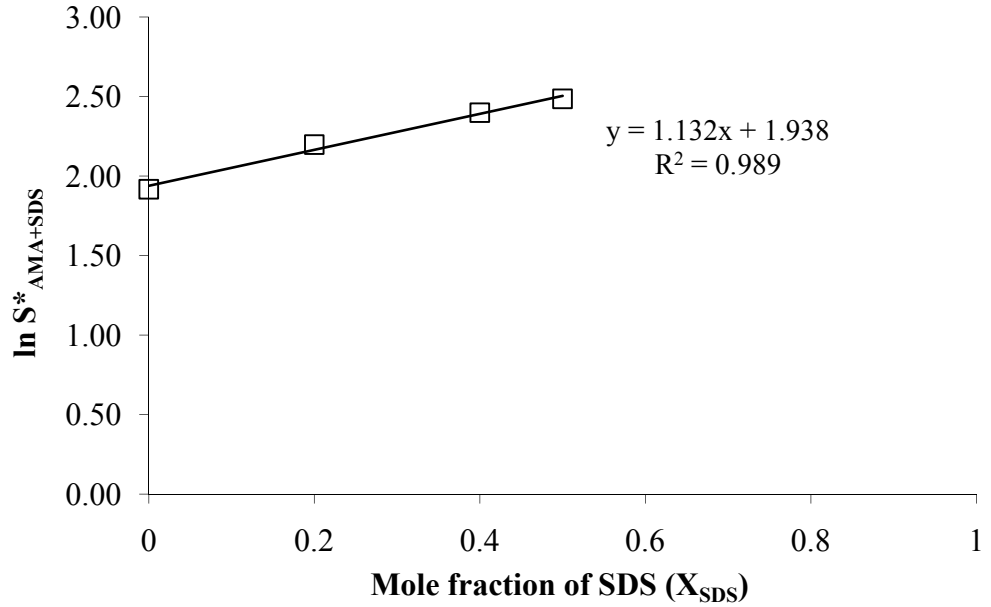

Figure 3.3. A plot of ln $S^*_{AMA+SDS}$ vs. SDS composition (X_{SDS}) in the mixed AMA-SDS system with limonene at constant 0.07 M total surfactant concentration and controlled temperature 25 ^oC.

Table 3.2. Summary of the σ value of conventional and extended surfactants

System	C_{12}-SO_4Na	$C_{12,15}$-$(EO)_2$-SO_4Na	$C_{12,13}$-$(PO)_8$-SO_4Na	Twin-tail C6 sulfosuccinate (AMA)	Twin-tail C8 sulfosuccinate (AOT)
σ	-2.46 ± 0.35	-2.97 ± 0.25	-0.784 ± 0.309	-0.933 ± 0.103	2.42 ± 0.16
K	0.10 ± 0.02[a]	0.062 ± 0.001[b]	0.087 ± 0.006	0.17 ± 0.02	0.17 ± 0.02
σ/K	-24.6	-49.5	-8.67	-5.47	14.2

[a] reference [20] and [b] determined from data in reference [34]

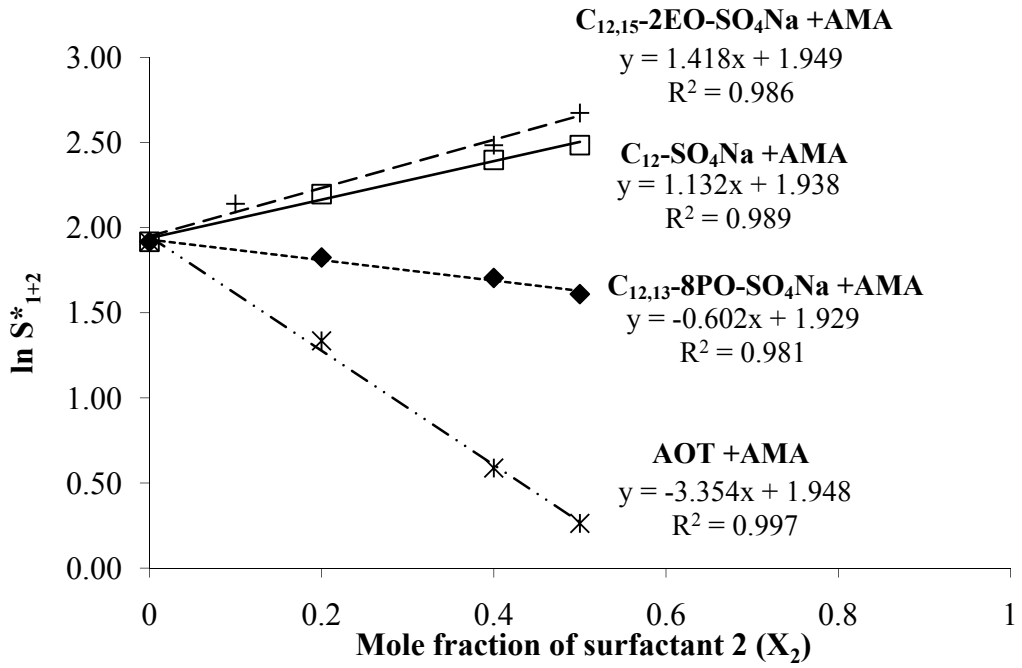

Figure 3.4. A plot of ln S^*_{1+2} vs. surfactant composition (X_2) of various surfactant mixtures with limonene at constant 0.07 M total surfactant concentration and controlled temperature 25 ^oC.

Similar to Figure 3.3, Figure 3.4 plots ln S* versus x_2 for four AMA-surfactant mixtures (including the AMA-SDS mixture shown in Figure 3.3). Three of the four surfactant combinations are a mixture of two conventional surfactants, AMA-SDS, AMA-AOT, and AMA-$C_{12,15}$-$(EO)_2$-SO_4Na systems, while the fourth, AMA-$C_{12,13}$-$(PO)_8$-SO_4Na, is a mixture of conventional and extended surfactants. The common component in each mixture is the AMA surfactant and the microemulsion phase study is carried out under the same conditions (limonene, 25 ^oC and no additives). Therefore, the variation of the slope of different surfactant combinations is a consequence of the change in the hydrophilic-lipophilic nature of

the surfactant mixtures, resulting from the nature of the surfactant blended with AMA.

Inspection of the plots in Figure 3.4 reveals a very interesting trend. Among the four combinations, the mixture of AMA and $C_{12,15}$-$(EO)_2$-SO_4Na surfactants has the highest positive slope value, followed closely by the AMA-C_{12}-SO_4Na system. The presence of eight propoxylated groups (POs) in $C_{12,13}$-$(PO)_8$-SO_4Na yields not only a significant drop in the slope, but also a negative slope value. The AMA and AOT system (a twin-tail C_8 sulfosuccinate) has the most negative slope value. As stated earlier, the slope has the reverse sign convention of the σ parameter. The σ values for these blended surfactants and the corresponding $\frac{\sigma}{K}$ values are summarized in Table 3.2. Therefore, the σ value is ranging from the most positive to the most negative for the surfactants studied as follows:

$$\text{AOT} > C_{12,13}\text{-}(PO)_8\text{-}SO_4Na > C_{12}\text{-}SO_4Na > C_{12,15}\text{-}(EO)_2\text{-}SO_4Na$$

In Table 3.2, it seems that the σ parameter (hydrophobic nature of surfactant) is influenced by the addition of EO and PO groups and the branching of surfactant hydrophobic tail. A straight-chain C_{12}-SO_4Na or SDS has the σ value of -2.46. The SDS surfactant is typically a water-soluble surfactant and tends to form oil-swollen micelles. In comparison to SDS, the $C_{12,15}$-$(EO)_2$-SO_4Na surfactant has approximately the same hydrocarbon tail length, so we would anticipate it to have a similar σ value with the SDS surfactant. However, the $C_{12,15}$-$(EO)_2$-SO_4Na shows a slightly more negative σ value (-2.97) which can be attributed to the addition of 2

EO groups inserted in the surfactant molecule. Because the σ value of $C_{12,15}$-$(EO)_2$-SO_4Na is more negative than that of SDS (-2.97 vs. -2.46), it implies that the $C_{12,15}$-$(EO)_2$-SO_4Na is somewhat more hydrophilic than SDS surfactant. This is consistent with the observation that the optimum salinity of the AMA-$C_{12,15}$-$(EO)_2$-SO_4Na mixture increases with increasing $C_{12,15}$-$(EO)_2$-SO_4Na mole fraction (Figure 3.4).

Unlike the effect of EO groups, the presence of 8 PO groups between the sulfate head and hydrophobic tail of $C_{12,13}$-$(PO)_8$-SO_4Na increases the value of the σ parameter to -0.78. This suggests that the $C_{12,13}$-$(PO)_8$-SO_4Na is more hydrophobic than SDS and $C_{12,15}$-$(EO)_2$-SO_4Na surfactants. As a result, lower optimum salinity is observed at higher $C_{12,13}$-$(PO)_8$-SO_4Na mole fractions.

These results are consistent with observations from the hydrophilic-lipophilic balance or HLB group contribution model as modified by Davies [16, 18]. Regarding this model, the addition of one EO group (-CH_2-CH_2-O-) contributes a value of 0.33 to the hydrophilic group number causing the HLB value to be higher and indicating that the surfactant is more hydrophilic. In contrast, the addition of one PO group ($\text{-CH}_2\text{-CH(CH}_3\text{)-O-}$) causes a reduction of -0.15 to the lipophilic group number, indicating the surfactant is more hydrophobic. For instance, the calculated HLB number of SDS and $C_{12,15}$-$(EO)_2$-SO_4Na are 40 and 40.66, respectively. Davies's HLB method has been widely used for estimating the hydrophilic-lipophilic balance of most conventional surfactants, however, it has not been evaluated for its ability to characterize the hydrophilic-lipophilic nature of extended surfactants. Additionally, it is interesting to mention that the EO and PO groups not only alters

the hydrophobicity of surfactant (σ value), but also the hydrophilicity (*K* value). This observation shows a deviation from Davies' HLB approach, where the EO group is only accounted for in the hydrophilic group contribution and the PO groups is mainly subjected to the hydrophobic subtraction group. The applicability of the HLB number on the molecular structure of extended surfactants will be revisited in the next section.

Besides the sensitivity of the σ parameter to the addition of EO and PO groups, the σ parameter is also susceptible to the branching and addition of a methyl group ($-CH_3$) on the surfactant hydrocarbon tail. The results shown in Table 3.2 indicate that by restructuring from a straight-chain C12 hydrocarbon tail of SDS to a twin-tail C6 AMA surfactant, the σ value is increased from -2.46 to -0.93. Furthermore, when the surfactant tails go from C6 to C8 in a twin-tailed structure (AMA to AOT), the σ value increases from -0.93 to 2.42. These results highlight a strong dependence of the σ parameter on the molecular structure of surfactant compounds.

Comparison of σ and $\frac{\sigma}{K}$ values in Table 3.2 leads to some interesting observations. On one hand, the $C_{12,13}$-$(PO)_8$-SO_4Na is suggested to be more hydrophobic than AMA surfactant due to the more positive σ value of $C_{12,13}$-$(PO)_8$-SO_4Na compared to that of AMA (-0.78 vs. -0.93, respectively). On the other hand, the $\frac{\sigma}{K}$ indicator suggests a the more hydrophilic behavior of $C_{12,13}$-$(PO)_8$-SO_4Na as

has a more negative $\frac{\sigma}{K}$ value (-8.67 vs. -5.47 for $C_{12,13}$-$(PO)_8$-SO_4Na and AMA surfactant, respectively). In this case, trends in the σ value are in good agreement with the experimental data (see Figure 3.4).

We speculate that is due to the way to calculate the $\frac{\sigma}{K}$ value of the $C_{12,13}$-$(PO)_8$-SO_4Na surfactant**.** While, the $\frac{\sigma}{K}$ term represents the surfactant characteristic for conventional anionic surfactants, there is a recommendation to use the combination of ethylene oxide number (EON) and the hydrophobic contribution (α) for nonionic surfactant [24]. The fact that nonionic surfactant requires modification of the equation, and the fact that extended surfactants have property of both anionic and nonionic surfactants, suggests some kind of modification of the equation is needed to calculate $\frac{\sigma}{K}$ for extended surfactants; evaluating the form of such a modified equation is beyond the scope of this work. Thus, without modifying the $\frac{\sigma}{K}$ term in this work, the σ value proves to be a better surfactant characteristic parameter for extended surfactants than the $\frac{\sigma}{K}$ value.

Comparison of the σ vs. HLB number. Table 3.3 presents the comparison between the HLB number calculated using Davies's equation and the σ value of some extended surfactants; note, the σ values in Table 3.3 come from the ln S* vs. x_2 data in Figure 3.5 using the same method as described previously for Figure 3.4.

From Table 3.3, while the HLB numbers of the surfactants are all quite similar, the σ values vary dramatically. Although the HLB numbers predict that surfactants with similar HLB numbers should behave in the same manner for a particular oil-water system [16, 18], the σ data generated in this work demonstrates otherwise.

Table 3.3. HLB number vs. σ value of various surfactants

Extended surfactant	Alkyl #	# PO	# EO	HLB[a]	σ
$C_{12,13}$-$(PO)_3$-SO_4Na	12-13	3	-	39.55	-1.77
$C_{12,13}$-$(PO)_8$-SO_4Na	12-13	8	-	38.80	-0.78
C_{12}-$(PO)_{14}$-$(EO)_2$-SO_4Na	12	14	2	39.51	0.74
C_{10}-$(PO)_{18}$-$(EO)_2$-SO_4Na	10	18	2	38.91	1.99

[a] Davies's HLB equation

HLB = 7 + Σ(hydrophilic groups) + Σ(lipophilic groups)

Each C = 0.475, SO_4 = 38.7, EO = 0.33, and PO = -0.15

Interestingly from Figure 3.5, extended surfactants exhibit hydrophilic-lipophilic behavior different from what their HLB values would suggest. For instance, both $C_{12,13}$-$(PO)_3$-SO_4Na and C_{12}-$(PO)_{14}$-$(EO)_2$-SO_4Na surfactants have very similar HLB values (39.55 vs. 39.51), but the slopes of these extended surfactants produce σ values opposite in sign (Figure 3.5a and Table 3.3). With increasing $C_{12,13}$-$(PO)_3$-SO_4Na mole fraction (see Figure 3.5a), the surfactant mixture requires more NaCl concentration to reach an optimum condition, indicating that the extended surfactant is more hydrophilic surfactant (positive slope value). On the other hand, the mixture of AMA-C_{12}-$(PO)_{14}$-$(EO)_2$-SO_4Na system requires less salt to attain the optimum condition, indicating that the extended surfactant is more

hydrophobic surfactant. The slope of the given examples yield the σ value provided in the last column of Table 3.3 as described below.

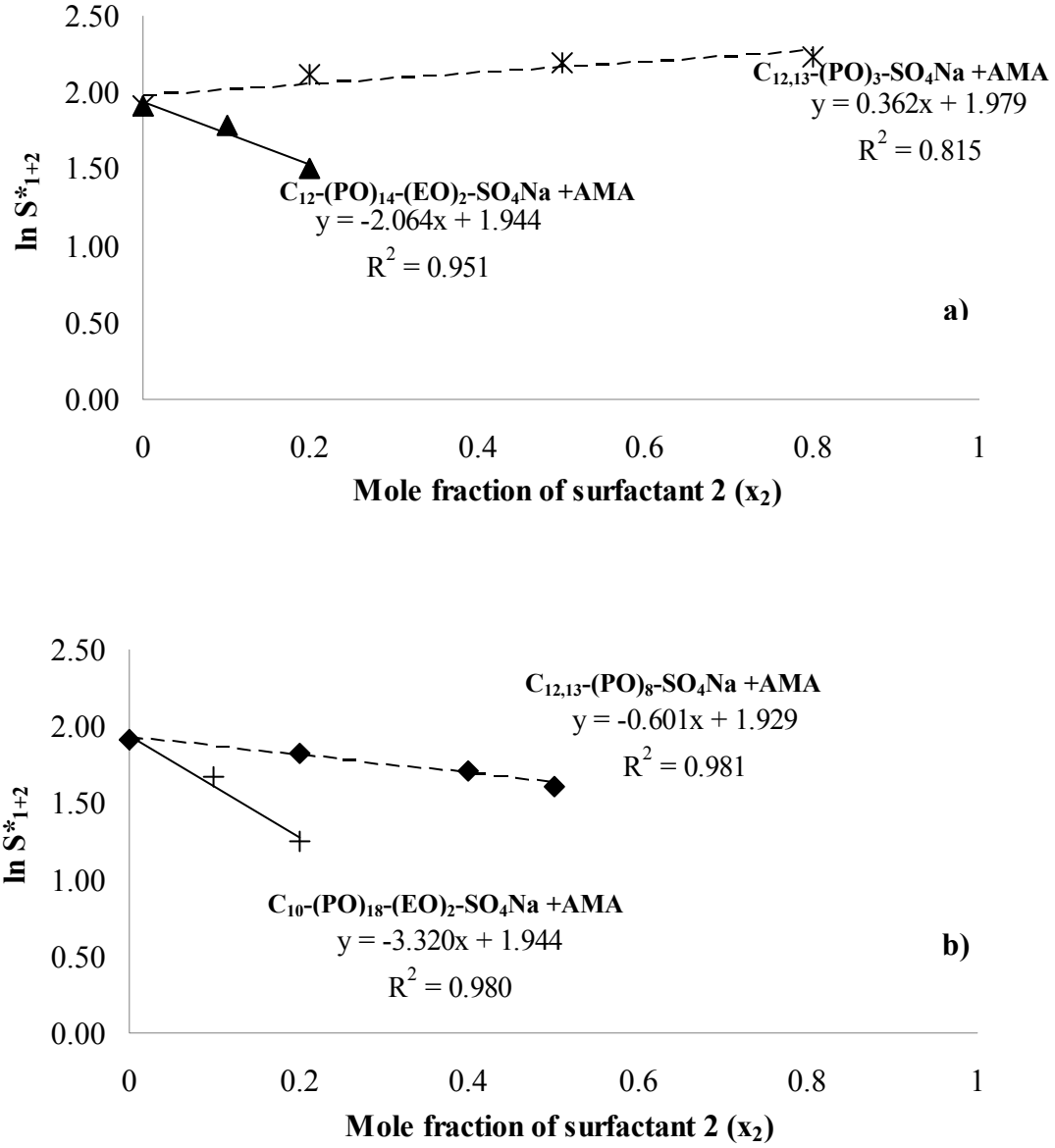

Figure 3.5. The σ value of mixed AMA-surfactant system with limonene oil at the optimum condition, 0.07 M total surfactant concentration, and 25 ^{o}C, a) AMA/$C_{12,13}$-$(PO)_3$-SO_4Na vs. AMA/C_{12}-$(PO)_{14}$-$(EO)_2$-SO_4Na systems and b) AMA/$C_{12,13}$-$(PO)_8$-SO_4Na vs. AMA/C_{10}-$(PO)_{18}$-$(EO)_2$-SO_4Na systems.

Regarding the calculated σ value, a distinctive hydrophilic-lipophilic behavior is observed between two extended surfactants. The $C_{12,13}$-$(PO)_3$-SO_4Na extended surfactant is a more hydrophilic surfactant with a σ value of -1.77, while the C_{12}-$(PO)_{14}$-$(EO)_2$-SO_4Na is a relatively more hydrophobic surfactant with the σ value of 0.74 (Table 3.3). The increase in a positive σ value of C_{12}-$(PO)_{14}$-$(EO)_2$-SO_4Na emphasizes the impact of the additional PO groups on the hydrophobic characteristic of extended surfactants. A similar observation is also found from another set of extended surfactants as depicted in Figure 3.5b. Both $C_{12,13}$-$(PO)_8$-SO_4Na and C_{10}-$(PO)_{18}$-$(EO)_2$-SO_4Na surfactants show the similar HLB numbers, however, the σ values of these two extended surfactants are quite different (-0.78 and 1.99, respectively).

These results demonstrate that the σ value is a superior indicator for determining extended surfactant behavior. The presence of PO and EO groups in surfactant structure undoubtedly plays a crucial role in modifying hydrophilic-lipophilic balance of extended surfactants.

Applications of the σ value. The HLD equation has been used for a number of purposes, including characterizing the hydrophobic nature of non-alkane oils [12, 31], predicting the optimum ethylene oxide number (EON*) of nonionic surfactant microemulsion [32], and quantifying phase behavior in food emulsion [33]. However, only limited research has focused on the σ parameter and its benefits. This last section thus seeks to demonstrate a practical use of the HLD equation using the σ values determined evaluated in this work.

Theoretically, the K and σ values represent fundamental surfactant characteristics; they should remain constant if the surfactant composition remains unchanged. Thus, in this work, we apply the K and σ values established previously to the modified HLD equation 8 for predicting the optimum salinity using the same surfactant system but different oils from the limonene used to establish the σ and K parameters. The surfactant system used in this task is the combination of AMA and AOT surfactants. The total surfactant concentration was fixed at 0.07 M and microemulsion phase study was performed at 25 ^{o}C without the addition of alcohol or other additives. Various surfactant mixture ratios were evaluated for making microemulsions with two oils; octane (EACN of 8) and decane (EACN of 10).

Figure 3.6 shows the comparison between the optimum salinity obtained from the HLD equation prediction and the microemulsion phase study experiment. For both oils, the optimum salinity predicted by the combination of the σ value established in this work and the HLD equation is in excellent agreement with the experimental data. These results demonstrate the advantages of utilizing the evaluated σ value in a simple HLD expression for guiding optimum formulation (in this particular case, it is the optimum salinity) of microemulsion systems, and also confirm that this surfactant characteristic parameter (σ value) is independent of oil nature as suggested previously by Salager *et. al.* [20, 24].

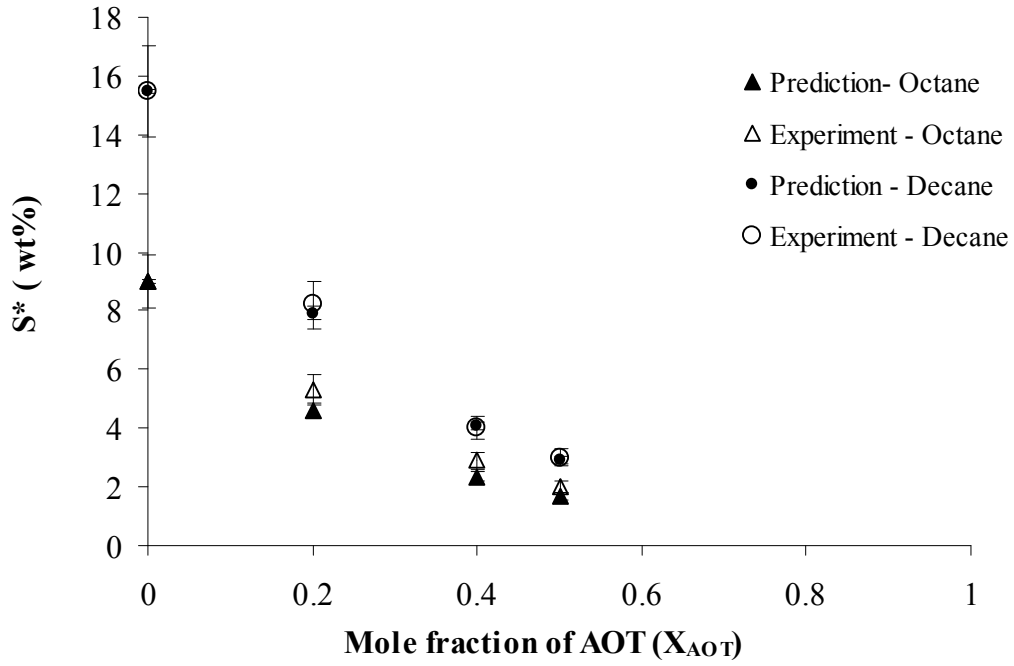

Figure 3.6. Comparison the optimum salinity (S*) obtained from the prediction using sigma parameter and the experimental phase study of a) AMA/AOT/Octane system (represented by the triangle bullet), and b) the AMA/AOT/Decane system (represented by the circle bullet). Total surfactant concentration of 0.07 M total surfactant concentration at 25 ^{o}C.

Conclusions

In this paper, we utilized the simple HLD technique for determining the σ and $\frac{\sigma}{K}$ of several conventional anionic surfactants and extended surfactants, the use of mixture of surfactants with AMA. The resultant parameters are evaluated as surfactant behavior indicators (i.e., as an alternative to the HLB number). To our knowledge, this is the first time that the HLD method and HLD index have been

used to capture the hydrophilicity/lipophilicity of extended surfactants. The results not only emphasize the impact of PO and/or EO groups inserted in the extended surfactant on the σ value, but also clearly demonstrate the sensitivity of the σ parameter to branching and additional methyl group on the surfactant hydrocarbon tail.

It should be noted that the σ parameter captures the nature of extended surfactants better than the $\frac{\sigma}{K}$ parameter. Further investigation evaluating the use of the σ and $\frac{\sigma}{K}$ values for extended surfactant systems is certainly important as well as additional modifications of the HLD approach accounting for the dual anionic-nonionic nature of extended surfactants.

In addition, the σ index was also demonstrated as more adequate indicator for representing extended surfactant characteristics than HLB number. Finally, the σ parameters evaluated in this work were combined with the HLD equation to illustrate its practical use for guiding the optimum salinity for a microemulsion system.

Acknowledgements

The authors would like to extend the special appreciation to Geoff Russell and Paul Filler, Sasol North America (Lake Charles, LA) and George Smith, Huntsman Petrochemical Corp. (Houston, TX) for providing extended surfactant samples. In addition, the authors would like to acknowledge Dr. Edgar J. Acosta at the University of Toronto for his suggestions and comments. Funding for this

research was provided by industrial sponsors of the Institute for Applied Surfactant Research at University of Oklahoma.

References

[1] J.H. Harwell, in: D.A. Sabatini and R.C. Knox (Eds.), American Chemical Society, Washington DC, 1992, p. 124.

[2] R.C. Knox, B.J. Shiau, D.A. Sabatini, J.H. Harwell, in: M.L. Brusseau, American Chemical Society, Washington DC, 1999, p. 49.

[3] L. Djordjevic, M. Primorac, M. Stupar, D. Krajisnik, Int. J. Pharm. Compd. 271 (2004) 11.

[4] A. Kogan, N. Garti, Adv. Colloid Interface Sci. 123 (2006) 369.

[5] P.K. Ghosh, R.J. Majithiya, M.L. Umrethia, R.s. Murthy, AAPS Pharm. Sci. Techol. 7 (2006) 3.

[6] M.J. Rosen, Surfactants and Interfacial Phenomena, John Willy & Sons, New Jersey, 2004, p. 353.

[7] C. Tongcumpou, E.J. Acosta, L.B. Quencer. A.F. Joseph, J.F. Scamehorn, D.A. Sabatini, S. Chavadej, N. Yanumet, J. Surf. Deterg.

[8] C. Tongcumpou, E.J. Acosta, L.B. Quencer. A.F. Joseph, J.F. Scamehorn, D.A. Sabatini, S. Chavadej, N. Yanumet, J. Surf. Deterg., 6 (2003) 205.

[9] N. Azemar, in: C. Salans and H. Kunieda (Eds.), Marcel Dekker, Inc., New York, 1996, p. 375.

[10] M. Minana-Perez, A. Graciaa, J. Lachaise, J.L. Salager, J. Colloid Interface Sci. 100 (1995) 217.

[11] C. Tongcumpou, E.J. Acosta, L.B. Quencer. A.F. Joseph, J.F. Scamehorn, D.A. Sabatini, N. Yanumet, S. Chavadej, J. Surf. Deterg., 8 (2005) 147.

[12] A. Witthayapanyanon, E.J. Acosta, J.H. Harwell, D.A. Sabatini, JSD 9 (2006) 331.

[13] J.L. Salager, R.E. Anton, D.A. Sabatini, J.H. Harwell, E.J. Acosta, L.I. Tolosa, J. Surf. Deterg., 8 (2005) 3.

[14] M. Bourrel, R. Schechter, Microemulsions and Related System, Marcel Dekker, Inc., New York, 1988.

[15] P.A. Winsor, Trans. Faraday Soc. 44 (1948) 376.

[16] J.T. Davies, International Congress on Surface Activity, London, England, 1948.

[17] W.C. Griffin, J. Soc. Cosmetic Chemists. 1 (1949) 311.

[18] P. Becher, Emulsions: Theory and Practice, American Chemical Society, Washington DC, 2001, p. 338.

[19] K. Shinoda, H.J. Arai, J. Phys. Chem. 68 (1964) 3485.

[20] J.L. Salager, J.C. Morgan, R.S. Schechter, W. H. Wade, E. Vasquez, Soc. Petrol. Eng. J. 19 (1979) 107.

[21] J.L. Salager, M. Bourrel, R.S. Schechter, W. H. Wade, Soc. Petrol. Eng. J. 19 (1979) 271.

[22] E.J. Acosta, E. Szekeres, D.A. Sabatini, J.H. Harwell, Langmuir 19 (2003) 186.

[23] J.L. Salager, R. Anton, J.M. Anderez, J.M. Aubry, Techniques de l' Ingenieur J. 2 (2001) 5.

[24] J.L. Salager, in: G. Broze (Ed), Marcel Dekker, Inc., New York, 1999, p. 253.

[25] M.J. Rosen, Surfactants and Interfacial Phenomena, John Willy & Sons, New Jersey, 2004, p. 5.

[26] J.L. Salager, Ph.D. Dissertation, University of Texas at Austin, Austin, Texas, 1978.

[27] E.J. Acosta, S. Yuanm, D.A. Sabatini, 95th AOCS Annual Meeting & Expo, Cincinnati, OH, 2005.

[28] S. Wacharasing, S. Chavadej, J.F. scamehorn, Sep. Sci. Techol., in press.

[29] J. Childs, E.J. Acosta, J.F. Scamehorn, D.A. Sabatini, J. Energy Res. Technol. 127 (2005) 153.

[30] C.H. Rodriguez, L.H. Lowery, J.F. Scamehorn, J.H. Harwell, JSD 4 (2001)

[31] V. Nardello, N. Chailloux, J. Poprawski, J.L. Salager, J.M. Aubry, Polym Int 52 (2003) 602.

[32] J. Poprawski, M, Catte, L. Marquez, M.J. Marti, J.L. Salager, J.M. Aubry. Polym Int 52 (2003) 629.

[33] R.K. Thakur, C. Villette, J.M. Aubry, G. Delaplace, Colloids Surfaces A: Physicochem. Eng. Aspects 301 (2007) 496.

[34] S.I. Chou, J.H. Bae, Soc. Petrol. Eng., 3 (1988) 778.

CHAPTER 4

Interfacial Properties of Extended-Surfactant-Based-Microemulsions

Abstract

Extended surfactants are surfactants with intermediate polarity groups, such as polypropylene oxide (POs) and polyethylene oxide (EOs), inserted in between the hydrophilic head and the hydrocarbon tail. Due to this unique molecular structure, extended surfactants exhibit enhanced surface activity without sacrifying water solubility. This results in superior solubilization and desirable IFT reduction, especially for highly hydrophobic oils and vegetable oils. However, extended-surfactant-based formulations struggle with slow kinetics. The present work seeks to evaluate both equilibrium and kinetic aspects of extended-surfactant-based microemulsions. To our knowledge, this is the first time that the interfacial morphology of extended surfactant membranes (i.e. characteristic length and interfacial rigidity) has been characterized. The results showed that additional PO groups increase the characteristic length (ξ) and the interfacial rigidity (E_r) of extended-surfactant-based-microemulsions. The relatively high rigidity of extended surfactant membrane was suspected to be due to the formation of liquid crystal or the structural arrangement of extended surfactant molecules. Based on the ξ and E_r values, the slow coalescence rate of extended surfactant-based system was also evaluated. Finally, we examined an approach to overcome the slow kinetics of

coalescence, while maintaining high solubilization and low IFT property by using combined linker and co-surfactant approaches.

Key words: microemulsions, extended surfactants, high solubilization, characteristic length, interfacial rigidity, coalescence rate

Introduction

The Winsor R-ratio is the conceptual framework for understanding microemulsion formulations. It was first introduced in 1948 by Winsor [1] as the surfactant interaction energy for both oil and water phases. By definition, R = 1 at the optimum condition where surfactant exhibits strong but equal affinity between oil and water, resulting not only in the formation of middle phase microemulsions, but also the maximum solubilization and minimum interfacial tension (IFT). In respect to this model [2-4], while maintaining R =1, systems with larger interactions with both phases produce lower minimum IFT values and greater solubilization than those with smaller interactions. A simple way to improve these interactions is by increasing simultaneously the hydrophilicity of the head and the length of hydrocarbon tail of the surfactant. However, this approach is limited by the loss in solubility associated with long hydrocarbon tails. Extended surfactants have been proposed as an alternative surfactant structure to achieve the Winsor's potential without sacrifying water solubility [4-7].

Unlike conventional surfactants, extended surfactants contain intermediate polarity groups such as the short-chain polypropylene oxide (POs) or polypropylene-polyethylene oxide (POs-EOs) inserted between the surfactant hydrophilic head and hydrocarbon tail. The presence of these intermediate groups provides two beneficial effects: extending the length of the surfactant further into both oil and water phase and offering a smoother interfacial transition from the polar aqueous to non-polar oil regions [3, 4, 7]. With this distinctive structure, extended surfactants have proven capable of forming middle phase microemulsions with large oil molecules, namely long-chain alkanes, triglycerides and vegetable oils [5, 8, 9]. Additionally, their microemulsions achieve both the high solubilization and ultra low IFT desirable in many applications [5, 7, 8, 10, 11].

Although extended surfactants achieve increased interfacial activity without losing water solubility, they face the challenge of slow kinetics. In our previous work [9], the equilibration time reported for optimum middle phase microemulsion was in the range of weeks to months. From an application standpoint, such formulations are inadequate for most processes which are operated under relatively short contact times (i.e. detergency, hard surface cleaning and surfactant-enhanced separation etc.). The time for extended-surfactant-based microemulsions to approach equilibrium is dependent on the coalescence rate of their corresponding macroemulsion droplets. We believe that the slow coalescence phenomenon is a result of the extended surfactants' unique structure: the presence of PO and/or EO groups. Achieving a better understanding of this relationship requires the

characterization of the surfactant membrane properties in extended surfactant systems. With this understanding we will be able to engineer formulations to achieve both equilibrium and dynamic properties suitable in application.

In addition to the concept of the Winsor R ratio, the correlation length or characteristic length (ξ) of the surfactant membrane can help guide us in producing the Winsor Type III microemulsion with high solubilization and low IFT properties. The structure of middle phase microemulsion has been considered as coexisting oil and water droplets stabilized by the surfactant membrane [12-14]. Using the opposite sign convention for the surfactant membrane curvature between oil and water droplets, a zero net-curvature corresponds to what is commonly known as a bicontinuous microemulsion structure (see Figure 4.1a). Sometimes this bicontinuous microemulsion phase is simply depicted as the microscopic lattice structure shown in Figure 4.1b. From Figure 4.1b, the characteristic length indicates the distance that oil or water molecules are separated from the oil/water interface yet still interact with the surfactant membrane. It limits, therefore, the maximum volume of oil (or water) to be solubilized in the middle-phase, thus determining the maximum solubilization capacity of the microemulsion system. Analogous to the solubilization parameter (SP), a larger characteristic length signifies a higher solubilization and also results in a lower IFT. Approaches to evaluate the characteristic length of interfacial membrane involve not only mathematical models, but also laboratory techniques such as X-ray reflectivity, neutron scattering, and dynamic light scattering [15-17].

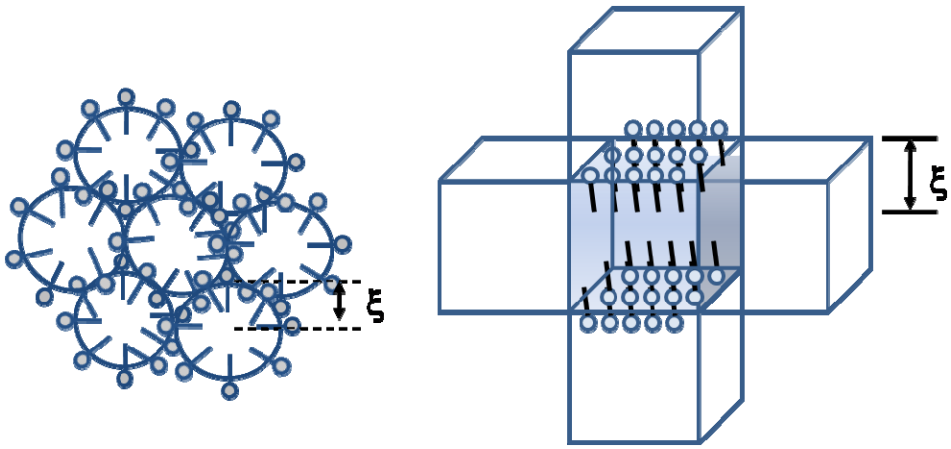

Figure 4.1. The structure of middle phase microemulsions at the optimum condition shown in accordance to (a) a zero net-curvature of coexisting oil and water droplets and (b) microscopic lattice model illustrating the characteristic length (ξ) of the surfactant dynamic membrane adapted from ref [4] and [19], respectively.

Another interesting property associated with the characteristic length is the rigidity of the surfactant membrane. Based on a series of phase studies, Acosta *et al.* [18] proposed empirical expressions to estimate these membrane properties as a function of IFT and phase volume. In subsequent work [6, 19-21], the correlation between characteristic length (ξ) and interfacial rigidity (E_r) with the addition of linker molecules was demonstrated. The result showed that both ξ and E_r values increase with an increase in surfactant hydrocarbon tail and the addition of lipophilic linker but decrease with the addition of hydrophilic linker. Addition of combined linkers produced an intermediate effect.

Interfacial membrane properties impact not only equilibrium properties, such as solubilization capacity and IFT reduction, but also dynamic properties of

microemulsions. The rate of oil solubilization and coalescence kinetics of macroemulsion droplets formed by shaking an optimum microemulsion sample are examples of dynamic features controlled by the property of surfactant film. The kinetics of macroemulsion in microemulsions coalescence has been studied as an indirect measure of microemulsion kinetics [19]; this approach will be used in the current study as well. It is also important to clarify that macroemulsion droplets form from the excess oil and water phases when equilibrium microemulsions are disturbed by shaking or mixing. But given sufficient time, these dispersed droplets will coalesce and reestablish the equilibrium microemulsion state; the rate at which this equilibrium is achieved is a function of the rigidity of the surfactant membrane.

Coalescence is a process in which two or more macroemulsion droplets collide to form a larger droplet [22]. It consists of three main steps; an approach of the droplets to form a plane-parallel film, the thinning of the film to a critical thickness, and the film rupture. Adsorbed surfactant at the oil-water interface forms a barrier for droplets to approach one another or film drainage to occur. Rosen [23] indicated that the close-packed adsorption of surfactants at the oil-water interface provided strong lateral intermolecular forces, causing high film elasticity, and thus resulted in decreasing the coalescence rate of dispersed emulsion droplets. Helfrich [24] proposed a mathematical model relating the film elastic modulus (K) to the free energy cost to create a new dynamic interfacial area. A highly elastic membrane is a rigid interfacial film. For a rigid membrane, more energy is required to deform the membrane as two droplets approach, thereby leading to a slower coalescence rate.

Acosta *et al.* [19], found that the addition of additives, like hydrophilic and lipophilic linkers, affects the rigidity of surfactant membrane and the subsequent coalescence. These prior studies underline the strong dependence of the coalescence rate on the rigidity of surfactant film.

Based on this overview, it is reasonable to speculate that, due to the elongated and bulky structure of extended surfactants they produce a thick and rigid surfactant membrane, which will result in a slow coalescence rate and a prolonged equilibration time of microemulsions. So although extended surfactants offer great potential based on their equilibrium properties, the utilization of extended surfactant-based formulations will be limited by their slow kinetics. In this present work, we start by demonstrating the ability of extended surfactants to form middle phase microemulsions with desirable high solubilization and low IFT properties in accordance to the Winsor's premise. Next, extended-surfactant-membrane kinetic properties will be characterized for the first time as a function of adding PO groups. Finally, we explore an approach to overcome the slow coalescence rate of extended surfactant-based systems, while still maintaining favorable low IFT and high solubilization for practical uses, by adding the combined linkers and co-surfactants.

Experimental procedures

Materials. Surfactants evaluated in this work are classified into two main groups; conventional surfactants and extended surfactants. In the first group, sodium dodecyl sulfate (C_{12}-SO_4Na or SDS) and bis(2-ethylhexyl) sulfosuccinate, sodium

salt (trade name Aerosol-OT or AOT), were utilized as representative of conventional anionic surfactants. The SDS (97% active) and AOT (99% + , anhydrous) were purchased from Sigma-Aldrich and used as received. The second group of surfactants evaluated is the extended surfactants containing various numbers of propoxyl groups (POs) inserted between the sulfate head and hydrocarbon tail ($R\text{-}(PO)_x\text{-}SO_4Na$). The hydrocarbon tail of extended surfactants studied consisted of either branched 12 to 13 carbons ($C_{12,13}$) or 14 to 15 carbons ($C_{14,15}$). These $R\text{-}(PO)_x\text{-}SO_4Na$ surfactant samples were provided by Sasol North American Inc. (Lake Charles, LA). All conventional and extended surfactants were used as received. The structure of the extended surfactant and their properties are illustrated in Figure 4.2 and Table 4.1.

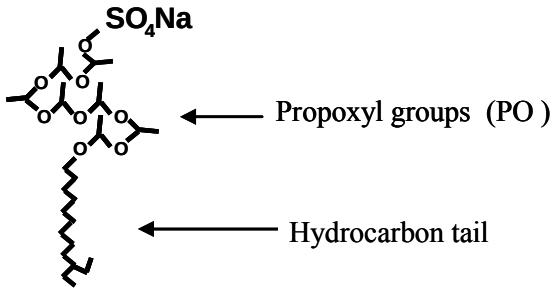

Figure 4.2. Proposed struture of PO-extended surfactants, ($R\text{-}(PO)_x\text{-}SO_4Na$), adapted from ref [7].

Table 4.1. Properties of conventional, extended surfactants, and co-surfactant.

Surfactants	HC	% Branch	# of PO groups	% Active	MW	a_i ($\overset{o}{A}^2$)
Conventional Surfactant						
$C_{12}H_{25}$-SO_4Na (SDS)	C_{12}	-	-	97.0	288	60.0[a]
Aerosol-OT	Twin-tail C_8	-	-	100	445	110[b]
Sec-butnaol	C_4	-	-	> 99.5	74	30.0[b]
Extended surfactants						
$C_{12,13}H_{25,27}$-$(PO)_4$-SO_4Na, 100 B	$C_{12,13}$	100	4	30.0	527	144.9[c]
$C_{12,13}H_{25,27}$-$(PO)_8$-SO_4Na, 100 B	$C_{12,13}$	100	8	30.7	766	61.73[c]
$C_{12,13}H_{25,27}$-$(PO)_8$-SO_4Na, 50 B	$C_{12,13}$	50	8	30.6	667	96.14[c]

[a, b] Values reported in the literatures (Ref. [6] and [23], respectively)

[c] Evaluated in this work with the presence of 0.2 M NaCl addition at 27 ^oC

a_i = cross sectional area per surfactant head group

Sodium chloride (99%+), sec-butanol (99%+, anhydrous) and straight-chain alkanes, namely octane (99%+, anhydrous), decane ((99%+, anhydrous), dodecane (99%+, anhydrous), and hexadecane (99%+, anhydrous) were purchased from Sigma-Aldrich (Saint Louis, MO) and used at the concentration shown without further purification.

Methods. *Microemulsion phase studies* were performed in flat-bottom test tubes with Teflon-lined screw caps. While holding surfactant concentration, temperature, and pressure constant, equal volumes of oil and water (5mL) were added into the vial at different NaCl concentrations (salinity scan). All test tubes were gently shaken to provide a well-mixed aqueous – oil solution. Subsequently, all samples were placed in a temperature-controlled water-bath at 27 ^{o}C, shaken once a day for the first 3 days and left to equilibrate for at least ten days. When the systems reached equilibrium, the relative phase heights and interfacial tension (IFT) values were quantified for each sample to determine the optimum condition (in this case, the salinity that producing the lowest IFT and highest volume of middle phase is known as the optimum salinity (S*) for the system). A sample determined as the optimum middle phase microemulsion of each surfactant system was then re-prepared and left to equilibrate for studying the rate of macroemulsion coalescence, where the macroemulsion was obtained by shaking a middle phase microemulsion.

Equilibrium interfacial tension (IFT) was measured using samples of pre-equilibrated microemulsion phases in a spinning drop tensiometer (University of Texas, model 500). The excess water phase of a middle phase microemulsion

(which was the dense phase) was added into the spinning drop tube. Then 1-3 μL of the excess oil phase was subsequently injected into the same tube. The IFT measurement was recorded after 15 minutes of spinning.

Characteristic length (ξ^*) and interfacial rigidity (E_r) of extended surfactant-based microemulsions at the optimum condition were evaluated from an empirical model developed by Acosta *et al.* [18]. The ξ and the E_r values were calculated from equations shown below.

For the characteristic length at the optimum condition (ξ^*):

$$\xi^* = \frac{6\phi_o\phi_w V_m}{A_S} \tag{1}$$

where ξ^* is the characteristic length at the optimum condition ($\overset{o}{A}$), ϕ_o and ϕ_w are the volume fractions of oil and water in the middle phase microemulsions, respectively, V_m is the total volume of a middle phase microemulsion, and A_S is the interfacial area making up the surfactant membrane (i.e. surfactants, co-surfactant, and/or hydrophilic linker) and can be calculated using the following equation.

$$A_S = \sum_i C_{S_i} V_W \phi_i (6.023\times10^{23}) a_i \tag{2}$$

where C_{S_i} is the initial concentration of surfactant *i* in the aqueous solution, V_w is the initial volume of the aqueous phase solution, ϕ_i is the fraction of surfactant or additives participating in the middle-phase volume with respect to the total surfactant

concentration, a_i is the cross-sectional area per molecule of the surfactant *i*, obtained from a Gibb surface tension plot at the appropriate electrolyte concentrations.

The interfacial rigidity at the optimum condition (E_r) can be calculated by:

$$E_r = 4\pi\xi^{*2}\,\gamma^{*} \tag{3}$$

where γ^{*} is the interfacial tension (either between middle phase/excess oil or middle phase/excess water) at optimum condition, the E_r is the interfacial rigidity expressed in k_BT unit at 300 K, and the ξ^{*} is the characteristic length at the optimum condition ($\overset{o}{A}$). In general, the E_r values for microemulsion systems are consistent with a bending modulus (K) of about 1 k_BT [17, 25].

Coalescence was measured using the turbidity device developed by Acosta *et.al.* [19]. The light source was a standard green LED and the detector was a cadmium sulfide cell (CDS) with a proportional resistance signal. Light transmission variation after the sample was placed in the device resulted in an increase or decrease in the resistance signal of the CDS detector. The change in the resistance was then registered via a multimeter (METEX M3850D) using a computer interface. The signal was converted into turbidity (τ) using the following equation:

$$\tau = \frac{1}{L}\ln\left(\frac{I_0}{I}\right) = \frac{1}{L}\ln\left(\frac{R}{R_0}\right) \tag{4}$$

where τ is the turbidity, L is the light path length, I_o and I are the intensity of light detected with the clear sample (blank) and with samples to be measured, respectively. The light intensity was measured and registered as the resistance (R).

Coalescence samples were obtained by shaking the optimum middle phase microemulsions. The light source and detector were aligned at the center of the test tubes because of the relationship between the equilibrium state of microemulsions and corresponding macroemulsions formed upon shaking. The turbidity curve was reported as a plot of turbidity vs. time as macroemulsion droplets coalesce and the system approached the equilibrium microemulsion condition.

From the turbidity results, a plot of inverse turbidity ($\frac{1}{\tau}$) vs. time (t) yields the coalescence kinetic constant (k_c) of the corresponding macroemulsion at the optimum condition.

$$\frac{1}{\tau} = k_c t + \frac{1}{\tau_0} \tag{5}$$

where τ and τ_o are the turbidity of samples at time *t* and that of the blank solution [19].

Results and discussion

Extended surfactant properties and the Winsor R-ratio. In this study, the ability of extended surfactants to form microemulsions is evaluated in comparison to a conventional surfactant having the similar hydrophilic head and hydrocarbon tail. Due to a limited number of extended surfactants, the extended surfactant $C_{12,13}$-$(PO)_8$-SO_4Na (50 % branch) and the conventional surfactant C_{12}-SO_4Na or SDS were the closest pair available. A microemulsion phase study was performed with a wide

range of alkane oils by varying NaCl concentrations (salinity scan) at a constant 0.07 M surfactant concentration and controlled temperature of 27 ^{o}C.

In both cases, a typical phase transition (Winsor Type I ➔ Type III ➔ Type II) was observed with increasing NaCl concentrations. However, it must be noted that while the extended surfactant $C_{12,13}$-$(PO)_8$-SO_4Na alone was capable of forming all three Winsor-type microemulsions with the studied oils, the conventional SDS surfactant system required the addition of 8.4 %wt sec-butanol to do so. In the absence of sec-butanol, the SDS either precipitated or exhibited a phase separation under the studied conditions. Sec-butanol has commonly been added to prevent strong surfactant tail-tail interaction and thus reduce surfactant precipitation in many microemulsion formulations without altering the optimum salinity (S*) of the surfactant system [3, 4].

To have a fair comparison between the $C_{12,13}$-$(PO)_8$-SO_4Na and the SDS/sec-butanol systems, their microemulsion properties were evaluated at the optimum condition (in this case, the optimum salinity). Table 4.2 summarizes the crucial microemulsion properties (i.e. optimum salinity (S*), solubilization parameter (SP*), and interfacial tension (IFT*)) of the $C_{12,13}$-$(PO)_8$-SO_4Na and the SDS/sec-butanol systems. In keeping with the Winsor's R-concept [1, 2], the optimum middle phase microemulsion is obtained when R =1. The R-ratio equation is listed as follows [1, 2]:

$$R = \frac{A_{SO-NET}}{A_{SW-NET}} \tag{6}$$

where $A_{SO\text{-}NET}$ and $A_{SW\text{-}NET}$ represent the net interactions between the surfactant and oil and the surfactant and water, respectively. Since electrolyte is required to reduce the $A_{SW\text{-}NET}$ to match the $A_{SO\text{-}NET}$ value, lower S* values suggest a larger $A_{SO\text{-}NET}$ interaction. As shown in Table 4.2 for a given oil, the extended surfactant $C_{12,13}$-$(PO)_8$-SO_4Na exhibits lower S* than the conventional SDS surfactant and sec-butanol mixture. Recalling that the presence of sec-butanol does not affect the optimum salinity of the surfactant formulation, the lower S* value of the $C_{12,13}$-$(PO)_8$-SO_4Na serves as strong evidence of an enhanced interaction by the lengthening PO groups of the extended surfactant molecule.

Table 4.2. Comparison of microemulsion properties at the optimum condition between the $C_{12,13}H_{25,27}$-$(PO)_8$-SO_4Na, 100 B and the SDS/sec-butanol mixture for a wide range of alkane oils at constant 0.07 M surfactant concentration and 27 ^oC.

Oil	ACN	$C_{12,13}$-$(PO)_8$-SO_4Na, 50 B			C_{12}-SO_4Na + sec-butanol		
		S*[a] (%wt)	SP*[a] (mL/g)	IFT* (mN/m)	S* (%wt)	SP*[b] (mL/g)	IFT* (mN/m)
Octane	8	6.50	6.78	0.0132	16.5	1.78	0.0292
Decane	10	8.00	5.91	0.00900	18.5	1.40	0.0528
Dodecane	12	9.50	6.26	0.00490	20.0	1.27	0.0562
Hexadecane	16	12.5	5.56	0.00430	24.5	1.01	0.105

[a] S* = optimum salinity

[b] SP* = total volume of middle phase (mL)/grams of surfactant

Concurrent with the low S* results, the middle phase microemulsion formed by the $C_{12,13}$-$(PO)_8$-SO_4Na surfactant exhibits a milky-bluish phase rather than transparent one. Such a microemulsion appearance was also observed by Salager *et al.* [4] and reflects larger microemulsion aggregates, which is expected for microemulsion in which high solubilization and low IFT properties were attained. Corresponding with the phase behavior and low optimum salinity, Table 4.2 reports that the SP* value of $C_{12,13}$-$(PO)_8$-SO_4Na are approximately four- to five-fold higher than the SDS-sec-butanol system, while the IFT values are at least one order of magnitude lower than the conventional surfactant system containing the SDS and sec-butanol. Moreover, it is also interesting to note that the solubilization enhancement and IFT reduction of the $C_{12,13}$-$(PO)_8$-SO_4Na formulation are more pronounced with long-chain alkanes like dodecane or hexadecane than for the medium-chain octane. This indicates that the additional PO groups not only promote the surfactant-oil interaction, but also result in a more hydrophobic nature of the extended surfactant.

It is also observed that as the oil becomes more hydrophobic (as indicated by an increase in ACN value), a larger S* value is observed. For example, the S* of $C_{12,13}$-$(PO)_8$-SO_4Na increases from 6.5 to 12.5 wt% when going from octane (ACN of 8) to hexadecane (ACN of 16). This result is expected since larger oil molecules tend to strongly interact with each other causing a smaller net interaction between surfactant and oil molecules ($A_{SO\text{-}NET}$). Therefore, more electrolyte must be added to lower the $A_{SW\text{-}NET}$ to equal the new $A_{SO\text{-}NET}$ value.

Characteristic length and interfacial rigidity of extended surfactant membrane. As stated in the introduction section, we proposed that with additional PO in the surfactant tails, extended surfactants will provide higher characteristic length (thicker surfactant membrane) and more rigid surfactant membranes. Therefore, the focus of this section is to quantitatively determine the characteristic length and membrane rigidity of extended surfactant-based formulations at the optimum condition. The formation of middle phase microemulsions with hexadecane was carried out by a salinity scan at 27 ^{o}C. The characteristic length (ξ) and interfacial rigidity (E_r) at the optimum condition were calculated using Equation 1 and 3. Other important data such as the values of a_i are summarized in Table 4.1.

Table 4.3 summarizes the solubilization parameter, characteristic length and interfacial rigidity of conventional and extended surfactant formulations at the optimum condition. For a majority of surfactants studied, there is a consistent trend between solubilization parameter and characteristic length, except for the $C_{12,13}$-$(PO)_8$-SO_4Na, 50 %branch. We will focus on the ξ^* value as an indicator for system solubilization in later discussions. In the case of the conventional surfactant SDS and alcohol mixture, it is interesting to note that the calculated characteristic length is lower than the reported value for a usual tail length of SDS [18] (11.64 $\overset{o}{A}$ vs. 18 $\overset{o}{A}$). The low value of the characteristic length indicates a very weak interaction between surfactant and oil; emphasizing an incompatibility between the surfactant and oil. The poor interaction of the SDS/sec-butanol system with hexadecane is in good agreement with the fact that this formulation produces a sponge-phase

microemulsion rather than a Winsor Type III microemulsion. A sponge-phase microemulsion refers to a middle phase microemulsion with very little oil solubilized. According to Equation 3, the interfacial rigidity is strongly influenced by the characteristic length; so the interfacial rigidity (Er) of SDS/sec-butanol system is found to be very low (0.2 k_BT). A value of $E_r < 1\ k_BT$ is quite common for systems containing high amount of short-chain alcohol or hydrophilic linker [18, 19]. Furthermore, the low E_r value in the SDS/sec-butanol systems is also consistent with the fact that their emulsion droplets immediately coalesce and approach equilibrium quickly after shaking creased (≤ 10 minutes).

In contrast to the SDS/sec-butanol system, all extended surfactant systems shown in Table 4.3 exhibited much higher characteristic length. However, characteristic length values varied depending on the number of PO groups inserted in extended surfactant molecules and the degree of branching. The results show that within the same extended surfactant series ($C_{12,13}$-$(PO)_x$-SO_4Na, 100 %branch), the characteristic length of extended surfactant notably increases from 211.8 $\overset{o}{A}$ to 270.1 $\overset{o}{A}$ by increasing the PO group inserted from 4 to 8 PO groups. Since higher characteristic length means thicker surfactant membrane and a better solubilization power of microemulsion systems, this partially verifies that the inserting PO groups increase the total length of surfactant molecules. However to confirm the lengthening structure of extended surfactant, the molecular structure and arrangement of extended surfactant at the interface must be characterized by

microscopic techniques such as X-ray reflectivity, neutron scattering, and dynamic light scattering, which is beyond the scope of this work.

Table 4.3. Characteristic length (ξ^*), interfacial rigidity (E_r) at optimum conditions, and equilibration time of conventional surfactant and extended surfactant systems for hexadecane.

Surfactant system	S* (%wt)	IFT* (mN/m)	V_{mp} (mL)	SP*[a] (mL/g)	ξ^* ($\overset{o}{A}$)	E_r (k_BT)	Equilibration time
Conventional surfactant-alcohol							
SDS/sec-butanol	24.5	0.105	0.530	1.01	11.64	0.23	≤ 10minutes
Extended surfactants							
$C_{12,13}H_{25,27}$-$(PO)_4$-SO_4Na, 50 B	12.8	0.0101	4.38	7.12	211.8	6.9	≈ 2 weeks
$C_{12,13}H_{25,27}$-$(PO)_8$-SO_4Na, 50 B	8.00	0.00750	5.70	6.53	270.1	8.3	months
$C_{12,13}H_{25,27}$-$(PO)_8$-SO_4Na, 100 B	12.5	0.00430	4.25	5.56	310.3	6.3	days

[a] SP* = total volume of middle phase (mL)/grams of surfactants

Similar to the trend of characteristic length, the E_r values are found to increase by increasing the number of PO inserted in extended surfactants. The calculated E_r values for the $C_{12,13}$-$(PO)_4$-SO_4Na and $C_{12,13}$-$(PO)_8$-SO_4Na surfactants containing 100% branch are 6.9 k_BT and 8.3 k_BT respectively. From the literature [17], the E_r value for typical middle phase microemulsion systems corresponds with the bending modulus (K) of 1 k_BT, whereas the $E_r \approx 10$ k_BT refers to lipid bilayers. Based on this scale, the relatively high rigidity of the extended surfactant membrane leads to two speculations. First, it is possible that the extended surfactants may form a middle phase microemulsion that coexists with liquid crystals. These liquid crystals could wrap around the emulsion droplets, inhibiting droplets from coalescing [2, 26-28]. Since extended surfactants produce a milky-bluish middle phase microemulsions, they require the laboratory device other than crossed polarizers to detect the formation of liquid crystal. This avenue will be further investigated in future work.

Another potential explanation of the high rigidity film is that extended surfactants contain PO groups, which not only are bulky molecules, but also may obtain different molecular arrangements at the interface. The additional PO groups may arrange themselves to coil and uncoil depending on the degree of PO groups inserted and/or formulation condition as it does in the polyethylene oxide (POE) [23]. By such effects, it potentially provides a steric hindrance, further preventing the approach of dispersed emulsion droplets or a thinning of the plane-parallel film. High E_r values of extended surfactants are also consistent with the observation of

persistent macroemulsion droplets and long equilibration time. In the later section, the coalescence of extended surfactant-based systems will be addressed quantitatively, and then several approaches will be proposed to overcome this problem.

Furthermore, Table 4.3 also shows that the characteristic length decreases with an increase in the degree of branching (310.3 $\overset{o}{A}$ vs. 211.8 $\overset{o}{A}$ for 50 % branch and 100 % branch $C_{12,13}$-$(PO)_8$-SO_4Na surfactants, respectively). This trend makes sense as the more linear tails would be expected to have stronger interactions with the oil phase. On the basis of characteristic length results, we would expect that the $C_{12,13}$-$(PO)_8$-SO_4Na, 50% branch yields more rigid membrane than the $C_{12,13}$-$(PO)_8$-SO_4Na, 100% branch. However, the results reveal similar E_r values (6.3 vs 6.9 k_BT for 50 % branch and 100 % branch $C_{12,13}$-$(PO)_8$-SO_4Na surfactants, respectively). In addition, the E_r value does not correlate well with the equilibration time as it did in previous cases. From the phase behavior observation, it was found that the $C_{12,13}$-$(PO)_8$-SO_4Na, 50% branch produces middle phase microemulsion that reaches equilibrium much faster (days) than that of the $C_{12,13}$-$(PO)_8$-SO_4Na, 100% branch (months) in spite of the fact that the E_r values are similar. This leads us to suspect compositional variation/impurities between these two extended surfactants may cause these observed trends. To our knowledge, the $C_{12,13}$-$(PO)_8$-SO_4Na with 50 % branch and the $C_{12,13}$-$(PO)_8$-SO_4Na, 100 % branch were produced from the different hydrocarbon feedstock (South Africa and Italy, respectively), thus it is possible that they might contain different types and degrees of impurities. Therefore, to further

investigate the effect of branching on the morphology of surfactant membrane will require extended surfactants with a high purity grade and controlled composition/impurities, which are not currently available.

Fish diagram of a single extended surfactant. An alternative way to represent microemulsion phase behavior is a gamma or fish diagram. This type of representation allows us to map a complete phase boundary (Winsor Type, I, II, III, and IV) as a function of surfactant and electrolyte concentrations. Since our knowledge on this relatively new class of extended surfactant-based microemulsions is still limited, it is valuable to examine the fish diagram of extended surfactant-based microemulsions. The $C_{12,13}$-$(PO)_8$-SO_4Na (50 % branch) was selected to demonstrate the fish diagram in this section. As discussed above, this extended surfactant has demonstrated to be a highly desirable candidate for forming microemulsions with long-chain alkanes. Therefore, the fish diagram of this extended surfactant will be established using hexadecane as a studied oil at controlled temperature of 27 ^{o}C.

Figure 4.3 shows a plot between surfactant concentrations (M) and salinity (wt%) of the $C_{12,13}$-$(PO)_8$-SO_4Na/brine/hexadecane system. From the plot, the microemulsion phase behavior is often portrayed in the gamma or fish-like shape, thus it is commonly referred as the gamma or fish diagram. The fish-shape boundary indicates the regions where the Winsor Type I, Type III and Type II microemulsions are formed, while the middle dashed-line specifies the optimal salinity at the given surfactant concentration.

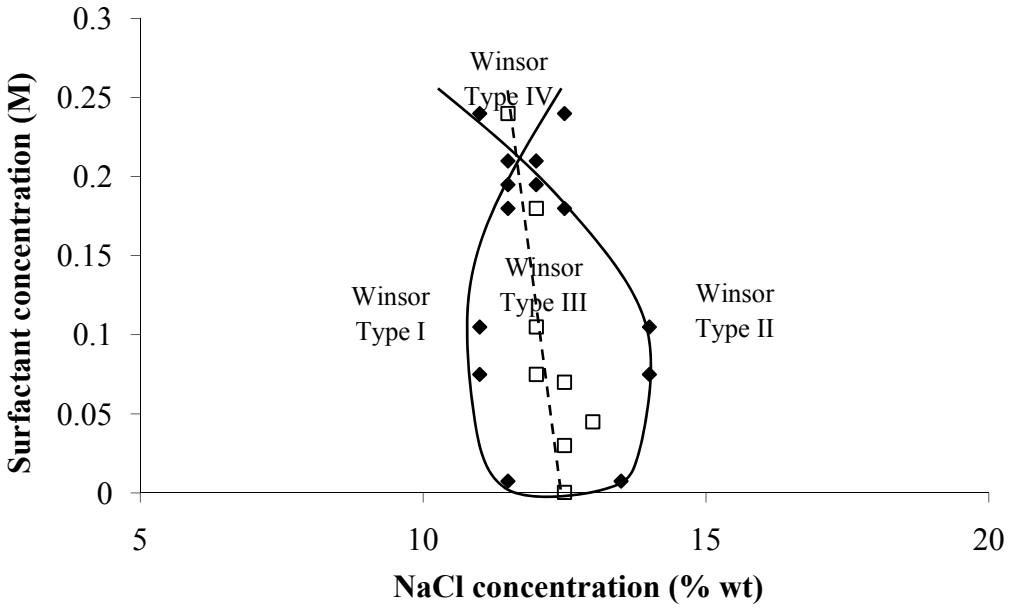

Figure 4.3. Fish diagram of the $C_{12,13}$-$(PO)_8$-SO_4Na, 50 B/brine/hexadecane microemulsion at constant 27 ^oC and W/O ratio = 1.

In addition to phase transition boundary, the fish diagram also offers two key surfactant concentrations, the critical microemulsion concentration (CμC) and the lowest surfactant concentration where a single phase (or Winsor Type IV) microemulsion is formed. This information is highly valuable for developing a cost-effective formulation. The critical microemulsion concentration (or CμC) is located at the bottom of the fish diagram boundary (at low surfactant concentration), yielding the minimum surfactant concentration required to form the first drop of middle phase microemulsion and attain the low IFT property [7, 20]. Conversely, the point in which three-phase lines merge at high surfactant concentrations indicates the lowest surfactant concentration where the Winsor Type IV system is observed (the entire volume of oil and water coexist in a single bicontinuous microemulsion phase). In

other words, this tri-critical point is an indicator of the solubilization capacity of surfactant formulation [2, 4]. Lower surfactant concentrations required to form the Type IV microemulsion indicate a better solubilization power of a system. From Figure 4.3, the CμC value and tri-critical point of the $C_{12,13}$-$(PO)_8$-SO_4Na surfactant are reported at 0.37 mM (0.03 wt%) and 0.20 M (13 wt%), respectively.

The fish diagram of the $C_{12,13}$-$(PO)_8$-SO_4Na, 50B shows a vertical orientation similar to what is typically observed for a high-purity single component conventional anionic surfactant system. There is very slight incline to the left at high surfactant concentrations. This slight slant which suggests stronger partitioning of surfactants into the oil phase at high concentrations, resulting in a larger surfactant-oil interaction and thus requiring less salt to maintain the R =1. The increase in the partitioning of the $C_{12,13}$-$(PO)_8$-SO_4Na, 50B at high concentration is attributed to heterogeneity in the PO distribution and hydrocarbon-tail length as well as the presence of impurities (e.g. unsulfated propoxylated alcohol) in the extended surfactant samples.

Approaches to the fast kinetics of coalescence in extended surfactant-based microemulsions. Recall that the macroemulsion droplets are generated by shaking equilibrium microemulsion samples. Therefore, the time required for the macroemulsion droplets to coalesce (coalescence rate) is representative of the equilibration time for the microemulsion systems. With the knowledge of interfacial rigidity (E_r) established above, extended surfactants are expected to have a rigid interfacial membrane, and thus demonstrate a slow coalescence rate. Therefore, in

this section we will introduce an approach to overcome the slow kinetics of coalescence while still maintaining desirable microemulsion properties

To enhance the rate of coalescence, the rigidity of extended surfactant membrane must be reduced. Literature reports [2-4, 15, 19, 21, 29-31] demonstrate an outstanding role of short-chain alcohols, linkers, and co-surfactants in decreasing the film rigidity. However, whether alcohols, linkers or co-surfactants are used, they must be selected with caution. On one hand, the presence of these compounds at the interface provides a disorder and flexibility to the surfactant membrane, leading to faster coalescence rate. On another hand, their presence at the interface can significantly reduce the surfactant interaction with water and oil phases, thus affecting the solubilization capacity and IFT property of the systems.

In this work, linker and co-surfactant molecules were utilized to modify the rigidity of extended surfactant membrane. The extended surfactant studied in this work was the $C_{12,13}$-$(PO)_4$-SO_4Na, 100 %branch; it was evaluated alone and in combinations with linkers and the co-surfactant. The four extended surfactant systems evaluated were the $C_{12,13}$-$(PO)_4$-SO_4Na-alone, the $C_{12,13}$-$(PO)_4$-SO_4Na/SMDNS/dodecanol, the $C_{12,13}$-$(PO)_4$-SO_4Na-/SMDNS/oleyl alcohol, and the $C_{12,13}$-$(PO)_4$-SO_4Na/AOT systems. The extended surfactant $C_{12,13}$-$(PO)_4$-SO_4Na was utilized at constant concentration of 0.07 M, unless stated otherwise. The amount of hydrophilic (SMDNS) and lipophilic linkers (dodecanol or oleyl alcohol) added was kept constant at 0.03 M. In the case of the $C_{12,13}$-$(PO)_4$-SO_4Na/AOT system, the total surfactant concentration was fixed at 0.07 M with the 50/50 $C_{12,13}$-$(PO)_4$-

SO_4Na-to-AOT ratio. The formation of middle phase microemulsion was carried out with hexadecane at 27 ^oC. In addition to quantifying the E_r value, to verify a change in the rigidity of interfacial membrane, the coalescence rates in the extended surfactant-alone and mixed formulations were tracked by the turbidity technique utilized by Acosta *et al.* [19].

Similar to Table 4.3, Table 4.4 summarizes the ξ^* and E_r values of the extended surfactant and mixtures at the optimum condition. Compared to the $C_{12,13}$-$(PO)_4$-SO_4Na-alone system, the ξ^* and E_r values decrease considerably with the addition of combined linkers and the co-surfactant AOT, while the IFT values remain relatively constant. This result highlights that the extended surfactant is a key component in producing the low IFT property. As mentioned above, the presence of additives like linkers or co-surfactants produces two different effects. A reduction in the ξ^* value indicates the decrease in the solubilization, while a decrease in E_r value suggests a less rigid surfactant membrane, which results in a faster coalescence rate (also a faster equilibration time).

Table 4.4. Characteristic length (ξ^*), interfacial rigidity (E_r), and coalescence rate constant (K_c) of the $C_{12,13}$-$(PO)_4$-SO_4Na-alone and mixture systems at the optimum middle phase hexadecane microemulsions and 27 ^oC. The $C_{12,13}$-$(PO)_4$-SO_4Na concentration was fixed at 0.07 M, unless stated otherwise. The ratio of SMDNS/lipophilic linker was kept constant at 0.03 M and added on the top of the 0.07 M $C_{12,13}$-$(PO)_4$-SO_4Na concentration. The ratio of $C_{12,13}$-$(PO)_4$-SO_4Na/AOT used was the 50/50 at constant 0.07M total surfactant concentrations.

Surfactant system	S* (%wt)	IFT* (mN/m)	V_{mp} (mL)	SP*[a] (mL/g)	ξ^* ($\overset{o}{A}$)	E_r (k_BT)	k_c (cm/min)	Equilibration time
$C_{12,13}H_{25,27}$-$(PO)_4$-SO_4Na	12.8	0.0101	4.38	7.12	211.8	6.9	4.0E-03	≈ 2 weeks
$C_{12,13}H_{25,27}$-$(PO)_4$-SO_4Na + SMDNS + dodecanol	17.5	0.0101	2.65	4.31	113.8	2.3	1.2E+00 ± 9.2E-02	≤ 10 minutes
$C_{12,13}H_{25,27}$-$(PO)_4$-SO_4Na + SMDNS + Oleyl alcohol	16.0	0.0117	3.18	5.17	136.3	2.9	3.9E-01 ± 3.5E-04	≤ 10 minutes
$C_{12,13}H_{25,27}$-$(PO)_4$-SO_4Na + AOT	5.80	0.0099	1.72	2.47	96.5	1.4	3.4E-01 ± 2.3E-02[b] 2.1E+01 ± 2.3E-02[c]	≤ 10 minutes

[a] SP* = total volume of middle phase (mL)/grams of surfactants

[b] the k_c value calculated from the first slope

[c] the k_c value calculated from the second slope

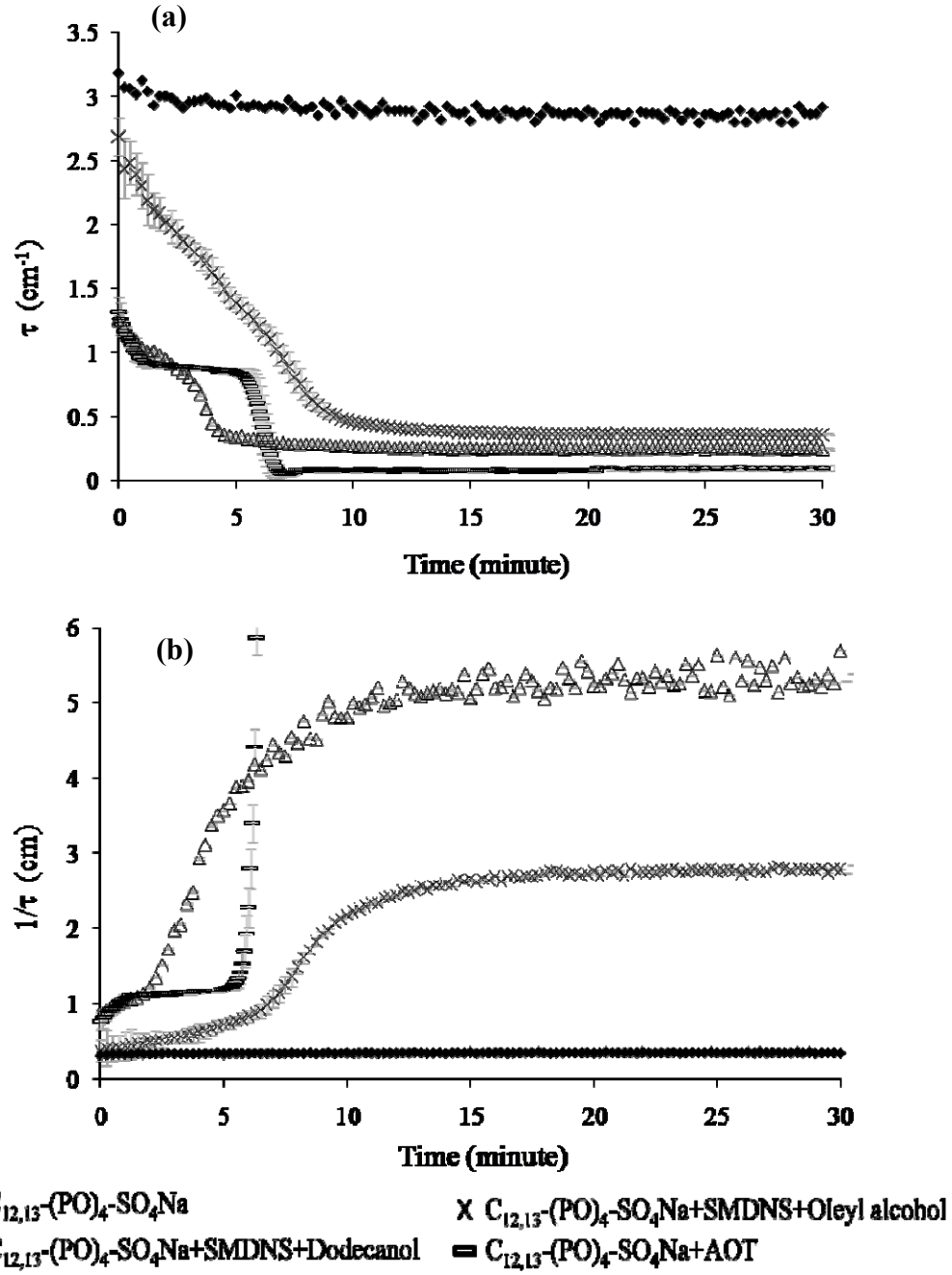

Figure 4.4. The turbidity (a) and inverse turbidity (b) curves during coalescence at 27 ^{o}C of the samples containing the 0.07 M $C_{12,13}$-$(PO)_4$-SO_4Na-alone, the 0.07 M $C_{12,13}$-$(PO)_4$-SO_4Na/0.03M SMDNS/0.03 M dodecanol, the 0.07 M $C_{12,13}$-$(PO)_4$-SO_4Na/0.03M SMDNS/0.03 M Oleyl alcohol, and the 0.035 M $C_{12,13}$-$(PO)_4$-SO_4Na/0.035 M AOT mixtures. Turbidity samples resulted from shaking the optimum middle phase hexadecane microemulsions.

Illustrated in Figure 4.4a is the turbidity curves during coalescence of macroemulsion made from the optimum Winsor III microemulsions of the extended surfactant-alone and the extended surfactant plus additive systems. The results show that the turbidity curve of a single $C_{12,13}$-$(PO)_4$-SO_4Na surfactant remains relatively constant over the entire study period (total of one hour), while the turbidity of the $C_{12,13}$-$(PO)_4$-SO_4Na-mixtures drop quickly and reaches a plateau within 10 minutes. It is noted that the turbidity curve is then correlated to the coalescence kinetic constant (k_c) by Equation 5 (repeated here for convenience):

$$\frac{1}{\tau} = k_c t + \frac{1}{\tau_0} \tag{5}$$

High k_c values indicate the fast coalescence of macroemulsions and quick equilibration time of microemulsion.

Figure 4.4b present the inverse turbidity curve for the same systems plotted in Figure 4.4a. Among formulations, the steepest slope (highest k_c value) is observed with the $C_{12,13}$-$(PO)_4$-SO_4Na/SMDNS/dodecanol system, while the smallest slope (smallest k_c value) is attained with the $C_{12,13}$-$(PO)_4$-SO_4Na-alone system. The calculated k_c values of studied systems are listed in Table 4.4. From Table 4.4, the $C_{12,13}$-$(PO)_4$-SO_4Na/SMDNS/dodecanol system has a k_c value three orders of magnitude higher than the $C_{12,13}$-$(PO)_4$-SO_4Na-alone system (1.2 E+00 vs. 4.0E-03 cm/s, respectively) indicating a faster coalescence rate while still providing good solubilization capacity and low IFT properties. Another added benefit of the linker modified formulation is that the magnitude of solubilization power, IFT reduction

and the kinetics of coalescence can be adjusted/optimized by simply changing the type of linker molecules as seen in the example of $C_{12,13}$-$(PO)_4$-SO_4Na-/SDMNS/oleyl alcohol formulation.

In the case of the $C_{12,13}$-$(PO)_4$-SO_4Na/AOT system, the turbidity plot shows a two-step reduction in turbidity (Figure 4.4a), which is different from prior systems. In our previous work [9], we introduced the σ parameter as a surfactant characteristic scale, alternative to the HLB number. Based on the basis of σ values, AOT was found to be much more hydrophobic than the extended surfactants. By considering the difference in their hydrophilic-lipophilic nature, it is suggested that the system with $C_{12,13}$-$(PO)_4$-SO_4Na and AOT may produce two different types of surfactant membranes or may transition over time in the composition at the interface, with the high ratio of AOT-to- $C_{12,13}$-$(PO)_4$-SO_4Na exhibiting different properties than the high fraction of $C_{12,13}$-$(PO)_4$-SO_4Na at the interface. This conclusion is speculative and should be explored in future research. In Table 4.4, two distinctive k_c values are calculated from the individual slopes in the $C_{12,13}$-$(PO)_4$-SO_4Na/AOT system. In addition, although the bicontinuous middle phase (MP) tends to be the continuous phase in macroemulsion systems, given the fact of disproportionate volumes between the bicontinuous micellar solution and excess oil and water phases, this MP phase also favor to be the dispersed phase. Therefore, in the case of the Winsor III microemulsion, it possibly consists of the coalescence of multiple emulsion systems (O/W, W/O, O/MP, and W/MP) and the coalescence rates are slowest for systems containing the MP as a continuous phase [22, 32]. Regarding this fact, it is possible

that the $C_{12,13}$-$(PO)_4$-SO_4Na/AOT system may produce multiple emulsions. A similar observation was also reported by Witthayapanyanon [33], who utilize various blending ratios between the extended surfactant and AMA surfactants. Further study is required to gain an improved understanding of this mixture behavior.

Acknowledgements

Funding for this research was provided by industrial sponsors of the Institute for Applied Surfactant Research at University of Oklahoma. The authors would like to extend deep appreciation to Geoff Russell and Victoria Stolarski, Sasol North America (Lake Charles, LA) for providing extended surfactant samples.

References

[1] Winsor PA (1948) Solvent Properties of Amphiphilic Compounds. Trans. Faradays Soc. 44: 736.

[2] Bourrel M, Schecter R (1988) Microemulsions and Related Systems, Marcel Dekker New York.

[3] Salager JL (1999) Microemulsions. In Broze G (ed) Handbook of Detergents: Part A: Properties. Marcel Dekker, New York, pp 253-302.

[4] Salager JL, Anton RE, Sabatini DA, Harwell JH, Acosta EJ, Tolosa LI (2005) Enhancing Solubilization in Microemulsions – State of the Art and Current Trends. J. Surfact. Deterg. 8(1): 3-21.

[5] Miñana-Pérez M, Graciaa A, Lachaise J, Salager JL (1995) Solubilization of Polar Oils with Extended Surfactants. Colloid Surfaces A 100: 217-224.

[6] Acosta E, Mai PD, Harwell JH, Sabatini DA (2003) Linker-Modified Microemulsions for a Variety of Oils and Surfactants. J. Surf. Deterg. 6(4): 353-363.

[7] Witthayapanyanon A, Acosta EJ, Harwell JH, Sabatini DA (2006) Formulation of Ultralow Interfacial Tension Systems Using Extended Surfactants. J. Surf. Deterg. 9(4): 331-339.

[8] Do L, Witthayapanyanon A, Harwell JH, Sabatini DA Environmentally friendly Vegetable Oil Microemulsions Using Extended-Surfactants and Linkers. submitted to J. Surf. Deterg.

[9] Witthayapanyanon A, Harwell JH, Sabatini DA (2008) Hydrophilic-Lipophilic Deviation (HLD) Method for Characterizing Conventional and Extended Surfactants. J. Colloid Interface Sci. 325: 259-266.

[10] Childs J, Acosta EJ, Scamehorn JF, Sabatini DA (2005) Surfactant-Enhanced Treatment of Oil-Based Drilling Cuttings. J. Energy Res. Technol. 127: 153-162.

[11] Yanatatsaneejit U, Rangsunvigit P, Scamehorn JF, Chavadej S (2005) Removal by Froth Flotation Under Low Interfacial Tension Conditions I: Foam Characteristics, Coalescence Time, and Equilibrium Time. Sep. Sci. Technol. 40: 1537.

[12] Scriven S (1976) Equilibrium Bicontinuous Structure. Nature 263: 123-124.

[13] Clausse M, Peyrelasse J, Heil J, Boned C, Lagourette B (1981) Bicontinuous Structure in Microemulsions. Nature 293: 636-638.

[14] Auvray L, Cotton JP, Ober R, Taupin C (1984) Evidence for Zero Mean Curvature Microemulsions. J. Phys. Chem. 88: 4586-4589.

[15] De Gennes PG, Taupin C. (1982) Microemulsions and the Flexibility of Oil/Water Interfaces. J. Phys. Chem. 86: 2294-2304.

[16] Acosta E (2004) Modeling and Formulation of Microemulsions: the Net-Average Curvature Model and the Combined Linker Effect. Dissertation, University of Oklahoma.

[17] Microemulsions. http://www.chm.bris.ac.uk/eastoe/surf_Chem/3%20Microemulsions.pdf.

[18] Acosta EJ, Szekeres, E, Harwell JH, Sabatini DA (2003) Net-Average Curvature Model for Solubilization and Supersolubilization in Surfactant Microemulsions. Langmuir 19: 186-195.

[19] Acosta EJ, Le MA, Harwell JH, Sabatini DA (2003) Coalescence and Solubilization Kinetics in Linker-Modified Microemulsions and Related Systems. Langmuir 19: 566-574.

[20] Acosta EJ, Harwell JH, Sabatini DA (2004) Self-Assembly in Linker-Modified Microemulsions. J. Colloid Interface Sci. 274: 652-664.

[21] Sabatini DA, Acosta E, Harwell JH (2003) Linker Molecules in Surfactant Mixtures. Current Opinion in Colloid and Interface Sci. 8: 316-326.

[22] Binks BP (1998) Emulsions-Recent Advances in Understanding. In Binks BP (ed) Modern Aspects of Emulsion Science, Royal Society of Chemistry, Great Britain, pp 1-55.

[23] Rosen MJ (2004) Surfactants and Interfacial Phenomena, John Wiley, New Jersey.

[24] Helfrich WZ (1973) Naturforsch. 28C: 693.

[25] Langevin D, Meunier J (1994) Interfacial Tension: Theory and Experiment. In Gelbart WM, Ben-Shaul A, Roux D (eds) Micelles, Membranes, Microemulsions and Monolayers. Springer-Verlag, New York.

[26] Tolosa LI, Forgiarini A, Moreno P, Salager JL (2006) Combined Effects of Formulation and Stirring on Emulsion Drop Size in the Vicinity of Three-Phase Behavior of Surfactant-Oil-Water Systems. Ind. Eng. Chem. Res. 45: 3810-3814.

[27] Wasan DT, McNamara JJ, Shaw SM, Sampath K, Aderangi N (1979) The Role of Coalescence Phenomena and Interfacial Rheological Properties in Enhanced Oil Recovery: an Overview. J. Rheol. 23(2): 181-207.

[28] Flumerfelt RW, Catalano AB, Tong CH (1981) the Coalescence Chatacteristics of Low Tension Oil-Water-Surfactant Systems. Proceeding of Symposium on Surface Phenomena for Enhanced Oil recovery, pp 571.

[29] Kazlov MM, Helfrich W (1992) Effects of a Cosurfactant on the Stretching and Bending Elasticities of a Surfactant Monolayer. Langmuir 8: 2792-2797.

[30] Gradzielski M (1998) Effect of the Cosurfactant Structure on the Bending Elasticity in Nonionic Oil-in-Water Microemulsions. Langmuir 14: 6037-6044.

[31] Meglio JM, Dvolaitzky M, Taupin C (1985) Determination of the Rigidity Constant of the Amphiphilic Film in “Birefringent Microemulsions”: the Role of the Cosurfactant. J. Phys. Chem. 89: 871-874.

[32] Hazlett RD, Schecter RS (1988) Stability of Macroemulsions. Colloids and Surfaces 29: 53-69.

[33] Witthayapanyanon A (2008) Extended Surfactants: Characterization and Microemulsion Properties. Dissertation, University of Oklahoma.

CHAPTER 5

Conclusions

The purpose of this chapter is to summarize important findings/understandings gained in the individual sections of this dissertation. This will be done by looking at major conclusions from each chapter, with some final conclusions at the end.

Chapter 2 investigated the role of additional PO and EO groups inserted in extended surfactant molecules in reducing IFT for a wide range of oils (e.g. hexadecane, triglycerides and vegetable oils). The dynamic IFT study was examined using two dilute extended surfactant formulations, sodium polypropyleneoxide sulfate ($R\text{-}(PO)_x\text{-}SO_4Na$), and sodium alkyl popypropyleneoxide-polyethyleneoxide sulfate ($R\text{-}(PO)_y\text{-}(EO)_2\text{-}SO_4Na$). The results showed that these intermediate groups provide an additional length to extended surfactant molecules, extending the extended surfactant further into the oil and water phases. This results in a stronger interaction between surfactant and oil (larger A_{SO}) and a corresponding larger surfactant-water interaction (A_{SW}). As predicted by Winsor's concept, systems with an equal increase in both A_{SO} and A_{SW} interactions attained the ultralow IFT property. Furthermore, when the oils studied were triolein and vegetable oils, the PO-EO extended surfactant offered superior IFT reduction capability as compared to PO-extended surfactants. In addition to the ultralow IFT property, extended

surfactants also exhibited low critical micelle concentration (CMC) and critical microemulsion concentration (CμC) as compared to other surfactants.

Another significant finding in Chapter 2 was the unexpected hydrophilic nature of triolein oil. Based on the equivalent alkane carbon number (EACN) estimation of the hydrophilic-lipophilic deviation (HLD), it was found that triolein behaved as a very polar oil, while all other vegetable oils displayed very hydrophobic behavior. This anomalous characteristic of triolien was suspected to be due to uncharacterized impurities (fatty acid and monoglyceride) in the triolein sample. One final remark from this chapter was that the HLB number did not correlate well with the hydrophilic-lipophilic nature of extended surfactants, probably due to a slightly polar environment induced by the presence of the PO groups.

In Chapter 3, while the overall goal was to utilize existing empirical models as a quick and easy-to-use tool for guiding the formation of extend-surfactant-based microemulsions, this effort first required an accurate determination of the hydrophilic-lipophilic nature of extended surfactants. As mentioned previously, the frequently used HLB number had failed to evaluate the extended surfactant hydrophilicity/lipophilicity because of their distinctive PO and EO attachment. In this work, the surfactant characteristic (σ) and associated σ/K parameters of the HLD expression were proposed as alternative surfactant behavior indicator for both conventional and extended surfactants. These parameters were easily characterized by means of a simple HLD technique and the use of mixed surfactant approach.

A major finding of Chapter 3 was that the hydrophilic-lipophilic behavior of both conventional and extended surfactant were very well defined by the σ and σ/K indexes. Regarding the σ basis, the more negative σ values corresponded with the more hydrophilic surfactant and the tendency to form O/W microemulsions, while the more positive σ values implied the more hydrophobic surfactants and the formation of W/O microemulsions.

In the case of extended surfactants, the σ parameter was found to capture the nature of extended surfactants better than the σ/K parameter. Additionally, the σ index was proven to be a more adequate indicator for representing extended surfactant characteristics than the HLB number. Further investigation revealed the opposite effect of adding PO vs. EO groups on the σ parameter. While the addition of PO groups increased the σ parameter to more positive values, suggesting a more hydrophobic extended surfactant, the presence of EO groups resulted in a more negative σ values, indicating a more hydrophilic surfactant. Furthermore, the σ parameter was also found to be very sensitive to the branching of surfactant hydrocarbon tails. The discussion was concluded by demonstrating the practical use of the combined HLD-established σ technique to predict the optimum salinity for microemulsions systems.

While collecting the experimental data for Chapter 2 and 3, the slow kinetics of extended-surfactant-based-microemulsions became painfully apparent. For example, the equilibration time reported for the optimum middle phase microemulsions of extended surfactants was often in the range of weeks to months.

Hence, although extended surfactants offered great potential based on their equilibrium IFT and solubilization properties, their practical utility is limited by this slow dynamic feature. It was found that the time for extended-surfactant-based-microemulsions to approach equilibrium was related to the coalescence rate of their corresponding macroemulsion droplets. These observations raised an interest in characterizing the film properties in extended surfactant systems.

The study in Chapter 4 displayed both equilibrium and kinetic aspects of extended-surfactant-based microemulsions as stated previously. From an equilibrium standpoint, extended surfactants showed an outstanding performance in forming the middle phase microemulsion with highly hydrophobic alkanes, superior to conventional surfactants. The fish diagram of extended surfactant/hexadecane/brine system was found to have a vertical orientation similar to those of high-purity single conventional anionic surfactant; the very slight incline to the left at high extended surfactant concentrations.

The interfacial morphology (characteristic length (ξ) and interfacial rigidity (E_r)) of the extended surfactant membrane was characterized using the net-average curvature model. As hypothesized, extended surfactants produced a thick and rigid surfactant membrane (high ξ and E_r values), thus demonstrating a slow coalescence rate and a prolonged equilibration time of their microemulsions. The results showed that the addition of PO groups played an important role in increasing both ξ and E_r values. A relatively high rigidity of extended surfactant membrane led to two

potential explanations; the formation of coexisting liquid crystal and the strong steric hindrance caused by the unique structure of extended surfactants.

With the knowledge of E_r basis, the coalescence rate in extended surfactant systems could be expedited by reducing the rigidity of extended surfactant membrane. Therefore, the last topic in Chapter 4 was to demonstrate the use of combined linker and co-surfactant approach to overcome the slow kinetics of coalescence while still maintaining desirable microemulsions properties. The remarkable findings of this section were that the addition of additives produced two different effects; the advantageous E_r reduction, resulting in a faster coalescence rate, and the detrimental decrease in solubilization capacity of systems. The choice of additives must be made carefully to optimize the best equilibrium and dynamic benefits. Moreover, it must be highlighted that extended surfactants were a key composition in achieving low IFT property. Lastly, the coalescence behavior of the conventional and extended surfactant mixture was addressed and discussed. However, further study is necessary to gain an improved understanding of this mixture behavior.

Finally, with the knowledge established in this work, the author hopes that formulating microemulsion using extended surfactants has been advanced in understanding and application. Thus formulators should be able to engineer the systems to achieve desirable microemulsion properties, both equilibrium and dynamic, suitable for widely varying applications.

APPENDIX A

Dynamic Interfacial Tension and the Critical Micelle Concentration (CMC) of Extended Surfactants (Chapter 2)

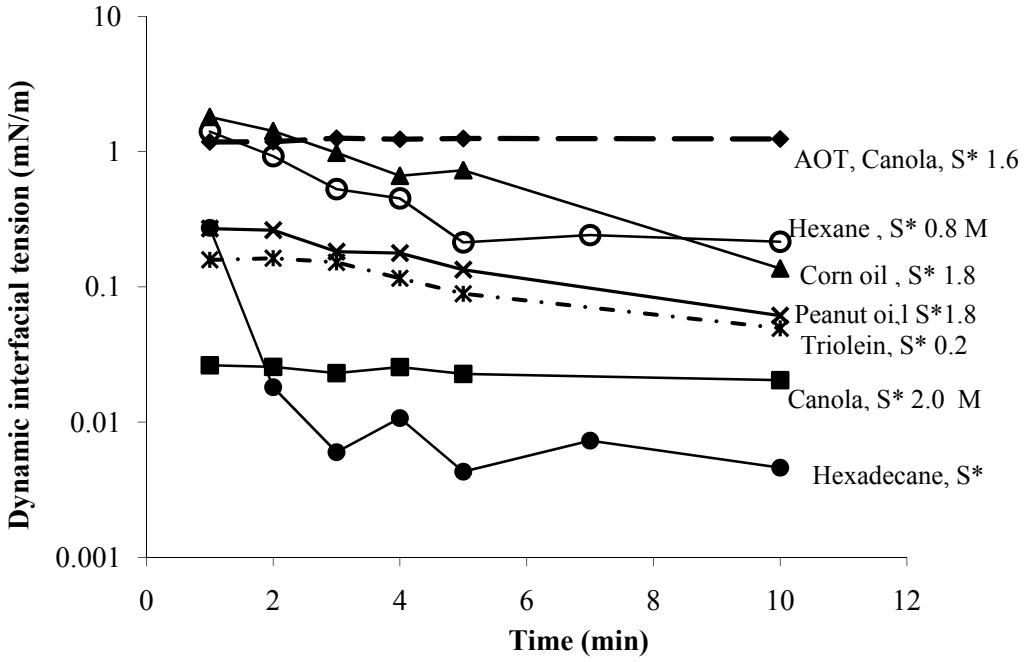

Figure 1. Dynamic IFTs at 10 min of various oils of 0.2 wt% $C_{14\text{-}15}$-$(PO)_8$-SO_4Na extended surfactant (except Canola, S* 1.6M used AOT), optimum salinity.

Table 1 Critical micelle concentration (CMC) and cross-sectional area (a_i) of extended surfactants without and with NaCl addition.

Extended surfactants	HC	% branch	# PO	# EO	No NaCl		0.2 M NaCl	
					CMC (μM)	a_i (Å^2)	CMC (μM)	a_i (Å^2)
R-$(PO)_x$-SO_4Na, 1st batch*								
$C_{12,13}H_{25,27}$-$(PO)_8$-SO_4Na	12, 13	100	8	-	130	153	14.0	68.0
$C_{14,15}H_{29,31}$-$(PO)_3$-SO_4Na	14, 15	100	3	-	253	141	20.0	44.6
$C_{14,15}H_{29,31}$-$(PO)_5$-SO_4Na	14, 15	100	5	-	60.0	133	11.7	80.5
$C_{14,15}H_{29,31}$-$(PO)_8$-SO_4Na	14, 15	100	8	-	33.4	134	5.00	116
$C_{12,13}H_{25,27}$-$(PO)_8$-SO_4Na	12, 13	50	8	-	171	139	24.5	96.1
R-$(PO)_x$-SO_4Na, 2 nd batch**								
$C_{12,13}H_{25,27}$-$(PO)_4$-SO_4Na	12, 13	100	4	-	75.3	172	25.0	145
$C_{12,13}H_{25,27}$-$(PO)_8$-SO_4Na	12, 13	100	8	-	50.6	121	2.50	61.7
$C_{14,15}H_{29,31}$-$(PO)_4$-SO_4Na	14, 15	100	4	-	94.6	117	3.00	46.1
R-$(PO)_y$-$(EO)_2$-SO_4Na*								
Linear $C_{12}H_{25}$-$(PO)_{14}$-$(EO)_2$-SO_4Na	12	linear	14	2	80.0	200	8.00	147

* CMC measurement at 30 ^oC

** CMC measurement at 27 ^oC

APPENDIX B

K- AND σ–Values of Conventional and Extended Surfactants

(Chapter 3)

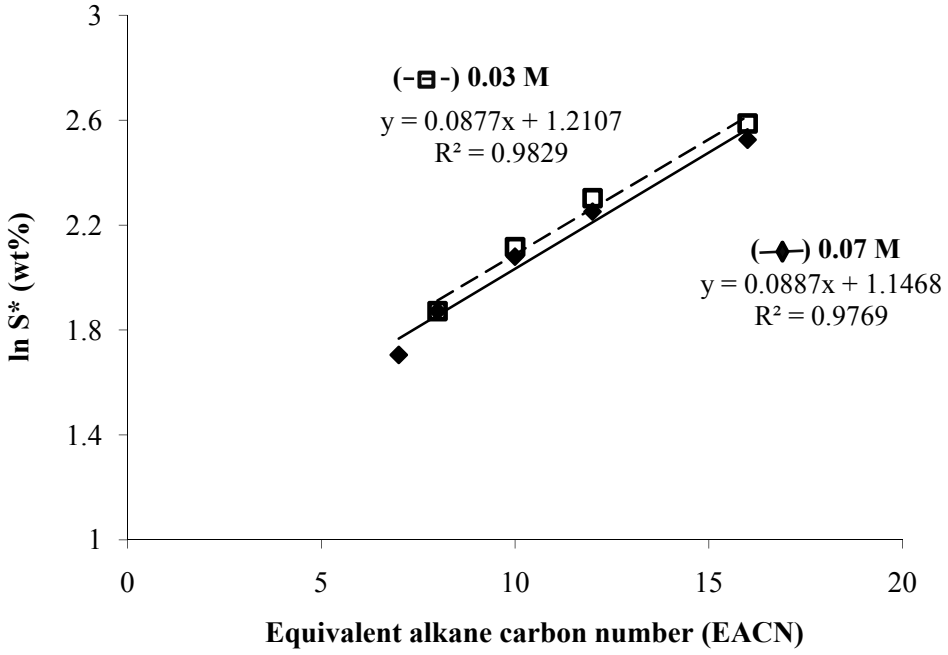

Figure 1. Verifying the independency of the K-constant of the HLD equation for the C12,13-(PO)8-SO4Na surfactant (50% branch) using microemulsion phase study at 0.03 M and 0.07 M surfactant concentrations and 25 ^{o}C.

Table 1. Comparison the optimum salinity (S^*) between the 0.07 M $C_{12,13}$-$(PO)_8$-SO_4Na-alone and the mixed 0.07 M $C_{12,13}$-$(PO)_8$-SO_4Na- 6.3 %wt sec-butanol systems at 25 ^oC.

Oil	EACN	$C_{12,13}$-$(PO)_8$-SO_4Na-alone	$C_{12,13}$-$(PO)_8$-SO_4Na-sec-butanol
		S* (%wt)	S* (%wt)
Pentane	5	unable to form MP	2.20
Heptane	7	5.5	3.50
Octane	8	6.5	4.00
Decane	10	8	5.50
Dodecane	12	9.8	7.50
Hexadecane	16	12.5	12.50

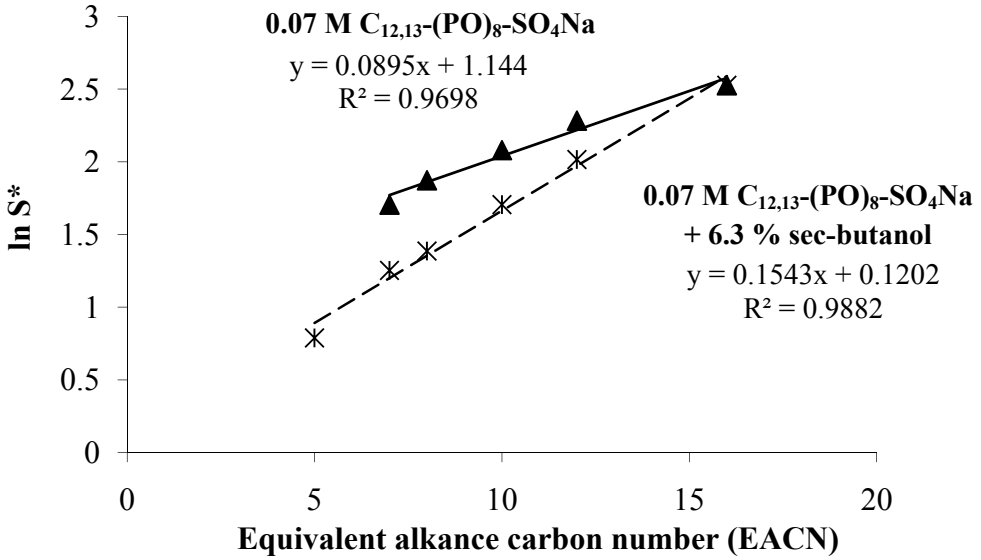

Figure 2. Effect of sec-butanol addition on the K-value of the extended surfactant system. The extended surfactant evaluated was the $C_{12,13}$-$(PO)_8$-SO_4Na (50 %branch) using microemulsion phase study at 0.07 M surfactant concentration and 25 ^oC (plotting from data reported in Table).

Table 2. Comparison of *K*-values at various ratios of AMA to $C_{12,13}$-$(PO)_8$-SO_4Na concentrations in the AMA/ C12,13-(PO)8-SO4Na/limonene/brine system, (a) a linear mixing rule prediction and (b) experimental phase studies at constant 0.07 M total surfactant concentration and 25 ^oC.

Mole fraction of surfactant 2(x_2)	Linear mixing rule		Experimental data		
		slope (K)		Intercept	
	$K_{prediction}$	K_{exp}	±	σ_{mix}	±
0	0.1600	0.1728	0.0188	-0.9333	0.1106
0.2	0.1412	0.1089	0.0192	-1.3360	0.1627
0.4	0.1224	0.0951	0.0180	-1.4390	0.1553
0.5	0.1131	0.0930	0.0184	-1.5214	0.1623
0.8	0.0849	0.0922	0.0006	-1.3796	0.0059
1	0.0661	0.0661	0.0122	-1.5476	0.1453

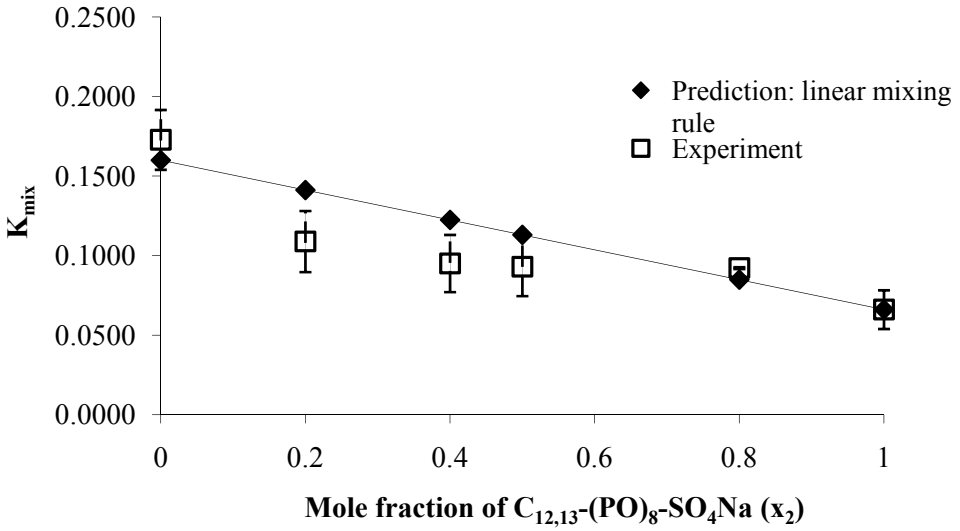

Figure 3. Comparison of *K*-values at various ratios of AMA to $C_{12,13}$-$(PO)_8$-SO_4Na concentrations in the AMA/ C12,13-(PO)8-SO4Na/limonene/brine system, (a) a linear mixing rule prediction and (b) experimental phase studies at constant 0.07 M total surfactant concentration and 25 ^oC (plotting from data reported in Table).

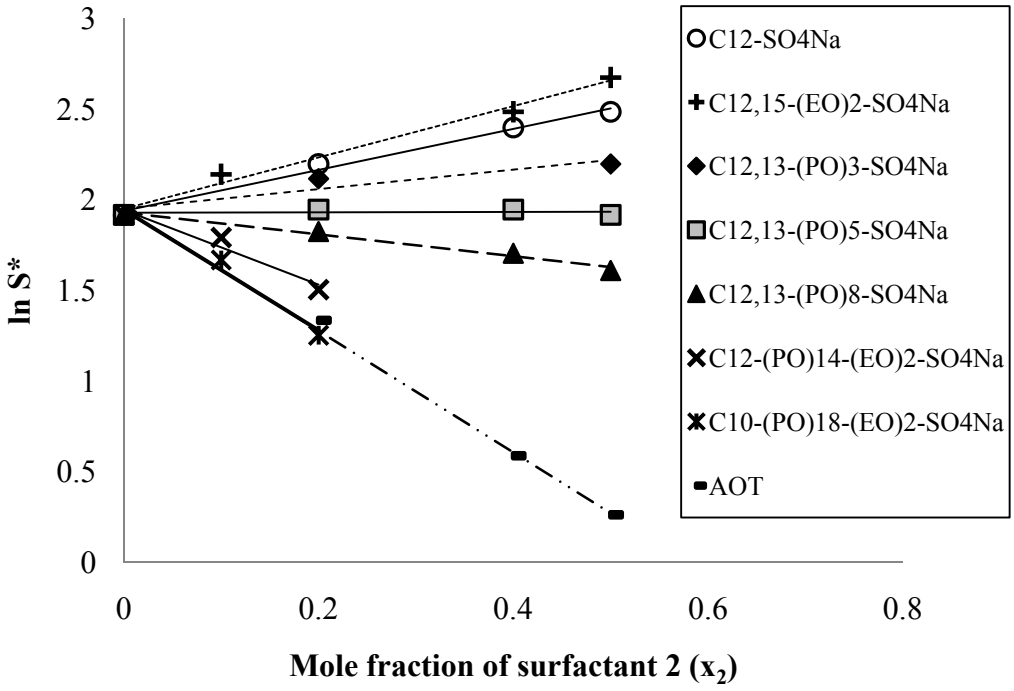

Figure 4. A plot of ln S* vs mole fraction of surfactant 2 (x_2) for conventional and extended surfactants.

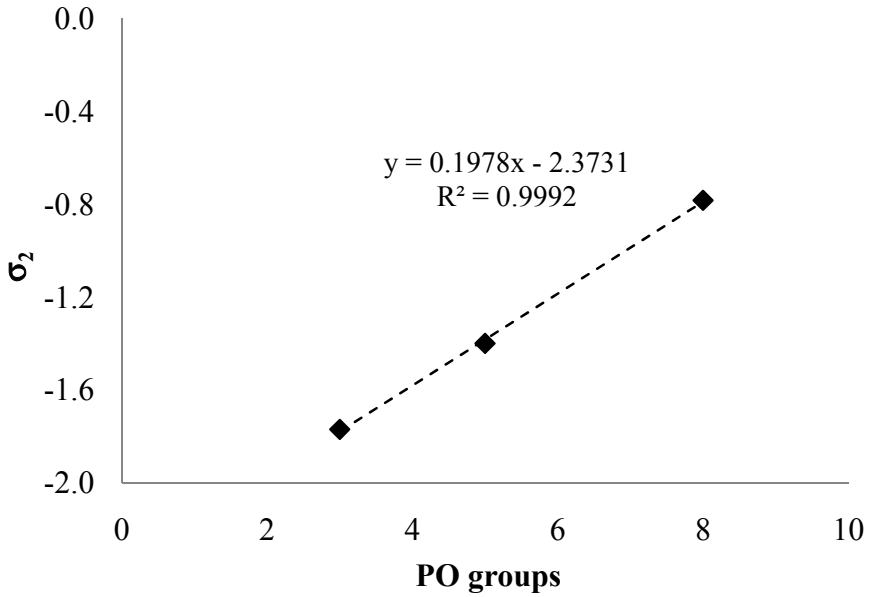

Figure 5. Effect of PO groups on the σ value of the $C_{12,13}$-$(PO)_x$-SO_4Na surfactant (50 %branch), x = 3, 5,and 8, respectively.

APPENDIX C

Dynamic Interfacial Property and Turbidity Measurement of Extended-Surfactant-Based Microemulsions (Chapter 4)

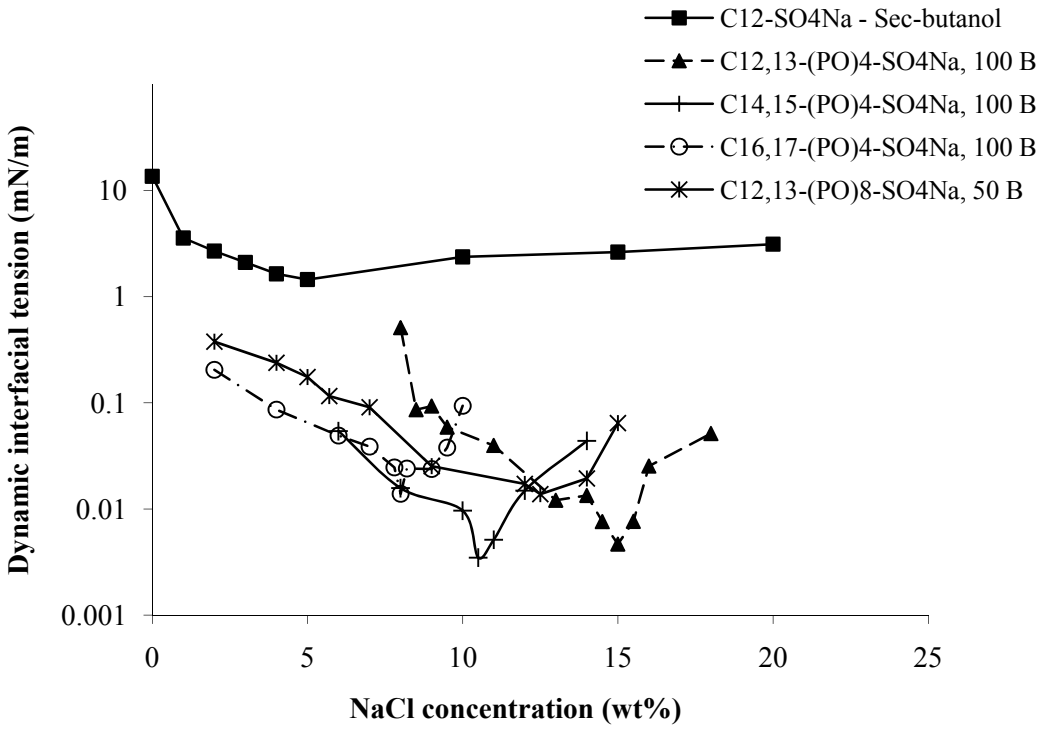

Figure 1. Dynamic interfacial tension at 10 minutes of dilute extended surfactant samples with hexadecane. Total surfactant concentration used was 0.003 M surfactant concentration at 27 ^{o}C.

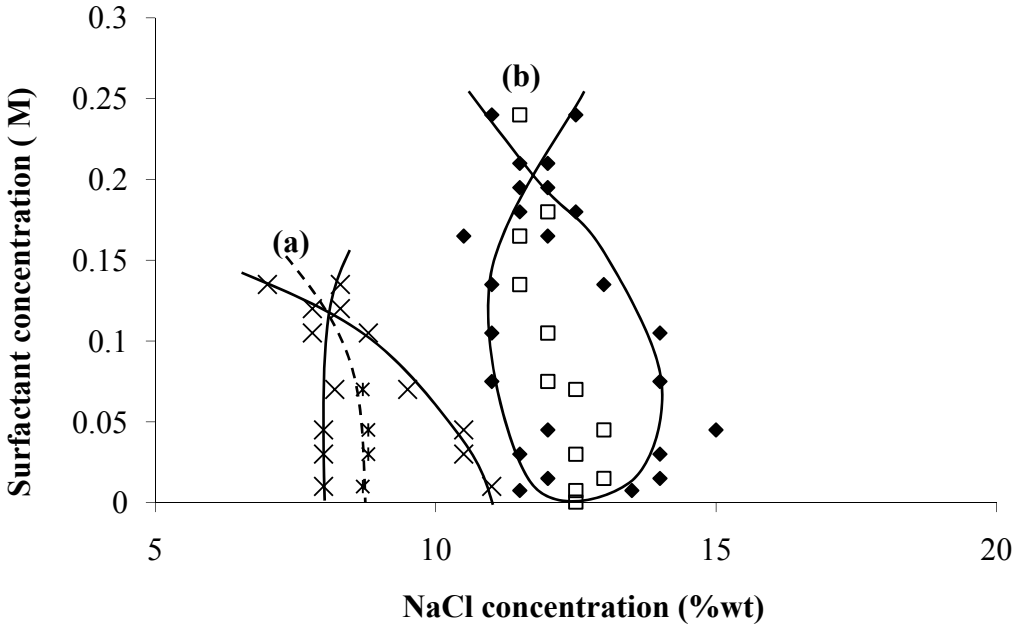

Figure 2. Fish diagram of the $C_{12,13}$-$(PO)_8$-SO_4Na/brine/hexadecane microemulsion at 27 ^oC: (a) 100 %branch hydrocarbon made from Italy crude oil and (b) 50 %branch hydrocarbon made from South Africa crude oil.

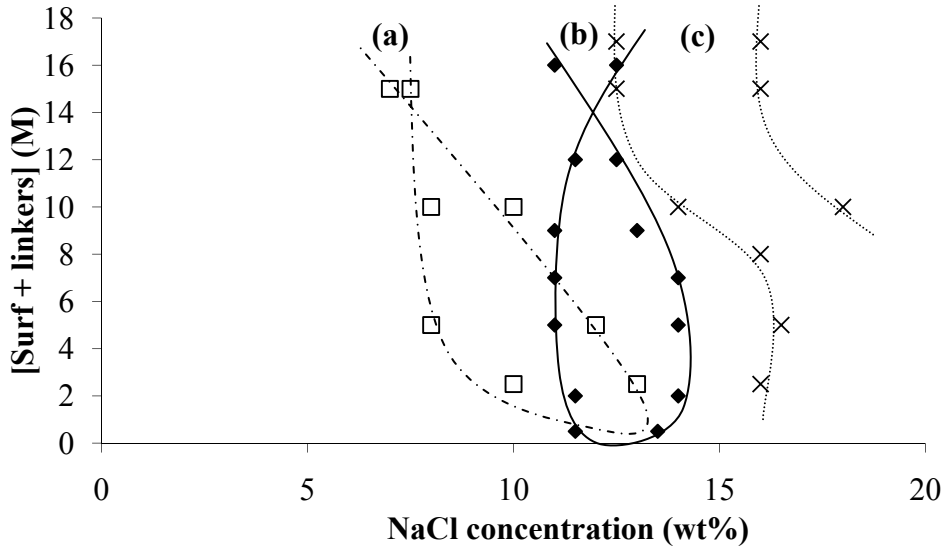

Figure 3. Fish diagram of (a) the $C_{12,13}$-$(PO)_8$-SO_4Na/SMDNS/oleyl alcohol, (b) the $C_{12,13}$-$(PO)_8$-SO_4Na-alone system, and (c) the $C_{12,13}$-$(PO)_8$-SO_4Na/hexyl glucoside/oleyl alcohol at 25 ^oC.

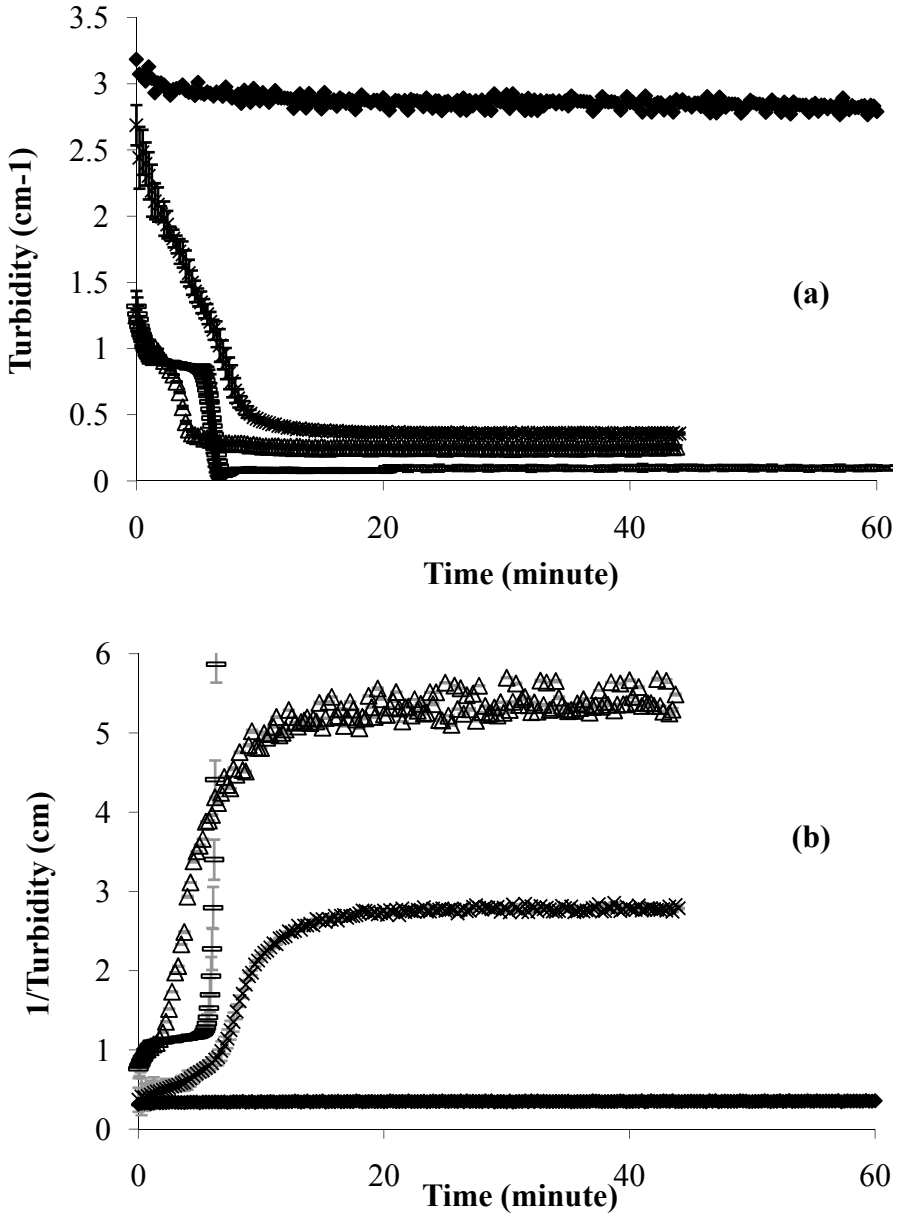

Figure 4. The turbidity (a) and inverse turbidity (b) curves during the 60-minute coalescence at 27 ^{o}C of the samples illustrated in Figure 4.4 (see Chapter 4). Turbidity samples resulted from shaking the optimum middle phase hexadecane microemulsions.

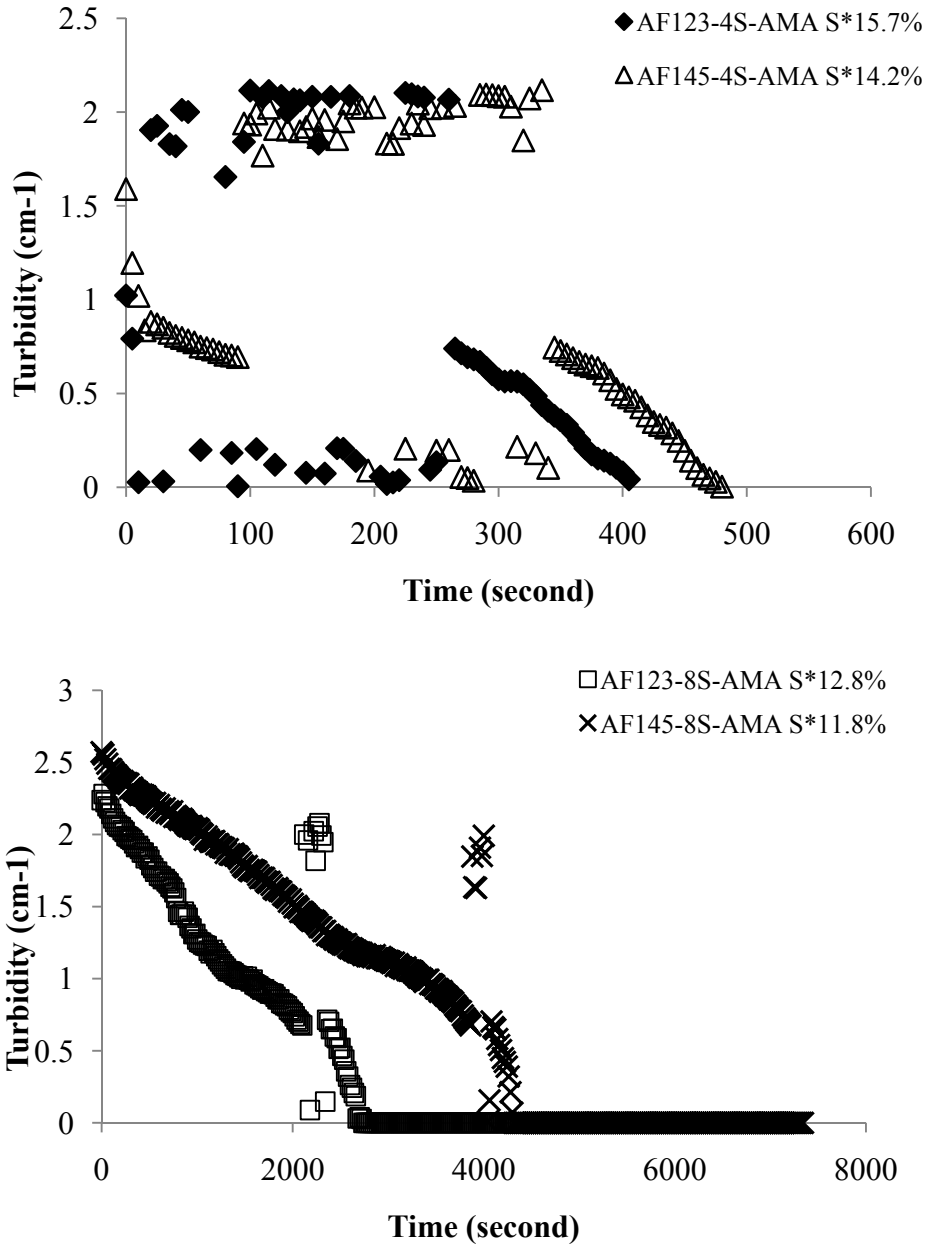

Figure 5. The discontinuous turbidity curve during coalescence at 27 ^{o}C of the 50/50 extended surfactant/AMA mixtures. The total surfactant concentration evaluated was 0.07 M. Turbidity samples resulted from shaking the optimum middle phase hexadecane microemulsions.

Table 1. The total time required to attain a complete coalescence in extended-surfactant-based microemulsion systems at the optimum salinity and 27 ^{o}C.

Surfactant system	S* (%wt)	Total time required to achieve a complete coalescence (second)
$C_{12,13}$-$(PO)_4$-SO_4Na 0.035 M + AMA 0.035 M	15.7	400.0
$C_{12,13}$-$(PO)_8$-SO_4Na 0.035 M + AMA 0.035 M	12.8	2720
$C_{14,15}$-$(PO)_4$-SO_4Na 0.035 M + AMA 0.035 M	14.2	475.0
$C_{14,15}$-$(PO)_8$-SO_4Na 0.035 M + AMA 0.035 M	11.8	4300

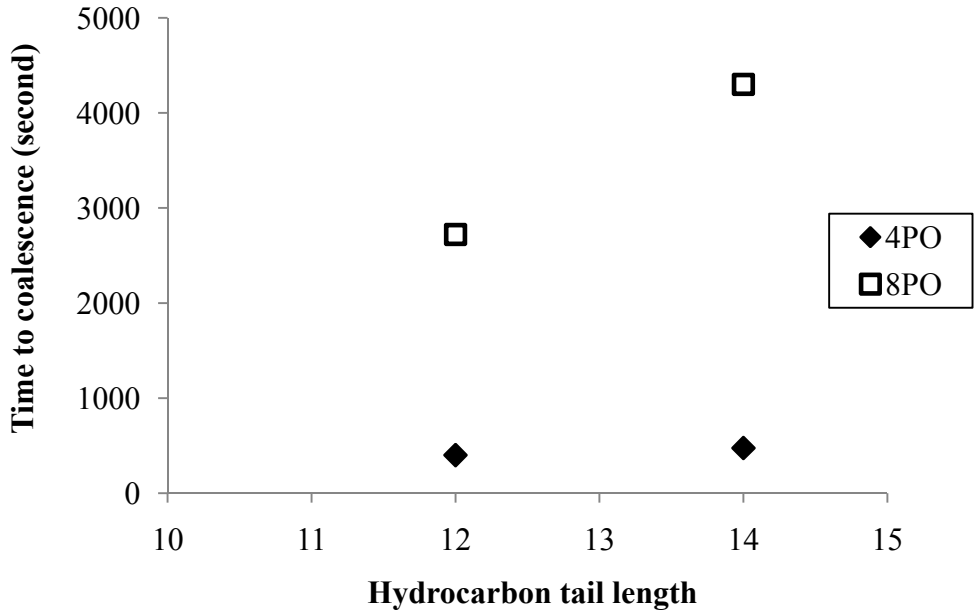

Figure 6. Effect of PO groups on total time required to achieve a complete coalescence in extended-surfactant-based microemulsion systems at the optimum salinity and 27 ^{o}C (plotting from data reported in Table).

APPENDIX D

Microemulsion-Enhanced Cleaning Performance

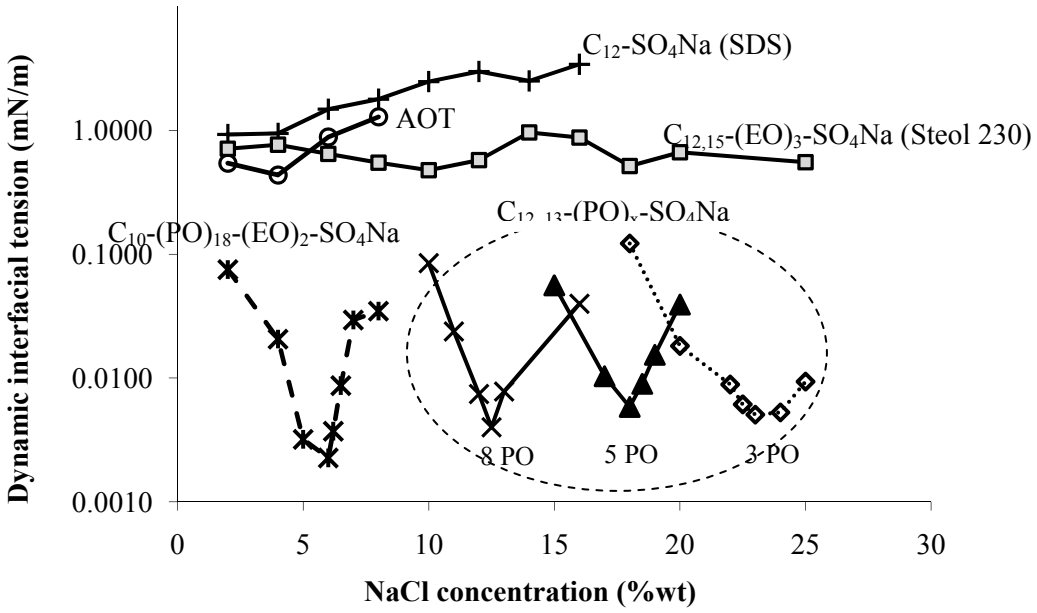

Figure 1. Dynamic IFTs at 10 min of various conventional and extended surfactants as a function of NaCl concentration with hexadecane oil. Surfactant samples were prepared at total surfactant concentration of 0.003 M (≈ 0.2 to 0.5 %wt) and 25 ^{o}C.

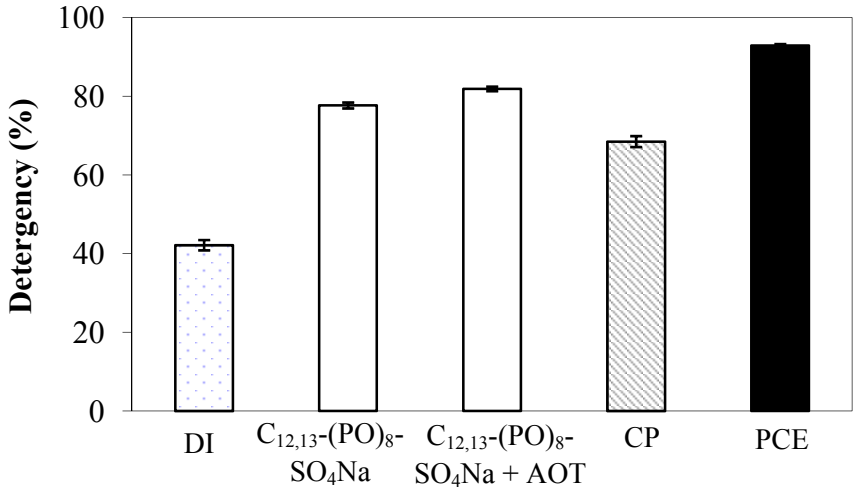

Figure 2. Removal of from 65/35 polyester-cotton (% detergency) using the $C_{12,13}$-$(PO)_8$-SO_4Na (50 % branch) and the mixed 50/50 $C_{12,13}$-$(PO)_8$-SO_4Na-AOT system at the optimum salinity compared to commercial detergent (CP) and organic solvent (PCE), the 0.003 M total surfactant concentration and constant 25 ^oC.

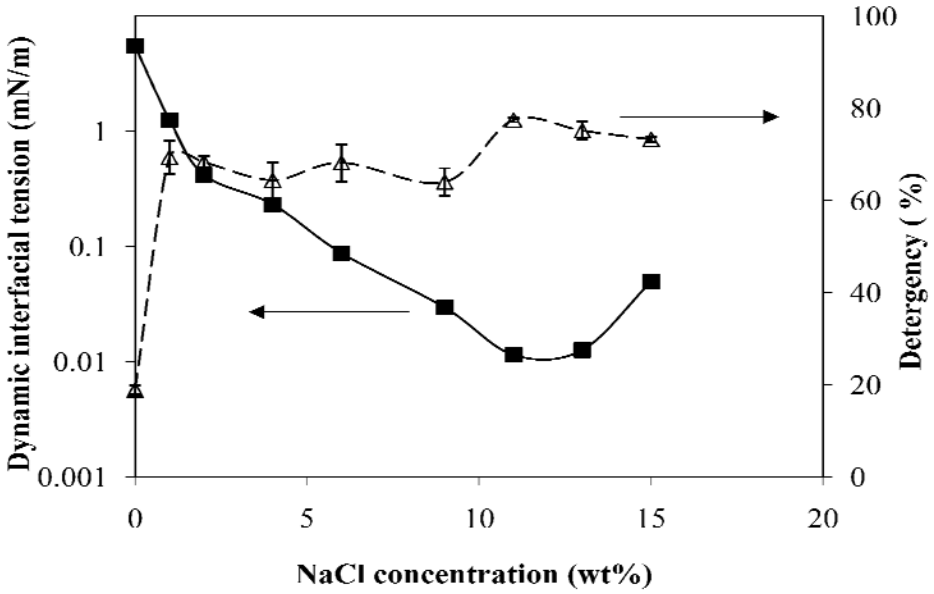

Figure 3. Dynamic interfacial tension and cleaning performance of the 0.003 M $C_{12,13}$-$(PO)_8$-SO_4Na (50 %branch) sample with hexadecane as a function of NaCl concentrations at 25 ^oC.

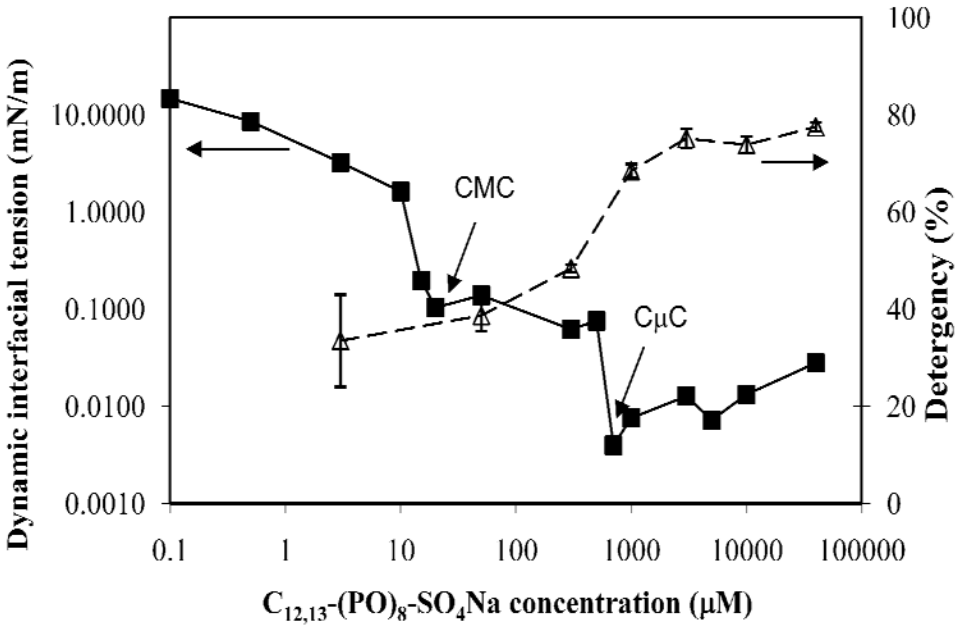

Figure 4. Dynamic interfacial tension at 10 minutes and cleaning performance as a function of the $C_{12,13}$-$(PO)_8$-SO_4Na (50 %branch) concentrations, hexadecane oil at 25 ^oC.

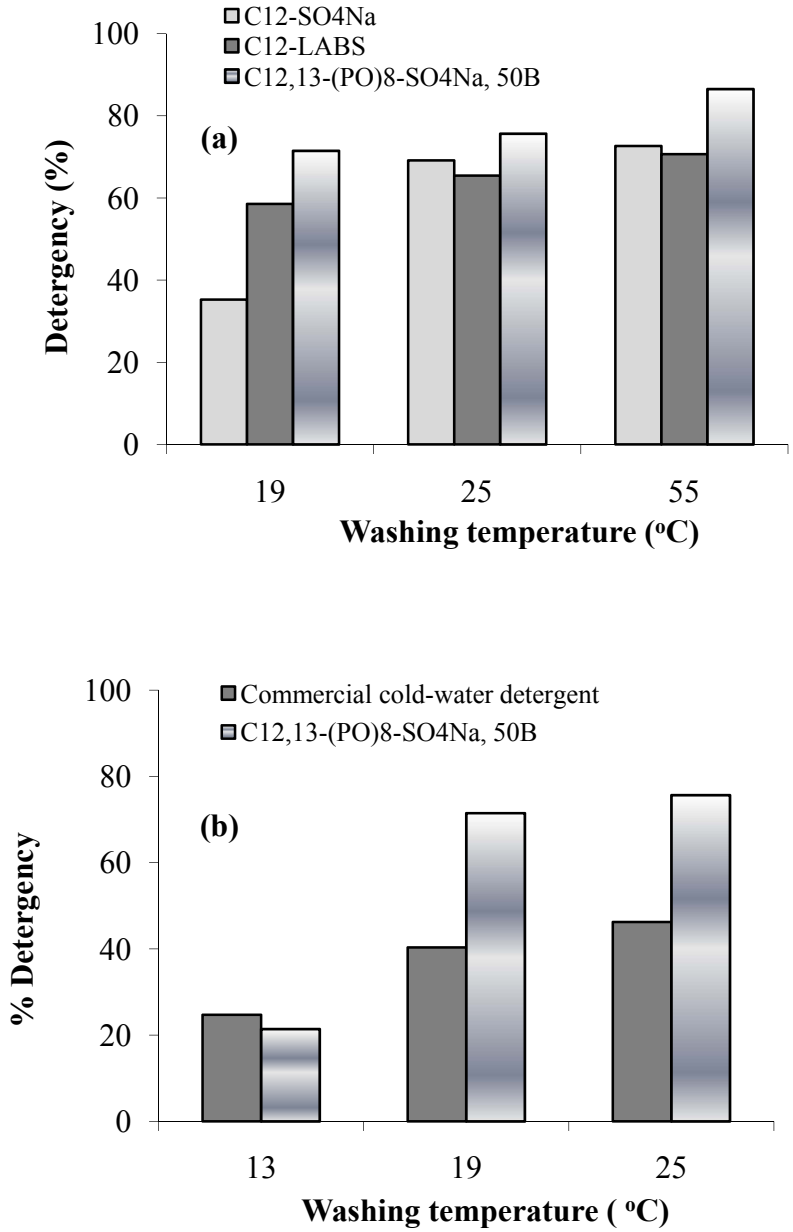

Figure 5. Effect of washing temperature on cleaning performance (% detergency) of (a) conventional vs. extended-surfactant systems and (b) extended surfactant vs. commercial detergent at the optimum salinity. The three surfactant systems studied were the C_{12}-SO_4Na (SDS), C_{12}-linear alkyl benzyl sulfonate, and $C_{12,13}$-$(PO)_8$-SO_4Na surfactants. The studied condition was at constant 0.003 M total surfactant concentration, hexadecane stained on the 65/35 polyester-cotton fabric.